



Spatial distribution of Nile perch in Lake Victoria using acoustic methods

Inês Dias Bernardes

Master of Science in Fisheries Biology and Management

Department of Biology, University of Bergen

2010



List of figures (from left to right):

Satellite image from Lake Victoria (source: <http://veimages.gsfc.nasa.gov/>);

Fishing boat arrival at Uganda (2006, source: <http://www.nationalgeographic.com>);

Nile perch being carried by a fisherman (source: <http://www.nation.co.ke/>);

Picture of an echogram of the LVFO August 2009 survey;

Picture of a boat used for transport of goods across the Lake's shore (Kayenze: Mwanza, August 2009)

Acknowledgments

This thesis would not be complete without the work and dedication of a vast number of people. To all of them I want to express my sincere gratitude for your dedication without which this work and experience would never be possible. With no disregard to all the people that have so much helped and allowed this master thesis, there are some that I would like to give a personal note.

First of all, I wish to thank to Berit for the enormous support, constant help and contagious good mood during this two years. To the University of Bergen for “sponsoring” this field work as for making possible my first and longtime wished trip to the African continent.

This thesis would never been possible without the dedication of Robert Kayanda, which have helped so much during all this time, in particular during the field work. Your guidance, support and efforts made this thesis possible.

To Egil Ona for “adopting” me in the middle of the way... For all your teaching, help and support with the acoustic data analysis and with the tuff writing process, as for always finding some time for me.

To all the people that helped me with the acoustic data. To Rolf Korneliussen, Ronald Pedersen for the great help for getting started with LSSS, but specially to Ingvald Svellingen for being always free for my never-ending questions.

To all the great people I had the chance of meeting and that made my experience in Mwanza unique, Ilse, Charles, Innocence, Happy and Koos. Also, to Mama Lucy and Father Malale for taking so good care of me in Mwanza. All the TAFIRI researchers and staff for making me feel so welcomed, with especial and sincere thanks to Katunzy and Ben Ngatunga for your efforts for this study. Oliva Mkumbo for your kind help in my data collection, by including me in the LVFO Survey. To all LVFO cruise personal, and in particular to the acoustics work group for all the special care, teaching as for the unforgettable time.

Greg Silsbe for kindly providing bathymetric data from Lake Victoria and Camilla Ilmoni for your assistance for working with this data.

To the ones that had the patience of reviewing my bad English and especially to my lovely mother that managed to not fall asleep while reading this work.

And of course, to Jeppe Kolding for this opportunity for working in Africa and for making this project possible.

Thank you all for so much.

Abstract

Lake Victoria supports Africa's largest fishery, being Nile perch the main contributor for the fishery revenues. Alerts for decreases in the commercial catches of Nile perch were reported during the mid 1990s. According to Kolding *et al.* (2008b), fish stocks are being affected mainly by eutrophication processes. The purpose of this work is to study if there is a relation between Nile perch spatial distribution and limnological data, in order to estimate the effects of enhanced eutrophication in the stock distribution. Acoustic data was used to obtain information on the Nile perch spatial distribution in association with limnological data (oxygen, chlorophyll *a* and temperature). Study limitations did not allow to conclude on relations between Nile perch densities and limnological data. However the results show a relation between Nile perch size and oxygen, and between Nile perch size and chlorophyll (for the three strata combined, as for the deep and inshore strata). Temperature showed to have no relation with fish size.

Key-words: Nile perch, Lake Victoria, acoustics, limnological data.

Acronyms

σ	Backscattering cross section [m^2]
Ψ	Equivalent beam angle [steradians]
π	Pi number
τ	Pulse duration [msec]
θ	Spherical angle [degrees]
χ	Trawl correction factor
Δz	Depth variation [m]
c	Sound speed [$m\ sec^{-1}$]
CTD	Conductivity, Temperature and Depth
GPS	Global Positioning System
KMFRI	Kenya Marine and Fisheries Research Institute
LSSS	Large Scale Survey System
LVFO	Lake Victoria Fisheries Organization
NaFIRRI	National Fisheries Resources Research Institute (Uganda)
NASC	Nautical Area Scattering Coefficient [$m^2\ nmi^{-2}$] (same as s_A)
N_V	Number of targets in the acoustic beam
R	Range [m]
r (f)	Relative frequency response
RMSL	Root mean square length [cm]
RV Victoria Explorer	Research Vessel Victoria Explorer
s_a	Area backscattering coefficient [$m^2\ m^{-2}$]
s_A	Area backscattering coefficient [$m^2\ nmi^{-2}$]
s_v	Volume backscattering coefficient [$m^3\ m^{-3}$]
s_V	Volume backscattering coefficient [$m^3\ nmi^{-3}$]
TAFIRI	Tanzanian Fisheries Research Institute
TL	Total length [cm]
TS	Target strength [dB]
TS_c	Compensated target strength [dB]
TS_u	Uncompensated TS [dB]
α	Absorption coefficient
ρ_A	Area density (referring to fish, [number of fish nmi^{-2}])
ρ_V	Volume density (referring to fish, [number of fish nmi^{-3}])

Units

cm	Centimeter
dB	Decibel
hp	horse power
kg	Kilogram
knots	nautical mile per hour (nmi hr ⁻¹)
l	Liter
m	Meter
mg	Milligrams (10 ⁻³ g)
min	Minutes
mm	Millimeters
msec	Milliseconds (10 ⁻³ s)
nmi	Nautical mile
°C	Degree centigrade
sec	Second
yr	Year
μg	Micrograms (10 ⁻⁶ g)

Table of contents

1	Introduction.....	1
1.1	Lake Victoria	1
1.2	Lake Victoria’s fishery	2
1.3	Nile perch	5
1.3.1	Growth and reproduction	5
1.3.2	Feeding habits.....	6
1.3.3	Distribution	7
1.4	Objectives.....	7
2	Materials and Methods	9
2.1	Field work.....	9
2.2	Data collection.....	10
2.2.1	Acoustic sampling	10
2.2.2	Environmental data collection	12
2.2.3	Biological data collection	12
2.3	Calibration	13
2.3.1	Acoustic equipment calibration	13
2.3.2	CTD profiler calibration	13
2.4	Data analysis.....	14
2.4.1	Echogram analysis	14
2.4.2	Target strength analysis	17
2.4.3	Density calculations	20
2.4.4	Limnological data analysis.....	21
2.4.5	Biological data analysis	22
2.5	Statistical analysis.....	24
3	Results.....	26
3.1	Limnological data analysis.....	26
3.1.1	Correlation between oxygen, chlorophyll a, temperature and depth	29
3.2	Target strength analysis	29
3.2.1	Validation of the TS measurements	30
3.2.2	Target strength distribution.....	32
3.3	Relation between limnological factors and mean TS	35
3.3.1	Oxygen	35
3.3.2	Chlorophyll a and temperature.....	37
1.1	Fish density distribution with depth	37
3.4	Comparison of fish densities between the sampled stations	39
3.5	Relation between limnological variables and fish density.....	40
3.6	Echogram analysis.....	42
3.7	Biological data analysis	43

4	<i>Discussion</i>	48
4.1	Limitations of this study	48
4.2	Target strength	50
4.2.1	<i>Validation of TS measurements</i>	50
4.2.2	<i>Spatial distribution of mean target strength</i>	52
4.3	Fish density distribution	52
4.4	Influence of limnological data on fish distribution	52
4.5	Bottom trawl and acoustic fish densities	54
5	<i>Conclusions</i>	57
6	<i>References</i>	58
7	<i>Appendixes</i>	67

Figure Index

Figure 1.1 – Pictures showing Dagaa. Picture on the left shows a fisherman’s drying Dagaa and picture on the right shows Dagaa before processing (Source: LVFO website).	2
Figure 1.2 – Map of Lake Victoria basin (source: Kayombo & Jorgensen 2005).....	3
Figure 1.3 – Some fishing boats used for the Lake fishery. Picture taken in Kayenze (Mwanza) near a Nile perch landing site (August 2009).	4
Figure 1.4 – Nile perch being carried by a fisherman (Source: http://www.nation.co.ke/).....	5
Figure 2.1 - Map of Lake Victoria showing the acoustic survey (lines) transects, the CTD (green squares) and bottom trawl locations (red squares), for the August 2009 LVFO survey. .	10
Figure 2.2 – Example of the layers used to divide the water column (Ruega station). The upper layer comprises mostly Dagaa and other small targets (the bracket on the left shows the surface layer not included in the analysis).	15
Figure 2.3 – Relative frequency response of targets to the two acoustic frequencies (70 and 120kHz). y-axis shows the ratio between the s_v at the two frequencies. The left figure a) shows the frequency response from smaller targets while the figure from the right b) shows the response from a bigger fish.	16
Figure 2.4 – Echogram showing the fish layer (limited with the red line). Black arrows show the areas where Nile perch targets were selected for mean TS calculations (Gozibar NE station). The color scale on the right corresponds to the s_v scale; depth scale is found on the left side and horizontal grids, for this station, are defined for 10 m intervals.....	18
Figure 2.5 – Zoomed echoes from Nile perch (Kamasi Station).	19
Figure 2.6 – Zoomed echoes from Nile perch (Kamasi Station). The three black lines show the single target detections.	19
Figure 2.7 – TS distribution and frequency response (from left to right) from the targets seen in fig. 2.6.....	19
Figure 2.8 – Variation of the fish target strength with fish length for the three equations describing the TS-TL relation for Nile perch. Blue dots show the relation for the equation $TS = 29,9 \text{ Log TL} - 79,3$; red dots show the data for $TS = 20 \text{ Log TL} - 66$; and green points for $TS = 30,2 \text{ Log TL} - 84,6$	23
Figure 3.1 – Mean oxygen (with standard error and standard deviation) level for each stratum. Values averaged for the water column.	26
Figure 3.2 – Mean chlorophyll <i>a</i> level (with standard error and standard deviation) for each stratum. Values averaged for the water column.	26
Figure 3.3 - Mean temperature (with standard error and standard deviation) level for each stratum. Values averaged for the water column.	26

Figure 3.4 – CTD profiles of inshore stratum (values averaged from the inshore stations).....	27
Figure 3.5 – CTD profiles of coastal stratum (values averaged from the coastal stations).	28
Figure 3.6 - CTD profiles of deep stratum (values averaged from the deep stations).	29
Figure 3.7 – Number of observations of targets distributed by target strength intervals. Y axis shows the number of TS observation and the x axis the target strength (in dB). Note: the y scale is not the same for all graphs; TS (x axis) scale from -65 to -20dB shown in graphs from 1 st row.	30
Figure 3.8 – Mean target strength calculated for each CTD station though the 3 different procedures. $TS_{Station}$ was calculated from the data from the entire water column; $TS_{Trawl\ area}$ show the mean TS calculated, for trawl stations, from the TS data on the trawl path (3m from the bottom); $TS_{Selected}$ represent the mean TS from selected Nile perch targets; $TS_{Trawl\ catches}$ show TS back-calculated from trawl catches.	31
Figure 3.9 – Target strength (in dB) in function of the number of fish in the acoustic beam (N_V). Graph includes data from all stations.	32
Figure 3.10 – Variation of TS and oxygen with depth for the inshore stratum. A second order polynomial trend was fitted to the TS data.....	33
Figure 3.11 – Variation of TS and oxygen with depth for the coastal stratum. A third order polynomial trend was fitted to the TS data.....	33
Figure 3.12 - Variation of TS and oxygen with depth for the deep stratum. A second order polynomial trend was fitted to the TS data.....	34
Figure 3.13 – Mean TS (in dB, with standard error) calculated for each stratum. The TS calculated for the two Gulfs – Emin Pasha and Speke – is also represented separately.....	35
Figure 3.14 – Mean TS data (with standard error and standard deviation), for all the stations, grouped by oxygen intervals (intervals of 0,5mg l ⁻¹).	36
Figure 3.15-3.18 – Mean TS data (with standard error and standard deviation) grouped by oxygen intervals. Graphs correspond to inshore, coastal deep strata and Speke Gulf, accordingly.	36
Figure 3.19 – Distribution of TS (averaged for each meter depth), dissolved oxygen, area backscattering coefficient (s_a), and TS detections over depth, for the inshore stratum. .	38
Figure 3.20 – Distribution of TS (averaged for each meter depth), dissolved oxygen, area backscattering coefficient (s_a), and TS detections over depth, for the coastal stratum...	38
Figure 3.21 – Distribution of TS (averaged for each meter depth), dissolved oxygen, area backscattering coefficient (s_a), and TS detections over depth, for the deep stratum.	39
Figure 3.22 – Fish density ($n^0\ nmi^{-2}$) for the entire water column, for each CTD station (figure on the left); and fish density distribution according to depth (figure on the right).	39
Figure 3.23 – Mean fish densities, with standard error and deviation, calculated for each stratum. .	40

Figure 3.24 – Mean fish density (\bar{x}) (with standard error [σ] and standard deviation [σ^2]) grouped by oxygen intervals (intervals of $0,5\text{mg l}^{-1}$).	40
Figure 3.25-3.28 – Distribution of fish density, grouped by oxygen interval for all strata and Speke Gulf.. Figures show the mean with standard error and standard deviation, for the inshore stratum, Speke Gulf, coastal and deep strata. Note: graphs are not at the same scale.....	41
Figure 3.29 – Total length distribution of Nile perch from all net hauls (11 bottom trawl hauls).	43
Figure 3.30 – Total weight for each specie captured from the bottom trawl catches.	44
Figure 3.31 – Comparison between estimated catch, from acoustic data, and trawl catches (kg haul^{-1}). Values are in Log scale.	45
Figure 3.32 – Relation between estimated catch, from acoustic sampling, and trawl data.	45
Figure 3.33 – Estimate from the frequency distribution of the expected total length from fish in the trawl area. Note: this graph should not be interpreted as the actual fish distribution, from the acoustic data.	46
Figure 3.34 - Estimate from the frequency distribution of the expected total length from fish, above 20cm, in the trawl area. Note: this graph should not be interpreted as the actual fish distribution, from the acoustic data.....	46
Figure 3.35 – Comparison between TS, calculated for each station, exported at 70 and 120 kHz frequencies.....	47

Table Index

Table 2.1 - Transducers and transceivers settings used for the acoustic survey.....	11
Table 2.2 – Parameter settings used during TS analysis using the LSSS post processing software.....	17
Table 3.1– Root mean square length calculated for Nile perch from the bottom trawl catch data. Maximum and minimum values for total length (TL) are also shown.	43

1 Introduction

1.1 Lake Victoria

The East African Rift Valley encloses the tropics' densest aggregation of lakes (Odada & Olago 2006; Johnson & Odada 1996). Lake Victoria is the largest of these, being also the world second largest freshwater lake, considering surface area (Awange & Ong'ang'a 2006).

Lake Victoria (00°20' N – 03°00' S, 31 °39' E – 34 °53' E) is the largest of the African Great Lakes (68 635km² of surface area; 2760km³ volume) and situated at an altitude of 1134 m (Kayombo & Jorgensen 2005). It is classified as a monomictic lake and has a high primary productivity (Bullock *et al.* 1995 in Klohn & Andjelic n.d.).

Lake Victoria is a shallow lake, being one quarter of the Lake's surface area less than 20 m deep (Silsbe 2004). It has an average depth of 40 m (Awange & Ong'ang'a 2006) and 80 m is the maximum depth found in the lake (Odada & Olago 2006).

Seasons differ between the North and Southern regions (Mkumbo 2002, Odada *et al.* 2004). Precipitation on Southern region of the lake is characterized by occurring in two main seasons, a dry and a rainy season (Mkumbo 2002). The two rain seasons occur between March-May (heavy rains), and October-December (Mkumbo 2002). Different rainfall patterns can be identified within Tanzanian waters; the highest annual precipitation levels are registered in the West region and the lower along the East shore (Kendall 1969). Wind patterns also reflect the seasonality, with strong winds increasing frequency between the months of February-March and July to November (Mkumbo 2002).

Lake Victoria is considered a closed system, having a long (140 yr) flushing time (Bullock *et al.* 1995 in Klohn & Andjelic n.d.; Bootsma & Hecky 1993). The majority of the lake's water inflow is supplied by rainfall (80 %) (Odada *et al.* 2004; Odada & Olago 2006; Awange & Ong'ang'a 2006) being the 17 tributaries responsible for less than 20% of the Lake's inflow (Yin & Nicholson 1998; Tamatamah *et al.* 2005). The White Nile is the only lake's outlet, located in the Ugandan part of the lake (Yin & Nicholson 1998; Tamatamah *et al.* 2005). About 82%, from the Lake's water inflow, is lost through evaporation (Hurst 1957 in Kendall 1969).

Annual water temperature variations found in Lake Victoria are small, with averages of 24 °C on the surface and 23 °C on deeper waters. Similarly, the annual air temperature variation reflects the mild climate, not exceeding 25 °C nor less than 19 °C (Awange & Ong'ang'a 2006). From May until August,

isothermal conditions characterize the water column; hence deeper waters are re-oxygenated throughout this period (Silsbe 2004). Successive higher temperatures in the water column are observed from September to December, influenced by deeper thermoclines observed (Silsbe 2004). A hypoxic layer is formed during the stratification period, consequence of the decomposition of organic matter (Hecky *et al.* 1994).

The variation of the limnological parameters reflect as well the season pattern; variations on the temperature, dissolved oxygen, depths of the thermo and oxycline, chlorophyll *a*, conductivity or water transparency are influenced by the hydrological factors (Mkumbo 2002).

1.2 Lake Victoria's fishery

There are considerable number of publications dedicated to the Lake Victoria and its ecological changes. An ecological shift was seen throughout the transition from the multispecies fishery in the 70s, comprising 24 species and dominated by cichlid species (Tilapiines and haplochromines) (Witte 2007, Matsuishi *et al.* 2006), to a relatively simple fishery of 4 species only (Mkumbo 2002). The prevailing species captured commercially in the Lake are Nile perch (*Lates niloticus*), Nile tilapia (*Oreochromis niloticus*), an endemic cyprinid Dagaa (*Rastrineobola argentea* TL_{max} = 6.8 cm, Figure 1.1) and some catfish species (Schofield & Chapman 1999, Scullion 2005).



Figure 1.1 – Pictures showing Dagaa. Picture on the left shows a fisherman's drying Dagaa and picture on the right shows Dagaa before processing (Source: LVFO website).

Two endemic species occupies the Lake's pelagic habitats, *Brycinus sadleri* and Dagaa, with increasing incidence in open waters (Schofield & Chapman 1999). Littoral waters of the Lake are populated by Nile tilapia and by the macrophyte feeder *Brycinus sadleri* (TL_{max} = 9.0 cm, Wanink & Joordens 2007).

The Lake's valuable natural resources supports Africa's largest fishery (Geheb *et al.* 2007). The Lake's waters are divided among the three countries bordering the Lake shore (Figure 1.2), Tanzania (49%), Uganda (45%) and Kenya (6%). Populations from the Lake Victoria region rely on the Lake as a source of water supply and of nutrition (Hecky 1993; Manyala 2005; Odada & Olago 2006), with fish contributing up to 27% of the total protein consumption in Tanzania (FAO 2007).



Figure 1.2 – Map of Lake Victoria basin (source: Kayombo & Jorgensen 2005).

Nile perch was introduced into the Lake Victoria during the 60s and by 1983 it was spread all over the Lake (Ogutu-Ohwayo 1988); Nile tilapia was together with Nile perch successfully introduced (Ogutu-Ohwayo 1988). The development of a multi-million export industry, the availability for fish in the local markets or the expansion of the artisanal fishing industry, are some of the economic benefits from Lake Victoria's non indigenous species (Cowx *et al.* 2003).

Estimates indicate that annual fish landings range between 450-500 thousand tons, valued at US\$500-US\$550 million (Manyala 2005). Nile perch forms the majority of the fishery exports' profits (FAO 2007) which are close to US\$129 million, just for Tanzania (Pfliegner 2008).

Given that the fishery is restricted to lakeshore regions, the sector has a considerable economic impact for such areas (Allison 2004). The Lake fishery comprises mainly artisanal fishers (FAO 2007; Salehe 2008), using small fishing crafts (length between 7 and 11m, see Figure 1.3), most of which

motorized with outboard engines; dug out canoes and dhows (LVFO 2008). The types of fishing gear with widespread use, in the Nile perch fishery, are gill nets and longlines (LVFO 2008). A slot size has been established for commercialization of Nile perch over the three partner states with a minimum and maximum size of 50 and 85cm, respectively (Salehe 2008).



Figure 1.3 – Some fishing boats used for the Lake fishery. Picture taken in Kayenze (Mwanza) near a Nile perch landing site (August 2009).

The Lake Victoria basin is quoted as a region that has experienced increasing ecological changes over time (Chapman *et al.* 2008). Reviews focusing the environmental degradation, fishery management problems have been widely published. The identified problems fit in two categories, one under the fisheries exploitation, where destructive fishing practices and overexploitation are focused; while the other concerns pollution of the Lake ecosystem (Odada *et al.* 2004).

Alerts for decreases in the commercial catches of Nile perch were reported during the mid 1990s (Bwathondi *et al.* 2001 in Odada *et al.* 2004; Scullion 2005; Matsuishi *et al.* 2006) and a decline on the stock biomass was also reported from Lake acoustic surveys (Getabu *et al.* 2003). Awareness for the excessive fishing pressure on the stocks has been repeatedly focused in publications, such as Ogutu-Ohwayo *et al.* (1991), Kitchell *et al.* (1997), Odada *et al.* (2004), Scullion (2005), Matsuishi *et al.* (2006) or van der Knaap *et al.* (2007). According to Kitchell *et al.* (1997) the fishing pressure is the main driver for the Lake and the fishery dynamics. Consequently, adoption of policy options to address overexploitation have been proposed, namely measures to limit the access to fishery (Odada *et al.* 2004).

The role of environmental stressors in the Lake Victoria ecosystem is not fully understood and research on its consequences is still lacking (Chapman *et al.* 2008). Hence, deviations from the option of management decisions that focus only top-down perspective have been stated in publications such as Kolding *et al.* (2008b). According to the authors, both top-down as bottom-up processes are affecting the Lake ecosystem, but eutrophication is indicated as the main driver affecting the fishery (Kolding *et al.* 2008b). The extent to which these two processes affect the Nile

perch stocks is unknown and is being investigated by the ongoing SEDEC project (Verreth *et al.* 2007), where this Msc project is integrated.

Anthropogenic changes in the watershed of Lake Victoria were in the base of the transition to an eutrophic state, from an mesotrophic system since the 30s (Hecky 1993, Chapman *et al.* 2008). Shifts in algal species composition, increasing incidence of algal blooms (Smith *et al.* 2006), oxygen reduction and decreasing in water transparency (Brönmark & Hansson 2005) are some of the most common effects from eutrophication described for Lake Victoria (Mwakosya *et al.* 2005, Hecky 1993). Oxygen reduction is believed to be the most important consequence of eutrophication, namely for freshwater fisheries (Doudoroff & Shumway 1970). Thus, the influence of this factor in the distribution of the Nile perch stock will be in focus.

1.3 Nile perch

A brief description of Nile perch biology, feeding habits and distribution follows in order to familiarize the reader with the species here in focus.

The Nile perch, the impacts of increasing eutrophication and it impacts for the fishery, constitute the framework from this study. This is due to its importance for the communities surrounding the Lake where the fishery constitutes an essential source of income.

1.3.1 Growth and reproduction

Nile perch (Figure 1.4) attains 1 kg during its first year and achieves the commercial size (50 cm), with 2 to 4 kg, with two or three years (Ogutu-Ohwayo 1994 *in* Kitchell *et al.* 1997).



Figure 1.4 – Nile perch being carried by a fisherman (Source: <http://www.nation.co.ke/>)

Sexual dimorphism is a feature characterizing Nile perch, as the females are larger than males (Hughes 1992a, Ogutu-Ohwayo 1988). Females can attain sizes of 173 cm (TL_{max}) when compared to

136 cm in males (Ogutu-Ohwayo 1988). Data collected from Tanzanian waters suggest that maturation (L_m) can occur at 54,34 cm and 76,71 cm length, in males and females respectively (Mkumbo 2002).

Nile perch reproduction is adapted to the stable and mainly non-seasonal environment, since ripe individuals can be found throughout the year (Hopson 1982 *in* Ogutu-Ohwayo 1988). Mkumbo (2002) reported small peaks in reproduction from May-July and October-November for Tanzanian waters, coinciding with the end and start of the rainy periods, respectively. A high reproductive potential is attributed to Nile perch which release its eggs in the pelagic environment (Ogutu-Ohwayo 1988). Shallow and sheltered areas are indicated as a possible preferential spawning area (Ligtvoet & Mkumbo 1990).

1.3.2 Feeding habits

Adult Nile perch occupies the top of the food web on the Lake Victoria (Ogari 1988 *in* Mkumbo 2002). It is a visual predator that depends on the light for feeding (Mkumbo & Ligtvoet 1992), being that there is an increased foraging activity during the morning hours (Mkumbo 2002).

Nile perch diet patterns seem to vary among the Lakes where it is found. Age of maturity (Schofield & Chapman 1999) and seasonality seem to influence its feeding patterns (Mkumbo & Ligtvoet 1992). Depth also showed to have an influence on the diet since Nile perch found at higher depths prey more in the shrimp *Caridina nilotica* and simultaneously less in Dagaa (Katunzi *et al.* 2006).

Several authors have reviewed Nile perch feeding habits for the periods following the decline of Haplochromine species. The habitat and prey abundance influence is clear (Katunzi *et al.* 2006). Small Nile perch (<5cm) feeds on zooplankton (Katunzi *et al.* 2006) while *Caridina*, *Rastrineobola* and juvenile perch are the main prey for Nile perch juveniles (>15cm) (Mkumbo & Ligtvoet 1992). Hughes (1992a, 1992b) attributed to *Caridina* an important role on the Nile perch diet, in particular for individuals <40cm. Above the referred size Nile perch started to prey on Dagaa (Mkumbo & Ligtvoet 1992) as on its own offspring (Mkumbo & Ligtvoet 1992; Kitchell *et al.* 1997), while Nile perch >100cm prey mainly on Tilapiines and its own juveniles (Ogutu-Ohwayo 2004).

Haplochromines are quoted as the preferential food item for Nile perch (Ogutu-Ohwayo 2004). They dominated Nile perch diet up to 1988, time when their abundance decreased being thus replaced by the other available prey types (Ogutu-Ohwayo 2004). Due to the recent recovery of some Haplochromine trophic groups (Witte *et al.* 2007) it is likely that its contribution for Nile perch's diet increases as well.

1.3.3 Distribution

Nile perch is a shallow water specie distributed along inshore habitats (Okemwa 1984); is described as a demersal

species (Ligtvoet & Mkumbo 1990) being found all over the water column (Mkumbo 2002), up to 60 m depth (Goudswaard & Witte 1985, Goudswaard 1988, Goudswaard & Ligtvoet 1988 *in* Witte & Van Densen 1995). Declines in Nile perch abundance are found with depth (Mkumbo 2002) with higher catch rates occur between 16 and 50 m deep (Witte & Van Densen 1995). A narrower range has been reported by Mkumbo (2002), being the highest Nile perch densities found between 30-39m. Nile perch juveniles (<11 cm) are also found all over the water column, although catches decline close to the surface (Goudswaard *et al.* 2004).

The seasonality, and the consequent mixing of the water column, is reflected on the Nile perch relative abundances (Mkumbo 2002). Nile perch spatial distribution may reflect the variation on limnological parameters, being the influence of the rainfall on the densities suggested in Mkumbo (2002).

The suggestion that oxygen levels could restrain the habitat distribution for Nile perch is a result of Fish's (1956) work. Low densities or absence of Nile perch from certain habitats, such as in swamp areas, is justified by its low tolerance to hypoxic environments (Chapman *et al.* 2002). Nile perch metabolic rates are higher than several haplochromines or tilapiine cichlids; hence, it justifies the absence of this big fish in environments with limited oxygen availability (Fish 1956, Schofield & Chapman 1999). This is reinforced by the findings by Schofield & Chapman (2000) which observed that Nile perch's has weak hypoxia compensating mechanisms.

The individual's oxygen consumption rate is dependent of several factors such life stage, body weight, activity level, environmental temperature, and feeding (Moyle & Cech 2004). In accordance, the suggestion that vulnerability differed among sexes, being the females more susceptible and the males more capable of tolerating hypoxic conditions has resulted from Kolding's *et al.* (2008a) work.

The susceptibility of Nile perch to low oxygen conditions and the awareness of a decrease in oxygen levels, as a consequence of increasing eutrophication in Lake Victoria, constitute the focus of this study.

1.4 Objectives

Through its integration on the SEDEC project, the purpose of this Master project is to study if there is a relation between the environment (limnological factors) on Nile perch spatial distribution. Under

this goal, the correlation between Nile perch density and distribution with oxygen, chlorophyll *a* and temperature will be examined, in order to estimate the effects of enhanced eutrophication in the stock distribution.

The research questions here focused relate to the relation between limnological factors and fish distribution are:

- I. Are fish densities related with differences in oxygen availability, temperature or chlorophyll *a* concentrations, over the water column?
- II. Is the distribution of different sizes of Nile perch related with variations in the limnological parameters?

In order to answer the research questions, acoustic data will be used to obtain information on the Nile perch spatial distribution and densities by depth. In addition, limnological data will allow to investigate the existence of correlations between these data and the stock. Comparisons between offshore locations with data collected within enclosed bays or inshore sites, considered more susceptible to limnological variations, will give indications of the relation between enhanced eutrophication and fish distribution.

2 Materials and Methods

2.1 Field work

The data collection was integrated in the SEDEC project, a joint initiative gathering institutions from Netherlands¹, Tanzania² and the Norwegian University of Bergen. The initial field work plan was to collect acoustic, gill net and limnological data over the water column. Data would be collected inside the Speke Gulf, a bay located in the South East (SE) of Lake Victoria, in areas exposed differently to eutrophication gradients. However, technical problems with the portable acoustic equipment dictated a change in the work plan. I was therefore kindly allowed to work with the data gathered under the LVFO biannual stock assessment survey, as well as to join the survey (from 16/08/09 to 22/08/09) while the vessel was in Tanzanian waters.

Lake wide acoustic surveys, directed for monitoring purposes have been conducted since 1999 under Lake Victoria Fisheries Organization (LVFO) programs (LVFO 2009; Getabu *et al.* 2003). These are lake wide surveys conducted under the LVFO in every 6 month interval and combine hydrographic, bottom-trawl and acoustic surveys, conducted for biomass estimate purposes.

The survey has a fixed grid of predetermined acoustic transects, as well as of fixed stations for collecting limnological data (oxygen, chlorophyll *a*, temperature and conductivity depth profiles) and bottom-trawl, covering both inshore and offshore waters (Figure 2.1). The survey was conducted using the TAFIRI's research vessel "Victoria Explorer" (RV Victoria Explorer), with scientific staff from the fisheries research institutes from the three countries bordering the Lake (TAFIRI, KMFRI and NaFIRRI). The RV Victoria Explorer is a stern trawler (LVFO 2009) with a propulsion power of 215 hp and length of 16,70 m (width 5,50 m; draft 2,20 m). The Research Vessel is registered on the Port of Mwanza and built in 1997 (Everson 2006).

The LVFO August 2009 survey went from the 16th of August, departing from Ilemela (Mwanza), to the 11th of September, finishing in Nyamikoma (Speke Gulf). The data used for my thesis was the correspondent to the Tanzanian waters (33 756 km² of surface area; 0° 59' S – 3° 00' S and 31° 37' - 34° 53' E³) and collected from 16/08/09 to 22/08/09 and in the 11/09/09.

¹ Aquaculture and Fisheries Group, Wageningen University; Aquatic Ecology and Water Quality Group, Wageningen University; Law and Governance Group, Wageningen University; Netherlands Institute for Ecological Research, Center for Limnology

² Tanzania Fisheries Research Institute; Faculty of Aquatic Sciences and Technology, University of Dar Es Salaam; Faculty of Arts and Humanities, University of Dar Es Salaam

³ Kayombo & Jorgensen 2005

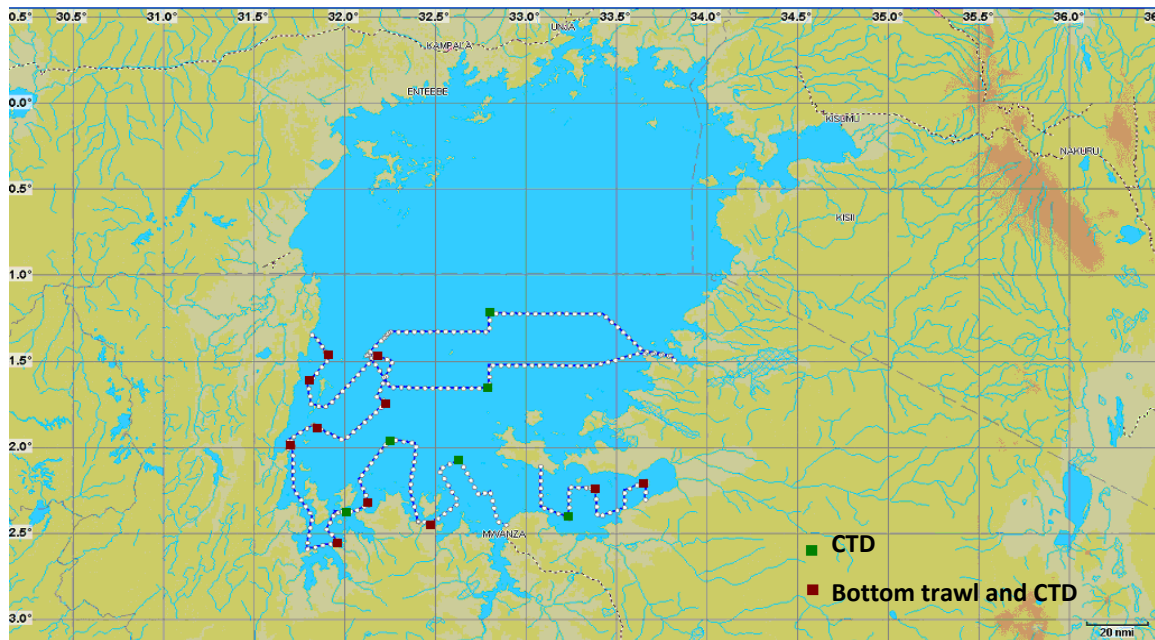


Figure 2.1 - Map of Lake Victoria showing the acoustic survey (lines) transects, the CTD (green squares) and bottom trawl sampling locations (red squares), of the August 2009 LVFO survey.

2.2 Data collection

2.2.1 Acoustic sampling

Within the LVFO surveys, sampling is limited to the daylight hours (from 7 am to 5 pm) as a general rule with exceptions in the days when the Lake has to be crossed (start of recordings at approximately 4 am). The restriction to daylight sampling, according to the LVFO standard operation procedures, is justified by the more “clear” echograms since there is less mixing of fish during that period (Everson 2006), facilitating the post-processing and scrutinizing of the acoustic data. Details regarding acoustic and biological sampling can be consulted in Appendix.

Vessel position was measured with a Garmin Global Positioning System (GPS), connected to a portable laptop, merging the data directly with the acoustic recordings. All the survey events, namely GPS position, CTD (Conductivity, Temperature and Depth) locations and net hauls were registered in a “Survey Event Log”, for later use in the post-processing analysis (Appendix II, Table 1).

Acoustic data was collected continuously, at an approximate cruising speed of 9 knots, with a SIMRAD EK-60 echo-sounder (Simrad, Kongsberg, Norway) operating with a vertical beam with 70 and 120 kHz split beam transducers. Both devices were hull-mounted at a depth of 1,80 m. The transducer and transceivers’ settings are displayed in the table 2.1 below.

Table 2.1 - Transducers and transceivers settings used for the acoustic survey.

<i>Transducers settings</i>		
<i>Transducer</i>	ES70-7C	ES120-7C
<i>Frequency (kHz)</i>	70	120
<i>Beam type</i>	Split	Split
<i>Athwartship beam angle (Deg)</i>	6,64	6,41
<i>Alongship beam angle (Deg)</i>	6,65	6,45
<i>Athwartship angle sensitivity</i>	23,00	23,00
<i>Alongship angle sensitivity</i>	23,00	23,00
<i>Equivalent beam angle (dB)</i>	-21,0	-21,0
<i>Gain (dB)</i>	26,3	25,99
<i>Depth transducer (m)</i>	1,80	1,80
<i>Transceivers settings</i>		
<i>Bandwidth (kHz)</i>	6,16	8,71
<i>Pulse duration (pulse length) (ms)</i>	0,256	0,256
<i>Sample interval (ms)</i>	0.064	0.064
<i>Sample distance (m)</i>	0,048	0,048
<i>Pulse interval (s)</i>	0.20	0.20
<i>Power (W)</i>	200	200
<i>Maximum ping range (m)</i>	120	120

In addition to the data collected along the survey transects, recordings were made during the net hauls and CTD sampling. Following the collection of the environmental data, the research vessel was kept drifting for 15 min which provides tracking data for single targets. Further details regarding the stations sampled can be consulted in Appendix IV.

The acoustic survey transects are classified according to stratum for analysis in the LVFO Acoustic surveys. Inshore, Coastal, Deep and Gulfs are the four types of stratum in use and defined as follows (Everson 2005):

Deep stratum – Stations with bottom depth over 40 m.

Coastal stratum – Stations included in a band of approximately 20 km, located between the deep stratum and the shore.

Inshore stratum – Areas close to islands and shallow waters.

Gulfs – The two gulfs found in the Tanzanian waters, Emin Pasha and Speke, are included in a different category for analysis according to LVFO procedures. However, for this thesis the two gulfs sampled were analyzed together with the data from the inshore stratum. Stations located in these two gulfs were included, for display as statistical analysis, in the inshore stratum since the number of samples collected in these two locations was insufficient to be analyzed separately.

The above described strata classification was used for this study.

All acoustic data was stored on a computer and backup was stored on an external hard disc in the end of each survey day.

2.2.2 Environmental data collection

Depth profiles for dissolved oxygen, chlorophyll *a*, conductivity and temperature were taken. Hydrographic samples were collected with a CTD profiler (CTD, Sea-bird Electronics®, Sea Cat SBE 19), equipped with oxygen, temperature, chlorophyll, conductivity sensors and pressure (depth) programmed to take measurements every 5 seconds. Vertical profiles from these parameters were taken approximately from a 0,4 m distance from the surface and bottom, due to the size of the protective structure from the sensors (LVFO 2009). Conductivity data is not analyzed in this study.

CTD vertical profiles were made prior to trawling, however the total number of net hauls was lower than the CTD measurements. CTD profile data from 17 stations are being considered in this study. The CTD devices were lowered manually, after a 3 minutes “warm up” period, and 2 or 3 measurements were taken in each meter. An average of 2 CTD stations was sampled by day, although exceptions occurred in the 19/08/09 and on the 20/08/09, where 3 and 1 location were sampled, respectively. Details of the CTD stations can be consulted in Table 1, Appendix IV.

2.2.3 Biological data collection

Biological samples were collected with a bottom trawl with V shape otter-boards, a 3,5 m vertical opening, a 24,4 m headrope and 27,6 m footrope (Agnew 2005). 15 m single sweeps were attached to 20 m upper and lower bridles (Mkumbo 2002).

Bottom trawl effort is predetermined in the Standard Operation Procedures for acoustic surveys (2 or 3 per day) (Everson 2005). These are however subject to fish availability in the sampling locations. A total of 11 bottom net hauls were done during this study period (see Table 2, Appendix IV), with a standard 30 min tow duration and a 3 knots towing speed. In order to also retain small species, such as shrimps (*Caridina niloticus*) and small size fish, a 4 mm mosquito net was incorporated into the cod end (LVFO 2009).

The net haul depths varied between 7,6 and 50,0 m (floatline) in the stations sampled. A schematic representation of the trawl used as well as further details regarding the trawling station's can be consulted in Appendix IV.

Following each haul, catch was sorted to the species level and then weighted using a spring scale balance, to obtain the weight proportion for all species. A regular kitchen balance (Salter Brecknell) was used for weighting smaller samples, when low numbers of small size fish were captured. Total length (TL) was measured for Nile perch individuals captured in the net hauls. Subsamples were taken when catches were numerically large, according to the Standard Operation Procedures for acoustic surveys (see Agnew 2005). For large catches, big fishes were sorted and measured to the nearest centimeter. A representative subsample (app. 200 fish) from the remaining fish was then selected for length measurements (Everson 2005).

2.3 Calibration

2.3.1 Acoustic equipment calibration

Two in situ calibrations on the hydroacoustic system were done, one of them two days prior the beginning of the survey (GPS location: 2°28'5''S, 32°52'37''E) and the second two days before the end of the survey (09/09/2009). The first calibration results were maintained in post-processing data analysis since values from both calibrations did not differ to a large extent.

Calibration was performed following the procedures described in the ER60's operator manual, by using a 32,1 and a 23,0 mm standard copper sphere, for the 70 and 120 kHz transducers. The theoretical target strength of copper spheres used were -39,1 and -40,4 dB respectively, at 25 °C. The sound speed (c) and absorption coefficient (α) were automatically calculated by the ER60 software. All the values obtained in calibration, as well the echo-sounder settings, are displayed in Appendix III.

2.3.2 CTD profiler calibration

Factory calibration settings were used during the survey. Accuracy limits for the CTD profiler are 0,1 ml l⁻¹ and 0,01 °C for the oxygen, temperature sensors respectively (Seabird 2009). Winkler titration method was used to assess the stability of the oxygen measurements from the CTD profiler. Oxygen concentration was determined by the method referred, previous to the start and following the end of the survey. Since no divergence was found between the methods, no adjustments to the oxygen profiles were necessary (LVFO 2009).

In addition, prior to the beginning of the survey a comparison was made between the CDT profiles from the CDT device used in the cruise (Sea-bird Electronics®, Sea Cat SBE 19) and an Hydrolab DS5

Multi Probe from the SEDEC Project. No difference in the limnological data was seen between both devices. Another CTD equipment, from NaFIRRI, and recently serviced by the manufacturer (LVFO 2009) was used during the survey to compare with the limnological data collected. Again, no divergence was found between the two equipments.

2.4 Data analysis

2.4.1 Echogram analysis

The post-processing analysis was done using the Large Scale Survey System – LSSS, version 1.4 (Korneliusson *et al.* 2006).

To account for the near field effect during vertical beaming, all echoes from 0,5 m from the transducer surface were excluded (Simmonds & MacLennan 2005). Similarly, the bottom exclusion zone was also set to 0,5 m above the bottom, which is the typical height for bottom bias in a transducer with a 7° beam angle, at 100 m depth (Ona & Mitson 1996). This value for the bottom exclusion zone was adopted for all stations even being most of them being shallower than 100 m.

Prior to processing, raw data was carefully inspected for removal of bottom detections errors, with some manual corrections to the bottom detection being made during the echograms scrutinizing. These corrections were mainly necessary when fish echoes, from schools or big fishes, were located close to the bottom, being then misclassified as bottom.

Wind and wave conditions were fairly good during the data collection, and also given the moderate depths, it was not necessary to apply noise removal.

Since the purpose of the analysis was to investigate the distribution of targets and relate it with environmental variables, the data considered for the post-processing was selected only from 1 nautical mile (nmi) distance from each CTD station, before and after the station. The acoustic analysis was done under the assumption that there is no spatial variation of the environmental data along the 2 nmi considered for analysis.

A volume backscattering coefficient (S_v) threshold of -70 dB applied to all echograms was used during scrutinizing as when exporting the scrutinized data to database, in accordance with the LVFO survey procedures (Everson 2005, LVFO 2009). This setting enabled the elimination of echoes from all the unwanted targets, such plankton and shrimp (*Caridina nilotica*).

Two layers were used to divide the fish echoes in the echograms. A shallower layer was set, generally within the upper 1/3 of the water column (see example Figure 2.2). This upper layer comprised mainly the dispersed echoes from smaller fish. This layer, referred as Dagua layer, was not considered for the analysis.

The other layer included a dense scattering layer of fish. This fish layer can be seen in all the echograms, although with different densities and at distinct depths.

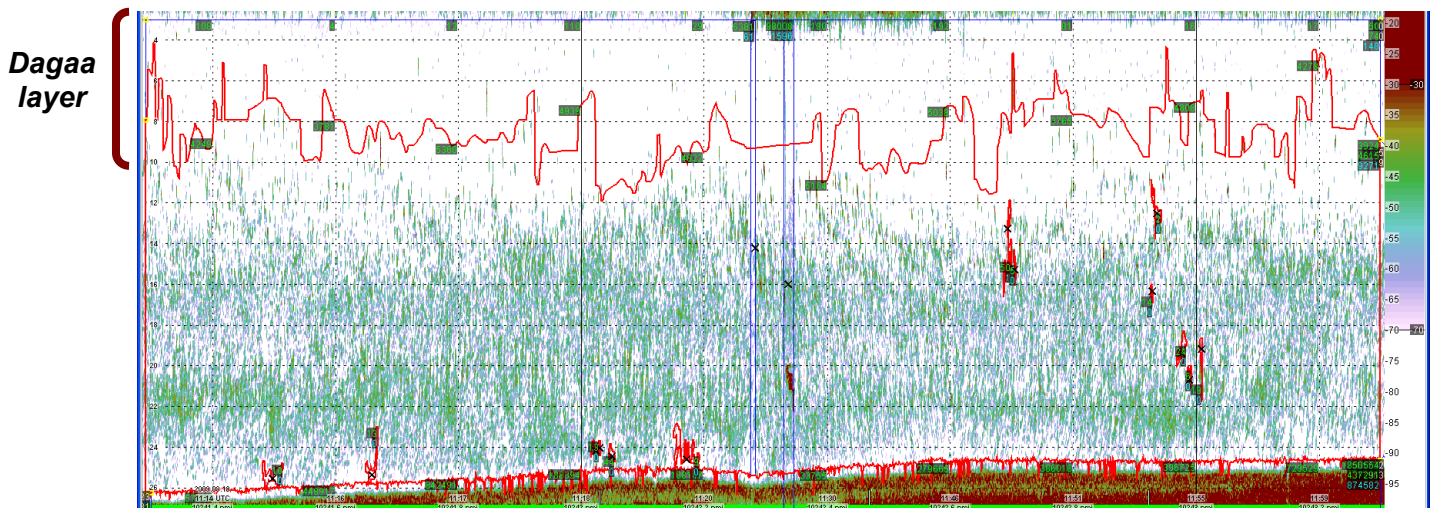


Figure 2.2 – Example of the layers used to divide the water column (Ruega station). The upper layer comprises mostly Dagua and other small targets (the bracket on the left shows the surface layer not included in the analysis).

Relative frequency response $r(f)$ is defined by the equation

$$r(f) = \frac{s_V(f)}{s_V} \quad (1)$$

(Korneliussen & Ona 2002)

and $s_V(f)$ is the volume backscattering coefficient (f) at a reference frequency, 70 kHz in this case. The frequency response of fish in the two layers was used to differentiate the type of fish present, as also the limits between the two fish layers. The type of frequency response of the fish, at 120 kHz differs according to the type of targets as with their size (Pedersen *et al.* 2009). Thus, smaller fish have a more flat frequency response line than bigger fish. Some examples of the frequency response from the upper layers are shown below, figure 2.3.

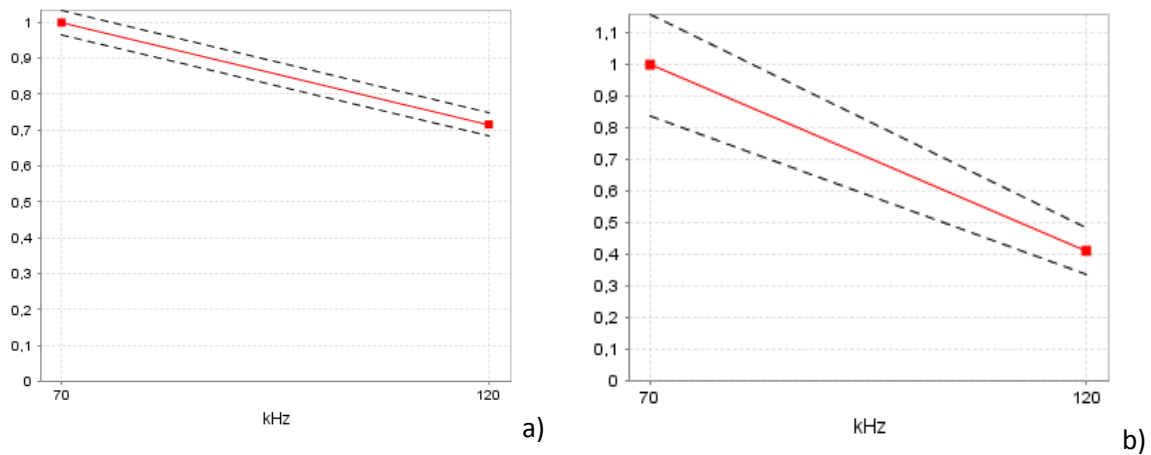


Figure 2.3 – Relative frequency response of targets to the two acoustic frequencies (70 and 120kHz). y-axis shows the ratio between the s_b at the two frequencies. The left figure a) shows the frequency response from smaller targets while the figure from the right b) shows the response from a bigger fish.

Due to the high mixing of fish species, it was not possible to differentiate the two layers basing on only the frequency response. The use of the single target detection mode in the echograms allowed the visualization and identification of the isolated targets. Then, target strength (TS) minimum and maximum detections visible in the echograms were manipulated and set to -80 and -66dB, respectively. This allowed identifying the layer where the smaller and unwanted echoes were concentrated. In one of the stations sampled (Bulamba) the water column was not divided in layers due to the shallow depths and since the mixing of targets was too high to allow visual separation.

An attempt of partitioning the echoes into species was made. However, this procedure was later dropped as only bottom trawl data was available which proved to be little representative for the acoustic recordings. There was no pelagic trawling, targeting the fish layer, as would be desirable; since the bottom trawl was limited to a layer of 3,5 m height from the bottom, the area sampled by the trawl did not correspond most of the times to the layer with dense fish scatters, as will be shown below. Thus, the separation of Nile perch based on the trawl catches was not performed.

The echo-integration has become an important technique for the measurement of fish abundance (Simmonds & MacLennan 2005). The measured “acoustic density”, the s_A values defined as the nautical area scattering coefficient (NASC), are the output from echo-integration. These are proportional to area density of the targets, averaged over a selected distance. The nautical area scattering coefficients exported to data files were averaged in analysis cells of 1 m vertically and 0,1 nmi horizontally. This corresponds to an average of 203 pings in the exported integrator cell.

Both TS and s_A data were exported for the 70 kHz frequency since there is a higher backscattering from fish at this frequency, as obvious from the frequency response measurements.

2.4.2 Target strength analysis

To convert the acoustic echoes into fish densities, the mean target strength of the fish echoes is necessary. Single target data, from the scattering layer close to bottom, was exported with LSSS and the parameters used for the single target analysis are shown in Table 2.2. Table 1 (Appendix VIII) shows an example of an exported TS file.

Table 2.2 – Parameter settings used during TS analysis using the LSSS post processing software.

<i>TS detection menu</i>	
Minimum TS value [dB]	-65
Maximum TS value [dB]	-20
Minimum echo length [relative to pulse length]	0.8
Maximum echo length [relative to pulse length]	1.8
Maximum gain compensation [dB]	6
Maximum phase deviation [phase steps]	8

The information generated from the LSSS includes compensated TS (TS_c) and the range of targets. TS_c was used to calculate the backscattering cross section (σ), through the formula:

$$\sigma = 4\pi 10^{TS_c/0,1} \quad (2)$$

(Ona 1999a)

A mean TS value was then calculated for each station, by

$$TS = 10 \text{Log}_{10} \left(\frac{\bar{\sigma}}{4\pi} \right) \quad (3)$$

(Ona 1999a)

While for the $\bar{\sigma}$ calculation the formula used was

$$\bar{\sigma} = \frac{1}{n} \sum_{i=1}^n \sigma_i \quad (4)$$

The calculation of mean TS was done under the assumption that no variation exists in single targets detected due to vessel and gear avoidance.

Average TS values (\overline{TS}) were also calculated for each meter depth, with the formulas (2), (4) and (3) described above, with the aim of assessing if there was any difference in the mean size of the targets

with depth. The number of TS detections was also averaged for each meter so that it could be compared with the s_v values.

2.4.2.1 Validation of TS measurements

High fish densities can affect and bias the mean TS calculated, since the probability of multiple targets being accepted as single targets increases (Rudstam *et al.* 2003). When several targets appear in the pulse volume, defined by the pulse duration and the beam cross section, the automatic filters in the echo sounder may not work ideally, and multiple targets may be erroneously accepted as originated from one single target. Thus, it was tried to establish a comparison of the mean target strength from the values extracted from the whole fish layer (designated as $TS_{station}$), along the 2 nmi, and some selected boxes with clear single targets ($TS_{selected}$), assumed to be Nile perch (see example in figure 2.4). If the $TS_{station}$ and $TS_{selected}$ did not differ, we assumed that the influence of multiple scatters is negligible in the single target detections.

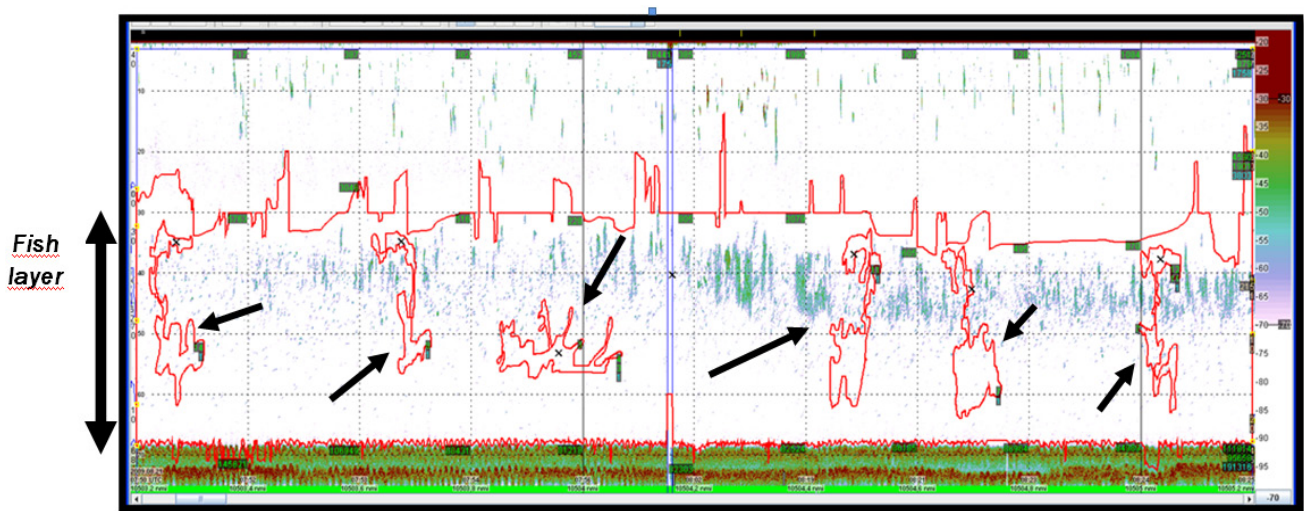


Figure 2.4 – Echogram showing the fish layer (limited with the red line). Black arrows show the areas where Nile perch targets were selected for mean TS calculations (Goziabar NE station). The color scale on the right corresponds to the s_v scale; depth scale is found on the left side and horizontal grids, for this station, are defined for 10 m intervals.

For this procedure, target locations were selected at least in five different locations (in the figure above, six locations were selected) from the echogram area; more than 100 single target detections in each of the selected areas was selected, when possible. In some stations, due to high fish densities, the number of TS detections was lower than 100 per location. The mean TS calculated from these targets ($TS_{selected}$) and the number of TS detections used for this calculation can be seen in Appendix VIII (Table 2). No targets were selected in Kome Channel, Senga, Nafuba and Bulamba since it was not possible to discriminate visually the echo traces. The two following figures show zoomed images of some selected echo traces (Figure 2.5 and 2.6).

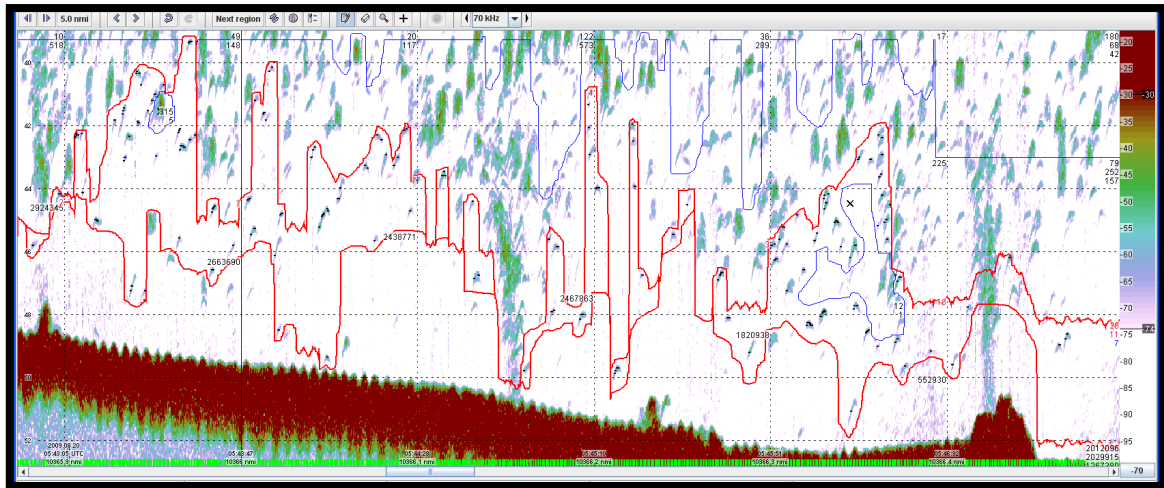


Figure 2.5 – Zoomed echoes from Nile perch (Kamasi Station; 0,6 nmi are shown).

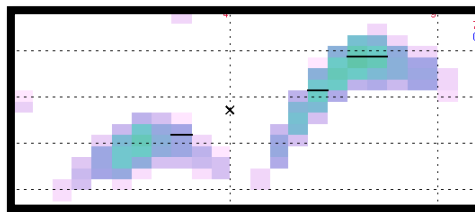


Figure 2.6 – Zoomed echoes from Nile perch (Kamasi Station). The three black lines show the single target detections.

Figure 2.7 show the relative frequency response as the TS distribution from the two fishes from the previous figure.

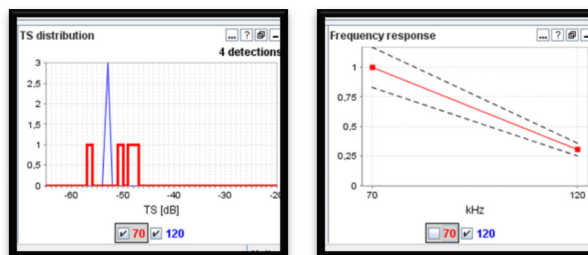


Figure 2.7 – TS distribution and frequency response (from left to right) from the targets seen in fig. 2.6. Left figure: y-axis shows the number of TS detections and x-axis the strength (from -65 to -20, in decibels) of the detections; right figure: y-axis shows the relative frequency response and the x-axis the two frequencies used.

Under the assumption that higher fish densities should reflect on a higher mean TS, the relationship between the mean target strength with depth and the correspondent density of scatters (s_v) was tested. Additionally, high density cells were identified by calculating the number of targets within the acoustic sampling volume (N_v).

$$N_V = \frac{c \tau \psi R^2 \rho_v}{2} \quad (5)$$

(Sawada *et al.* 1993 in Parker-Stetter *et al.* 2009)

c refers to the sound speed (m sec^{-1}), τ to the pulse duration (msec), ψ to the equivalent beam angle (steradians), R to the depth of the targets and ρ_v the fish density by volume. High density cells are defined by Parker-Stetter *et al.* (2009), based on previous studies for the North American Great Lakes, as cells with N_V higher than 0,1 being thus excluded for TS calculations.

Other procedure was used to calculate the mean TS for the sampling stations (referred as mean TS_{Trawl area}). This procedure was done only in the locations where bottom trawl was performed. TS was calculated repeating the procedure done for the whole water column, but including only the single target detections from the bottom trawl path, ie, 3m from the bottom. This was done with the objective of investigating the relative contribution of other fish species for the TS detections, besides Nile perch, and was based on the assumption that bottom trawl hauls reflect the fish abundance.

Even if the trawl data is not representative of the fish biomass, it is likely that it still reflects the species composition in the trawl area. As such, TS_{Trawl area} of each station was compared, being that the trawl data showed variations in the trawl catches between 2 and 98 % of Nile perch. This was done based on the assumption that stations with higher proportion of Nile perch would have a higher mean TS value.

2.4.3 Density calculations

Mean s_A values (6) and standard error (7) were calculated for each pelagic channel. The pelagic channels generated in the reports, output from the LSSS, were defined for 1 m depth.

$$\bar{x} = \frac{1}{n} \sum_{i=1}^n x_i \quad (6) \quad \text{Std. Error} = \frac{s}{\sqrt{n}} \quad (7)$$

where n is the number of samples and s the sample standard deviation.

Since in some of the stations there was a steep bottom, such as in Maisome and Kamasi, the number of samples considered for the calculations was reduced in these stations. For the calculations of the mean s_A , only the samples that had a number of pelagic channels $\pm 3\text{m}$ from the CTD location were considered. Therefore, for Maisome only 1nmi, before the CTD sampling, was included for the mean s_A calculations while for Kamasi the distance considered was 0,6 nmi before the CTD sampling.

Fish densities were calculated from the s_A values, generated from the LSSS reports, under the assumption that there was no variation in fish densities as a result of vessel movement or gear avoidance.

The nautical area scattering coefficient (s_A , [$m^2 \text{ nmi}^{-2}$]) was first converted to area scattering coefficient (s_a , $m^2 \text{ m}^{-2}$), since

$$s_A = 4\pi (1852^2) s_a \quad (8)$$

(Simmonds & MacLennan 2005)

The area backscattering coefficient quantifies the energy returned from the water column, between two depths (Δz) (Simmonds & MacLennan 2005). It is also the integral of s_v (volume backscattering coefficient) within the same depth. The volume backscattering coefficient was calculated as

$$s_v = \frac{s_a}{\Delta z} \quad (9)$$

(Ona 1999a)

The area (ρ_A) and volume (ρ_v) fish densities were calculated, dividing the area scattering coefficients by the mean backscattering cross section (σ), through the use of the equations, respectively

$$\rho_A = \frac{s_A}{\sigma} \quad (10)$$

$$\rho_v = \frac{s_a}{\sigma} \quad (11)$$

(Ona 1999a)

2.4.4 Limnological data analysis

Oxygen, chlorophyll, temperature and conductivity measurements were averaged for each meter (approximately 3 measurements per meter were taken), using the following formula:

$$\bar{x} = \frac{1}{n} \sum_{i=1}^n x_i \quad (6)$$

CTD depth profiles were plotted using Statistica 8.0 software and averaged for each stratum for graphical illustration and statistical analysis.

2.4.5 Biological data analysis

The high fish density and the mix of the species in the same layer of the water column, made impracticable to separate the echoes visually. Trawl data was not used for separating the fish echoes as mentioned, which will be discussed later.

As described in the biological sampling, length data was collected for Nile perch individuals. The length frequency was plotted for each station and the root mean square length (RMSL, in cm) was calculated (Ona *et al.* 2001 in Ha 2008).

$$RMSL = \sqrt{\frac{\sum n_j L_j^2}{\sum_{i=1}^n n_j}} \quad (12)$$

The backscattering cross section (σ) relates to the acoustic properties of the target reflected at a certain frequency, while the target strength (TS) is the logarithmic conversion of the backscattering cross section, expressing the size of the echo (Simmonds & MacLennan 2005; Horne 2000). The relationship between the TS and the fish total length (TL, in cm) is described mathematically (equation 13), assuming that the backscattered sound is proportional to the reflecting organs which depend on the fish size (MacLennan 1990; Horne 2000).

$$TS = m \text{Log}_{10} (TL) + b_{20} \quad (13)$$

where m is approximate to 20 according to Foote (1987). The b_{20} is a constant relating the fish length to the target strength (Simmonds & MacLennan 2005) and for Nile perch this value is -66, according to Getabu *et al.* (2003). The stock of Nile perch in Lake Victoria have been monitored, using acoustic methods, twice a year. The relation between fish length and target strength published for Nile perch is

$$TS = 20 \text{Log}_{10} (RMSL) - 66 \quad (14)$$

This relation was established based on cage experiments with Nile perch with a 120 kHz transducer (Getabu *et al.* 2003). In the recent surveys a new relationship has been in use. The equation shows the following relation between fish length and TS: $TS = 29,9 \text{Log}_{10} (TL) - 79,3$ (15) and was calculated using the deformed cylinder model (LVFO 2009). Another relation has been developed more recently, based on *in situ* target strength and trawl data, as $TS = 30,2 \text{Log}_{10} (TL) - 84,6$ (16)

(Kayanda 2010, unpublished data). The distribution of the target strength regressed against the logarithm of the fish length, for the described TS-TL equations can be visualized in Figure 2.8.

Variation of fish target strength with total length

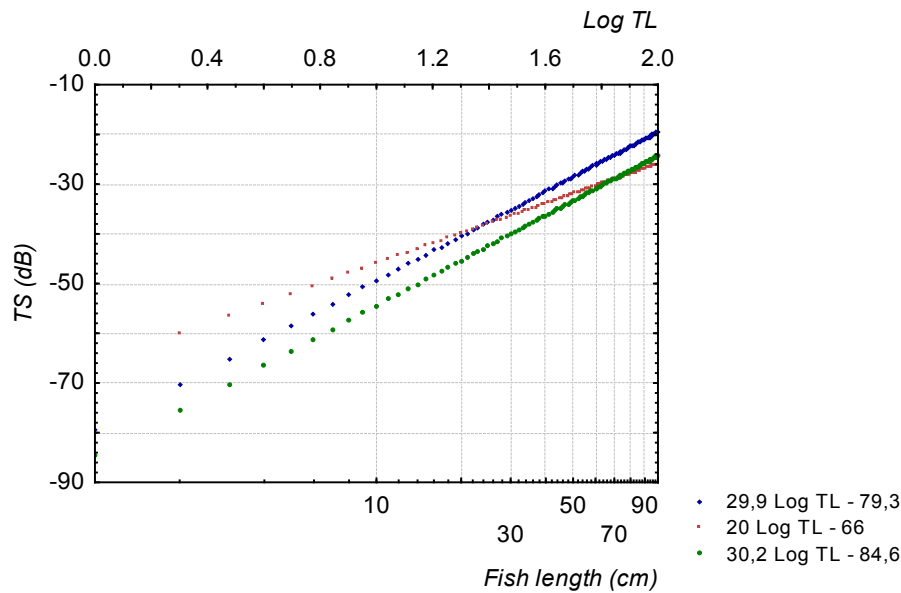


Figure 2.8 – Variation of the fish target strength with fish length for the three equations describing the TS-TL relation for Nile perch. Blue dots show the relation for the equation $TS = 29,9 \text{ Log TL} - 79,3$; red dots show the data for $TS = 20 \text{ Log TL} - 66$; and green points for $TS = 30,2 \text{ Log TL} - 84,6$.

The adoption by any of the three models, describing the relation between the size dependence of target strength, does not have an influence in the results discussed. The importance for such equations is mainly to provide a more familiar measure to the reader, by referring then to a size measure of fish other than to its intensity of backscattered echo.

A faster increase in TS with fish length has been suggested for physoclist species, such as cod. These models were however based on *ex-situ* experiments and a decrease in the slope was suggested for the wild (MacLennan 1990). 20Log L dependence of TS is suggested by Foote (1987) for physoclist fish species in wild. The eq. 14 was thus used for describing the TS-TL relation. Despite the TS model (eq. 14) was derived from experimental evidences on a 120 kHz transducer, Godlewska *et al.* (2009) suggested that there is no differences in the TS measured by 70 and 120 kHz transducers. Thus, data was exported at 70 kHz under this assumption.

From the RMSL of the Nile perch individuals, \overline{TS} was calculated for each station ($TS_{\text{Trawl catches}}$). Mean TS values, calculated from bottom trawl hauls as from the acoustic data were plotted for all stations.

Fish biomass was calculated for each trawl station according to the procedures described in the Standard Operation Procedures for Bottom Trawl surveys, for Lake Victoria (Agnew 2005). The area swept by the trawl ($A_{i,j}^{sw}$, nmi²) was calculated by

$$A_{i,j}^{sw} = V_{i,j} t_{i,j} h_{i,j} \chi \quad (17)$$

$v_{i,j}$ is the towing speed of the vessel (nmi h⁻¹) at haul j of stratum i , $t_{i,j}$ is haul duration in hours, $h_{i,j}$ is the head rope length (m), χ is the correction factor standardized as 0.33 (Ligtvoet *et al.* 1995). The weight density (kg nmi⁻²) of all the species from haul j of stratum i is obtained through the formula

$$D_{i,j} = \frac{W_{i,j}}{A_{i,j}^{sw}} \quad (18)$$

$w_{i,j}$ is the total weight from the haul (kg) and $A_{i,j}^{sw}$ the trawl swept area.

The theoretical catch was also calculated from the acoustic densities, so that it could be compared with the catches from the bottom trawl. The estimated catch (number per haul) was calculated by

$$C = \rho_{Trawl} A_{i,j}^{sw} \quad (19)$$

(Ona 2009)

where ρ_{trawl} refers to the acoustic fish densities (fish number nmi⁻²) from the trawl path, 3 m above the bottom. In order to transform the catch to weight, the mean weight for the fish used for the calculations was 10 g. This value was estimated since there was no collection of length-weight data neither for Nile perch nor for the other species captured.

2.5 Statistical analysis

Graphical representations of the results were done using Statistica 8.0 software system (Stat Soft, Inc) and PASGEAR data base package (Pasgear II clx, version 2.4; Kolding & Skålevik). Data was grouped by strata (Inshore, Coastal, Deep) for plotting and for statistical analysis. The division within strata was done according to the LVFO acoustic survey procedures. Data from the Emin Pascha Gulf and from Speke Gulf were included in the inshore stratum.

Statistical analysis was done using Statistica 8.0 software system. Since the variables showed to not follow a normal distribution, non parametric statistical analysis were used to test the hypotheses. With the aim of testing if there was a relation between the limnological parameters and both fish

densities as size of targets, the independent variables selected to be tested were the mean values of oxygen, chlorophyll a and temperature. The depth was also added as independent variable in order to rank its relation with the targets' distribution. Target strength (TS) and fish density (ρ_v) were tested as dependent variables.

The correlation of the different limnological factors on the fish densities and the respective TS was tested by using Spearman's rank correlation. This test was used to test the correlation between fish density and TS with depth and limnological parameters (oxygen, chlorophyll and temperature). TS and fish densities, averaged for each meter depth were used for this test. The tested null hypotheses were:

- I. H_0 : There is no relation between fish density and the tested variables.
- II. H_0 : There is no relation between the fish size (seen through TS) and the tested variables.

The null hypothesis were rejected when $p < 0.05$.

With the aim of testing if there was an effect of strata on the fish densities and size of targets, these were selected as independent variables. TS and ρ_v were tested as the dependent variables.

Kruskal-wallis Anova was used to test if there was a difference in fish density or in the mean size of targets, in function of strata. The average TS and density values for each CTD station were used to test the hypotheses. The null hypotheses tested were:

- III. H_0 : There is no difference in fish density for the three strata.
- IV. H_0 : There is no difference in fish size (seen through TS) in the three strata.

3 Results

3.1 Limnological data analysis

The CTD variables show distinct features with depth at each of the locations sampled. Mean oxygen, temperature and chlorophyll, calculated for the water column for each stratum, are shown in figures 3.1 to 3.3. Mean values calculated for all CTD stations can be consulted in Appendix V (Table 1).

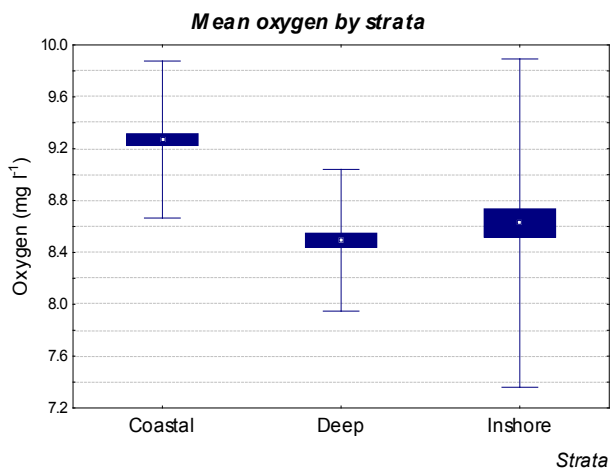


Figure 3.1 – Mean oxygen (with standard error and standard deviation) level for each stratum. Values averaged for the water column.

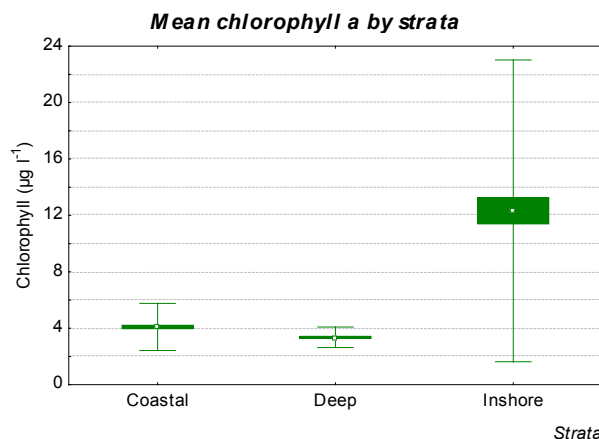


Figure 3.2 – Mean chlorophyll *a* level (with standard error and standard deviation) for each stratum. Values averaged for the water column.

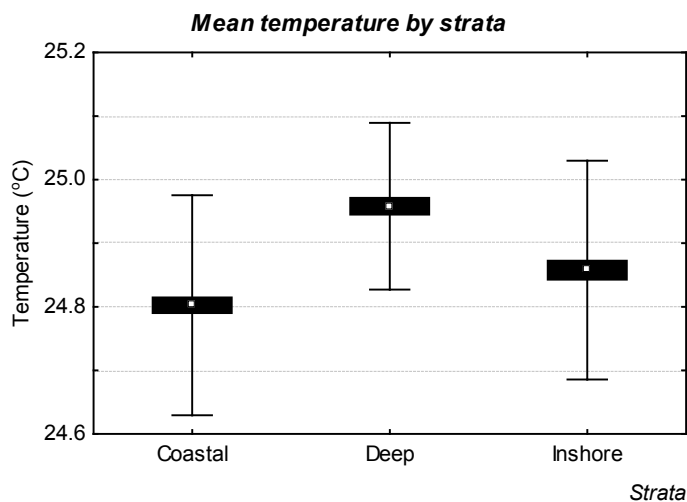


Figure 3.3 - Mean temperature (with standard error and standard deviation) level for each stratum. Values averaged for the water column.

The mean values shown were calculated from the depths where exist observations on fish density or single target detections; i.e., only the CTD data from the depths where Nile perch targets were found was included since only this data was used to relate with fish densities and sizes.

The highest mean oxygen levels are observed in the coastal stratum, followed by inshore. Strata showed to have a statistical relation ($p=0,000$) with oxygen level. When analyzing the variation between two strata, the deep and inshore did not show a statistical significant difference ($p=0,051$). When comparing the coefficient of variation from all the strata, it is observed that the inshore stations show a larger variation over the water column (Table 2 in Appendix V); moreover, there is also a big variation in the oxygen levels between the stations included in the stratum. In regards to mean chlorophyll *a*, values observed in the inshore stations are higher than in the other strata (Figure 3.2; see Table 3 in Appendix V). A significant difference in mean values ($p=0,000$) between the three strata is found. The coefficient of variation for chlorophyll *a* is higher in inshore stations, followed by the coastal stratum. In the deep stations the mean temperature is higher (Figure 3.3) and there is a significant difference ($p=0,000$) among strata. The difference in temperature ranged 0,15 °C between deep and coastal stations, where the higher and lowest temperatures were recorded, accordingly. The overall variation of the temperature over the water column is small for each stratum; the maximum variation was 1,3 % and was observed in the upper 10 m from the inshore stratum (Table 3, Appendix V).

The limnological parameters profiles, averaged for each stratum, are shown in figures 3.4 to 3.6. The vertical distributions of the limnological data differ within the CTD sampling locations; profiles for each of the station can be consulted in Appendix V (Figures 1 to 17).

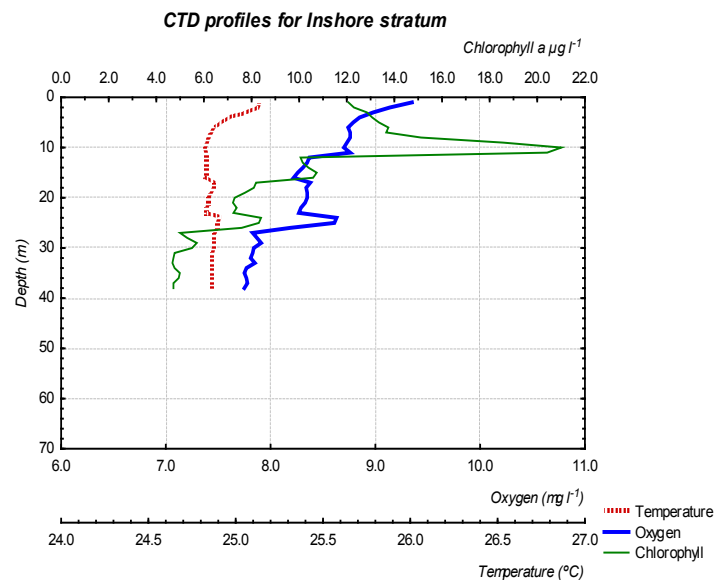


Figure 3.4 – CTD profiles of inshore stratum (values averaged from the inshore stations).

In the Inshore stratum, the oxygen levels are higher in the layers close to the surface. There is a gradual decrease of the oxygen level over the water column; a small increase is observed around 25

m depth. Chlorophyll *a* also shows a decreasing trend over the water column, however there is a peak in the chlorophyll *a* level from 8 to 10 m. This peak is explained by the values from two sampling locations, Kome and Senga, where the chlorophyll level reached values of 46 and 70 $\mu\text{g l}^{-1}$, respectively. In inshore stations, only three locations have a maximum depth over than 25 m (Ruega, Bumbure and Makibwa); the variation of the chlorophyll *a* on the shallower stations is considerably bigger when compared with the deeper stations. Data on temperature does not show a big variation along the water column; even though, it is in the surface where the biggest variations are seen (ranging from 24,5 to 26,2 °C in inshore stations).

CTD profiles for coastal stratum are displayed in figure 3.5.

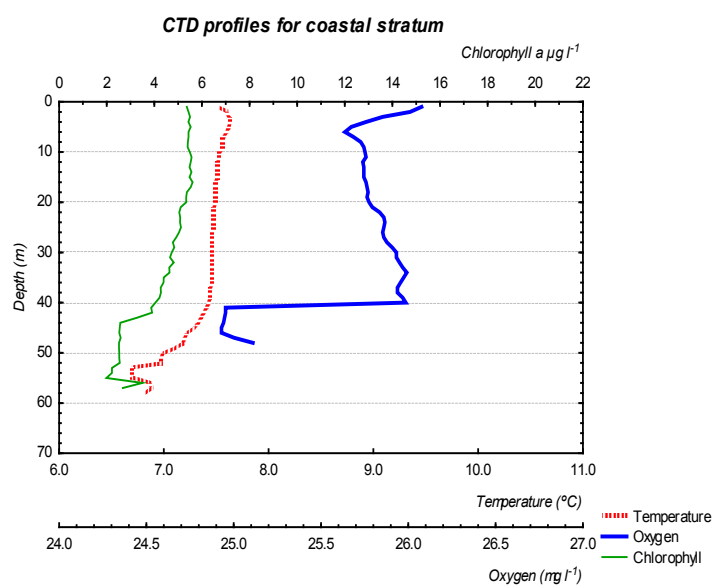


Figure 3.5 – CTD profiles of coastal stratum (values averaged from the coastal stations).

In the coastal stratum, there is a decreasing trend of the oxygen level, up to approximately 5 m depth, from where there is an overall increase until the 40 m depth. This is observed in most of the CTD stations but with some divergence below 40 m depth. Chlorophyll *a* show a decreasing trend, relatively constant over depth. At 42 m depth there is a more abrupt decrease followed by an increase at 55 m; this variation is due to a sudden decrease in the chlorophyll *a* values in Miendere station, at that depth. Temperature values do not show major differences over the water column, as seen in the figure 3.5; however, a small decrease in temperature, below 40 m is seen in the graph and is observed due to a decrease (0.3 °C) between 40-50 m in three of the coastal stations (Miendere, Cherenche and Bumbire).

CTD profiles for the deep stratum are shown in figure 3.6.

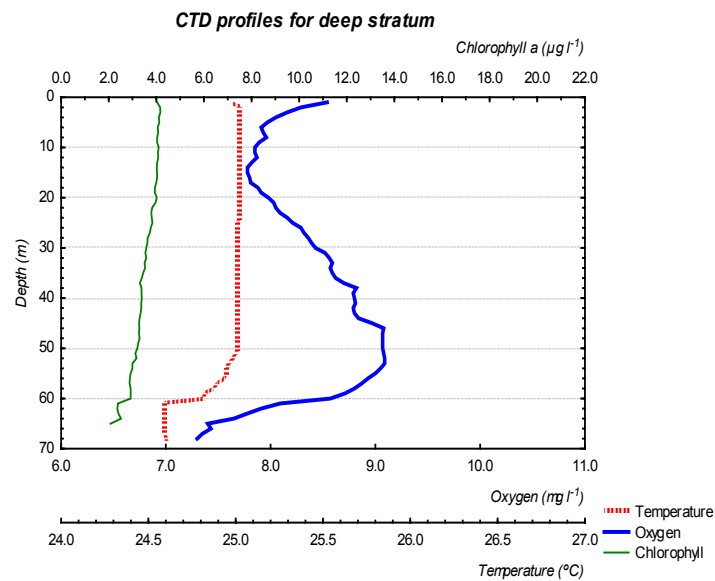


Figure 3.6 - CTD profiles of deep stratum (values averaged from the deep stations).

The data shown from the deep stratum correspond to two sampling stations (Kamasi and Gozibar). The oxygen pattern over the water column is similar in the two stations, with a first decrease in the oxygen level, followed by an increase until 45 m approximately; below 45 m, there is a different pattern in the two stations, since the oxygen stabilizes in Kamasi but decreases sharply in Gozibar. Chlorophyll *a* levels vary from 4,1 to 2,4 $\mu\text{g l}^{-1}$, with a constant decrease over the water column. In temperature there is no big variation over depth. Only for one of the stations (Gozibar), there is a decrease from 50 until the 60 m (from 25,0 to 24,6 $^{\circ}\text{C}$), which can be seen in the graph.

3.1.1 Correlation between oxygen, chlorophyll *a*, temperature and depth

The correlation between the limnological variables, as their relation with depth, was tested with Spearman Rank correlation test for each stratum (see Table 1, Appendix VI). For the inshore stratum, no relation between depth and temperature was found ($p=0,119$). Also, no correlation was observed between temperature and chlorophyll *a* ($p=0,133$), for the same strata. All the other variables showed a statistical significant correlation in inshore stations; in the coastal stratum, temperature and depth were the only variables that did not show relation with oxygen (0,073 and $p=0,134$); in the deep stratum, correlation was found between all the variables tested.

3.2 Target strength analysis

Figure 3.7 show the distribution of the detected single targets along the 2 nmi sampled, for each CTD station. The TS distribution varies among stations, alternating between uni and bimodal distribution.

The number of TS detections in each station differs also from station to station (see Apendix VIII, Table 2).

Frequency distribution from the TS detections for each station

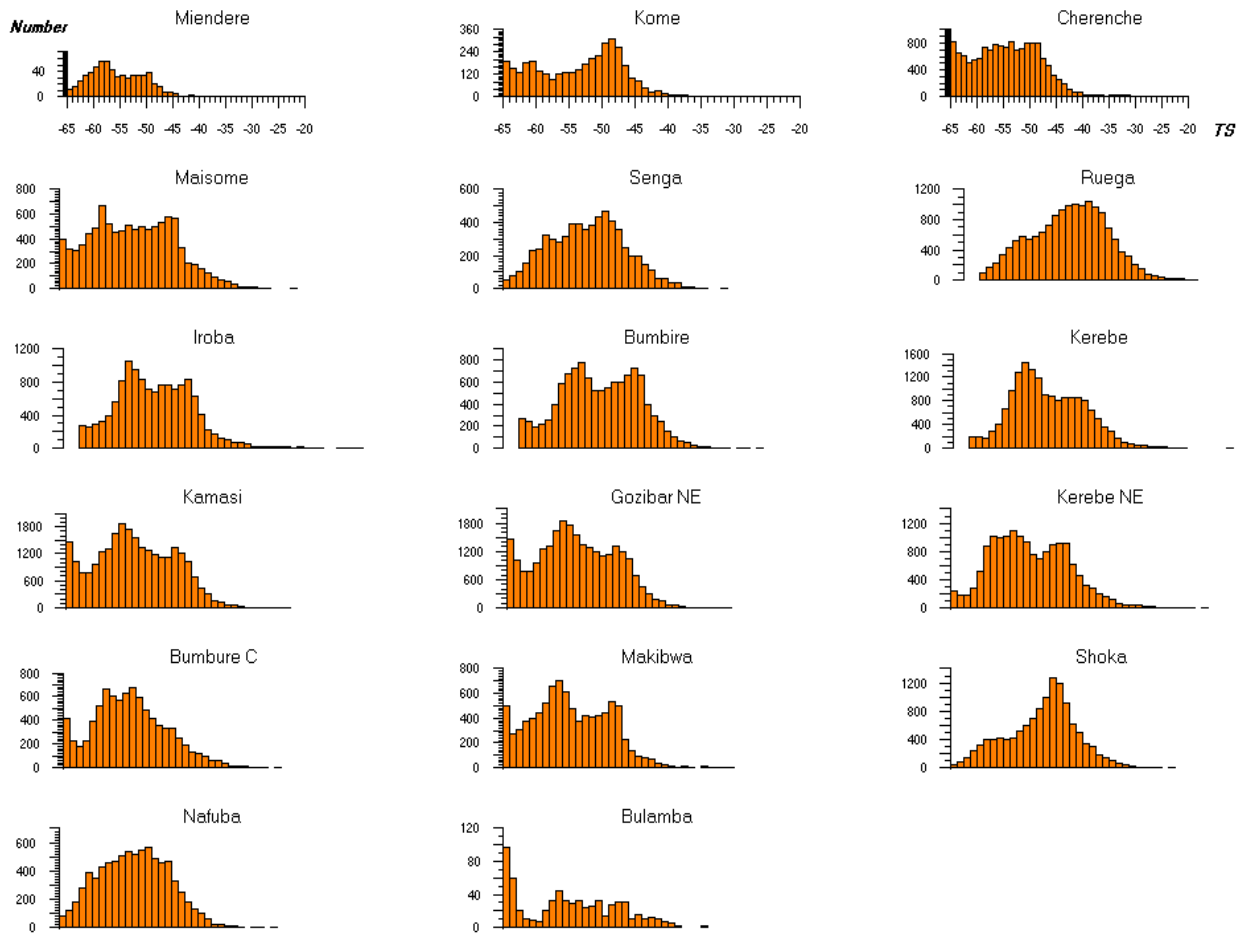


Figure 3.7 – Number of observations of targets distributed by target strength intervals. Y axis shows the number of TS observation and the x axis the target strength (in dB). Note: the y scale is not the same for all graphs; TS (x axis) scale from -65 to -20dB shown only in graphs from 1st row.

3.2.1 Validation of the TS measurements

The contribution of multiple targets for the single target detections was evaluated through the combination of the procedures described in the material and methods section.

Mean target strength calculated for each station

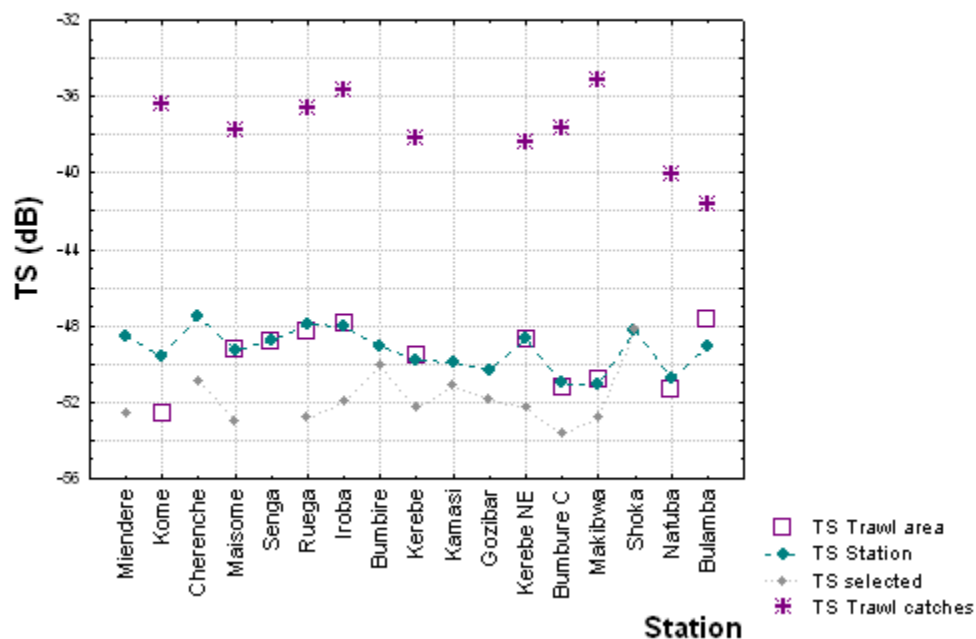


Figure 3.8 – Mean target strength calculated for each CTD station through the 3 different procedures. $TS_{Station}$ was calculated from the data from the entire water column; $TS_{Trawl\ area}$ show the mean TS calculated, for trawl stations, from the TS data on the trawl path (3m from the bottom); $TS_{Selected}$ represent the mean TS from selected Nile perch targets; $TS_{Trawl\ catches}$ show TS back-calculated from trawl catches.

The calculations of the mean TS, from the selected echo traces of Nile perch, are shown in the graph ($TS_{Selected}$). These values are lower comparing with $TS_{station}$ values, with differences from 0 up to 5 dB (Shoka and Ruega, respectively). The highest $TS_{Selected}$ is -48,18 dB (Shoka) while the lowest is -53,67 dB (Bumbure C). The distributions of $TS_{station}$ and $TS_{Selected}$ can be consulted in Appendix XI (Figures 1 to 26). Most of the stations showed a similar frequency distribution from the TS data, from $TS_{station}$ and $TS_{Selected}$. Maisome, Gozibar and Kerebe NE are the stations that show some differences in the distribution; an increase in the number of bigger targets is seen in $TS_{station}$.

The comparison of mean TS from $TS_{Station}$ and $TS_{Trawl\ area}$ was done to assess the relative contribution from other fish species besides Nile perch to the single target detections (Figure 3.8). In most of the locations mean $TS_{Trawl\ area}$ was approximate to the $TS_{Station}$. However, in Kome there is a smaller TS value (difference of -1,60 dB) in the mean $TS_{Trawl\ area}$.

Results from the Sawada equation and correlation between fish density and TS were combined. In most of the sampling stations there were analysis cells with $N_v > 0,1$ (percentage of cells with $N_v > 0,1$ ranged from 7 to 49 %). Correlation between TS and fish densities was found significant ($p < 0,05$) for 7 stations sampled (see Appendix XI, Figure 27).

Kome was one of the stations with a significant relation between fish density and TS; however, the calculation of N_v revealed that in this station there were no cells with high fish density. On the other hand, high fish densities are observed in Ruega, both seen in the echogram and from the number of cells with $N_v > 0,1$ (from 13 up to 26 m all the cells have $N_v > 0,1$); in this station however, no correlation is found between TS and densities. A figure showing number of targets within the beam volume (N_v) plotted against TS follows (Figure 3.9).

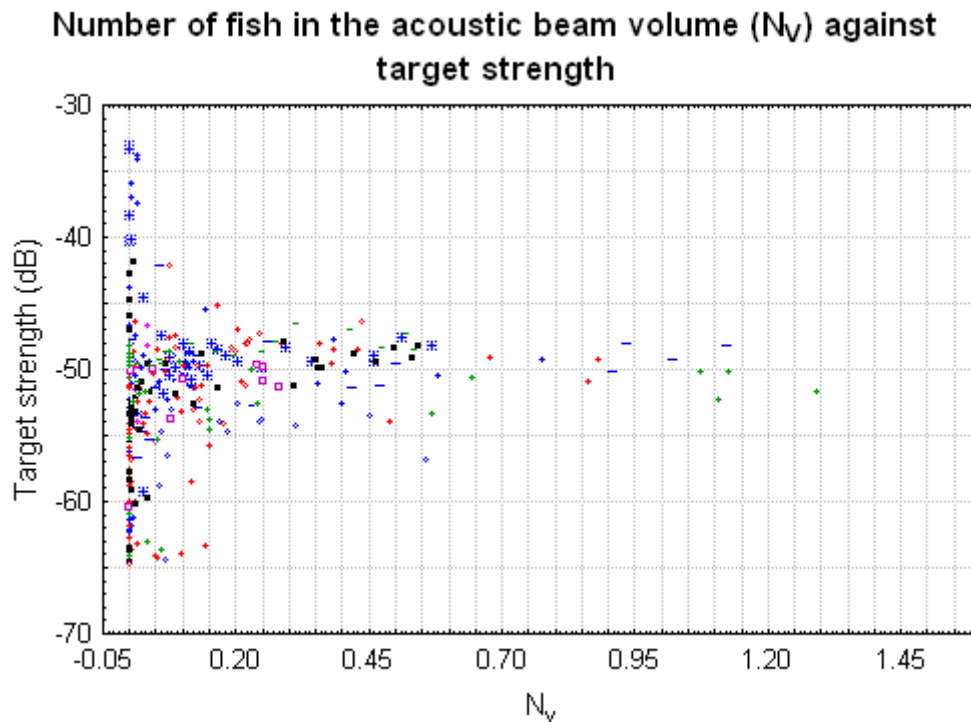


Figure 3.9 – Target strength (in dB) in function of the number of fish in the acoustic beam (N_v). Graph includes data from all stations.

No apparent relation can be identified between TS and fish densities from the graph. All the bigger targets (> -45 dB) were found at fish densities below the limit applied in Rudstam *et al.* (2003).

3.2.2 Target strength distribution

The estimated mean target strength ($TS_{Station}$), calculated for each sampling station, ranged from -47,25 dB (Cherenche) to -51,05 dB (Makibwa) (Figure 3.8). Table 2 in Appendix VIII show the mean TS values for each station, with the three methods used, as well as the TS values back-calculated from the trawl catches ($TS_{Trawl\ catches}$). The mean TS values for the bottom trawl stations were back-calculated from the trawl catch data ($TS_{Trawl\ catches}$) and values range from -35,15 dB (Makibwa) to -41,66 dB (Bulamba). The comparison between the $TS_{trawl\ catches}$ and $TS_{Station}$ show a discrepancy in the mean TS values of around 10 dB.

The mean target strength shows a distinct pattern, over depth, for the three strata (Figure 3.10-3.12).

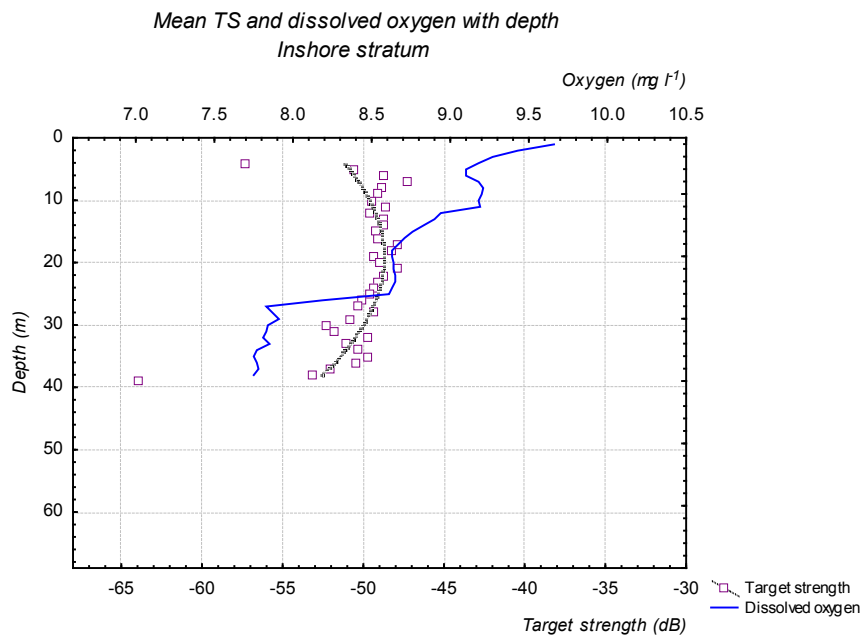


Figure 3.10 – Variation of TS and oxygen with depth for the inshore stratum. A second order polynomial trend was fitted to the TS data.

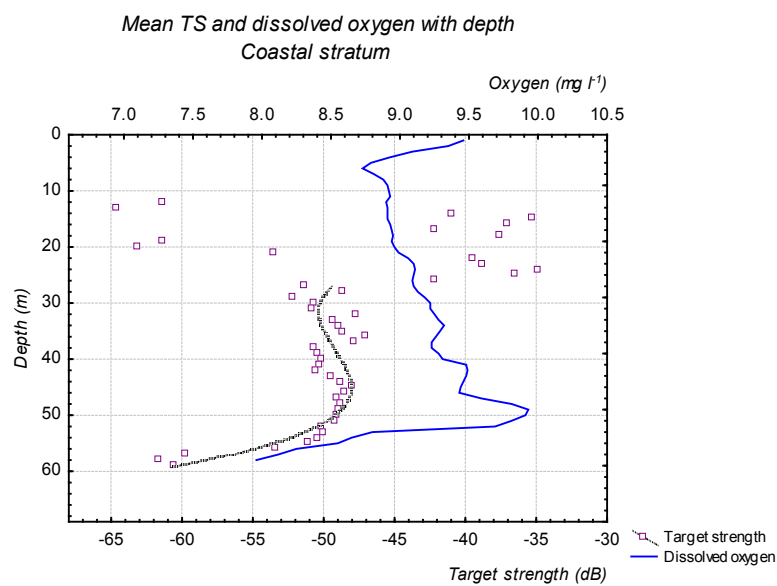


Figure 3.11 – Variation of TS and oxygen with depth for the coastal stratum. A third order polynomial trend was fitted to the TS data.

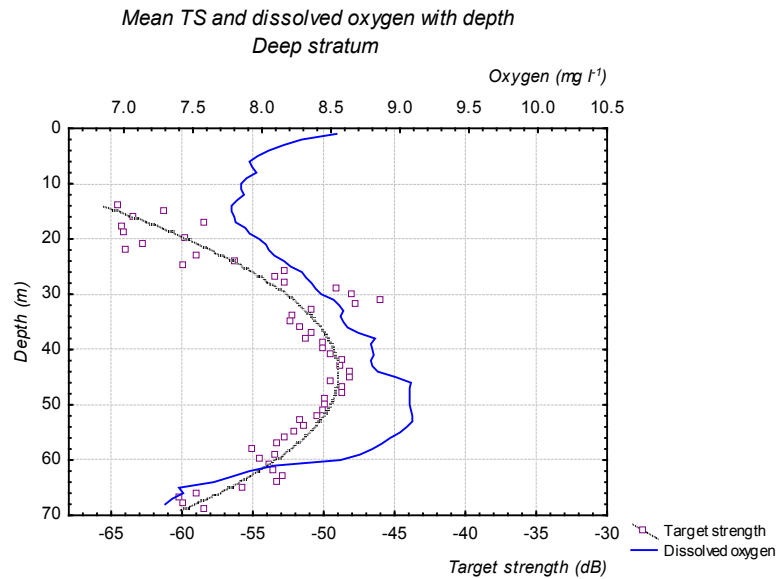


Figure 3.12 - Variation of TS and oxygen with depth for the deep stratum. A second order polynomial trend was fitted to the TS data.

In the inshore stratum, the majority of TS are between -53 to -47 dB. TS distribution graphs for each station, can be consulted in Appendix IX (Figures 1 to 17); in most of the stations, a higher standard error in the target size is found in the upper areas of the fish layer.

In the coastal stations (Figure 3.11) there is a big variance in the mean TS for depths above 35 m approximately; most of the fish detections for these stations are distributed beyond 27 m depth and deeper than 30 m depth, a 3rd order polynomial trend can be identified in the TS distribution. There is a decreasing trend in the TS up to 45m, followed by an increase until 55 m and a subsequent decrease. In the deep stratum, the majority of TS range between -65 to -46 dB.

In the deep stations (Kamasi and Gozibar), most of TS detections distribute from 25 m until 50 m. A unimodal pattern can be observed in the TS distribution from the deep stratum, with an inflection at 45 m depth; the mean TS range from -60,2 to -47,1 dB.

A comparison of the mean TS for the three strata is illustrated in Figure 3.13. TS values calculated for the two Gulfs – Emin Pasha and Speke – can also be seen in the graph. Note that these two are included in the inshore stratum as well.

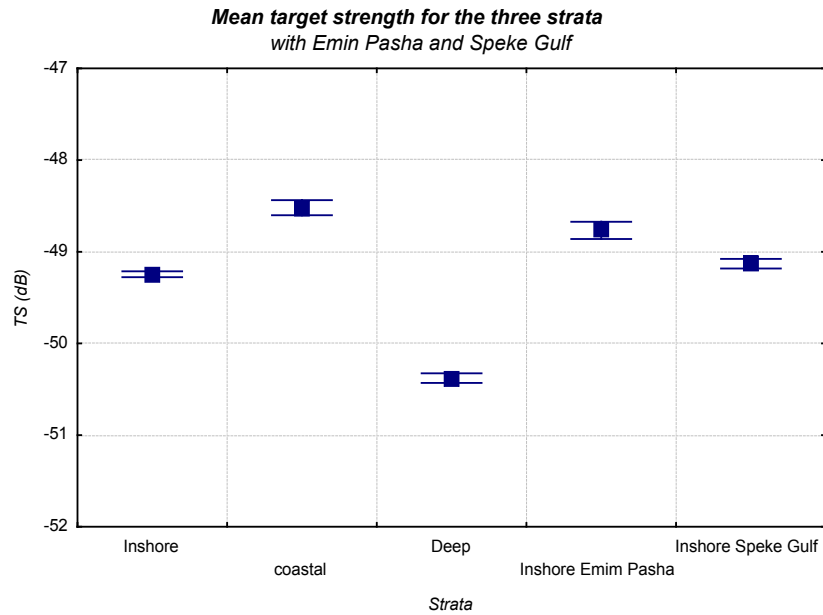


Figure 3.13 – Mean TS (in dB, with standard error) calculated for each stratum. The TS calculated for the two Gulfs – Emin Pasha and Speke – is also represented separately.

The mean size of the targets shows to differ significantly with strata ($p=0,003$, see section 8.4, Appendix VIII for statistical analysis results). Coastal stations have, on average, bigger targets while deep stations have smaller fish.

3.3 Relation between limnological factors and mean TS

3.3.1 Oxygen

TS values, combined from all the stations, were grouped in $0,5 \text{ mg l}^{-1}$ oxygen intervals (Figure 3.14). In the graph is possible to observe a positive trend of the target strength with an increase of oxygen level ($p=0,000$). However, in the first oxygen interval (from $6,5$ to $7,0 \text{ mg l}^{-1}$) the TS values found are relatively high, contrasting with the observed trend. The mean TS values included in this interval are all from one single station - Shoka (located in Speke Gulf); this was the location with the lowest oxygen averaged for the water column (see Table 1 in Appendix V).

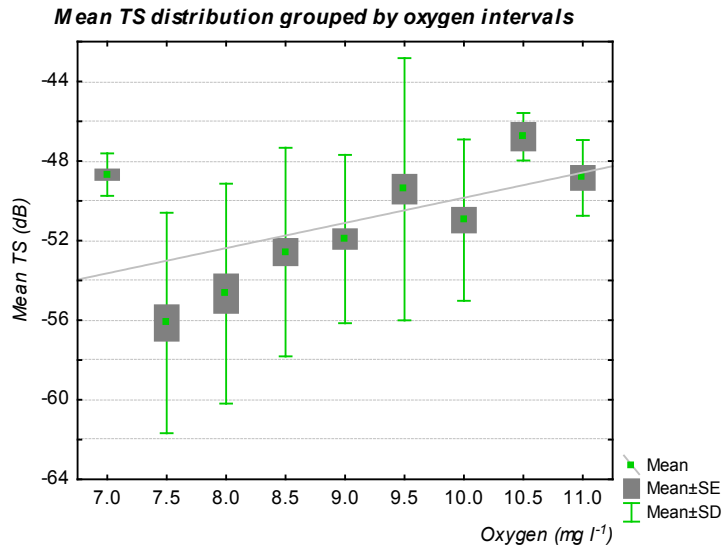


Figure 3.14 – Mean TS data (with standard error and standard deviation), for all the stations, grouped by oxygen intervals (intervals of 0,5mg l⁻¹).

When separating the data by strata, the trends observed correspond to the one seen in figure 3.14. There is an increasing tendency of TS with the increase of oxygen, in all strata (figure 3.15 to 3.18).

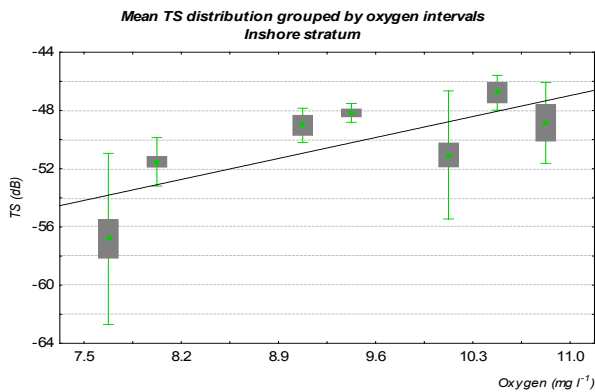


Figure 3.15

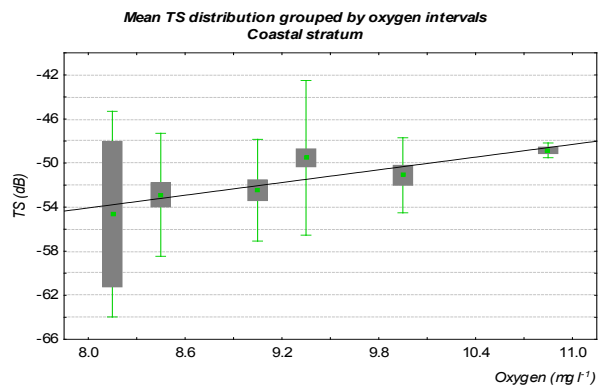


Figure 3.16

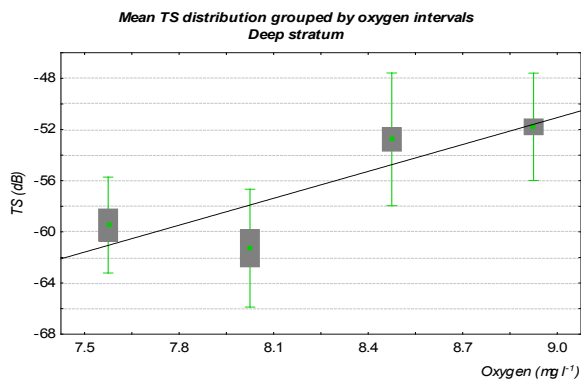


Figure 3.17

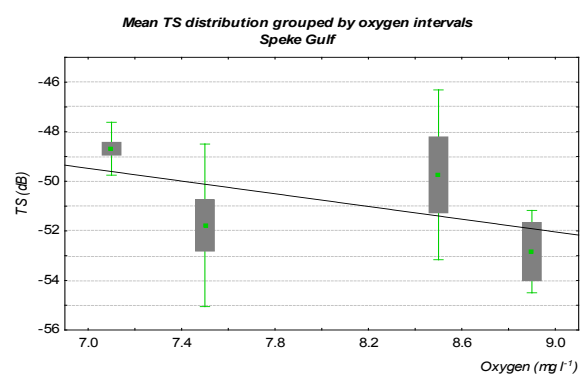


Figure 3.18

Figure 3.15-3.18 – Mean TS data (■) (with standard error [■] and standard deviation [⊥]) grouped by oxygen intervals. Graphs correspond to inshore, coastal deep strata and Speke Gulf, accordingly.

The relation between oxygen level and the size of the targets is found to be statistically significant when testing for the three strata ($p=0,022$, $p=0,043$, $p=0,000$: inshore, coastal and deep strata, respectively).

Stations from Speke Gulf (Shoka, Nafuba and Bulamba) showed the lowest mean oxygen content from all the stations sampled. This was the grounds for plotting separately the data from the 3 stations located in this Gulf (Figure 3.18). Speke Gulf data show an opposite tendency in the TS relation with oxygen when comparing with the other strata.

3.3.2 Chlorophyll *a* and temperature

TS values were plotted in function of chlorophyll *a* for the three strata (see Figures 1 to 4 in Appendix X); the data shows a distinct variation pattern for each. When all stations are plotted together, a trend in the data is not easily identified; however, a significant correlation between chlorophyll *a* level and TS is found ($p=0,003$).

In the coastal stratum, there is a slight positive tendency in the TS distribution with the increase of chlorophyll ($p=0,000$); while, in inshore stations there is a negative, non significant ($p=0,950$), trend in the TS distribution when the chlorophyll level goes above $25 \mu\text{g l}^{-1}$; in deep stations, the TS showed an increase up to $3 \mu\text{g l}^{-1}$ chlorophyll level, after which decreased ($p=0,008$). When grouping target sizes in function of temperature it is not possible to observe a pattern in data distribution (Appendix X, Fig. 6 to 9). In accordance, no statistical correlation is found from Spearman rank correlation test, for any strata.

1.1 Fish density distribution with depth

Fish distribution have distinct patterns over the water column among the stations sampled. Figures 3.19 to 3.21 show the mean target strength, the area backscattering coefficient ($\text{m}^2 \text{m}^{-2}$), the number of TS detections and the oxygen variation over depth; these are shown for the inshore, coastal and deep strata, accordingly. Similar graphs, done for each station sampled, can be consulted in Appendix IX (Figures 1 to 17).

When comparing the area backscattering coefficient (s_a) from the three strata, a clear distinction of the inshore stratum, with higher s_a values, can be identified.

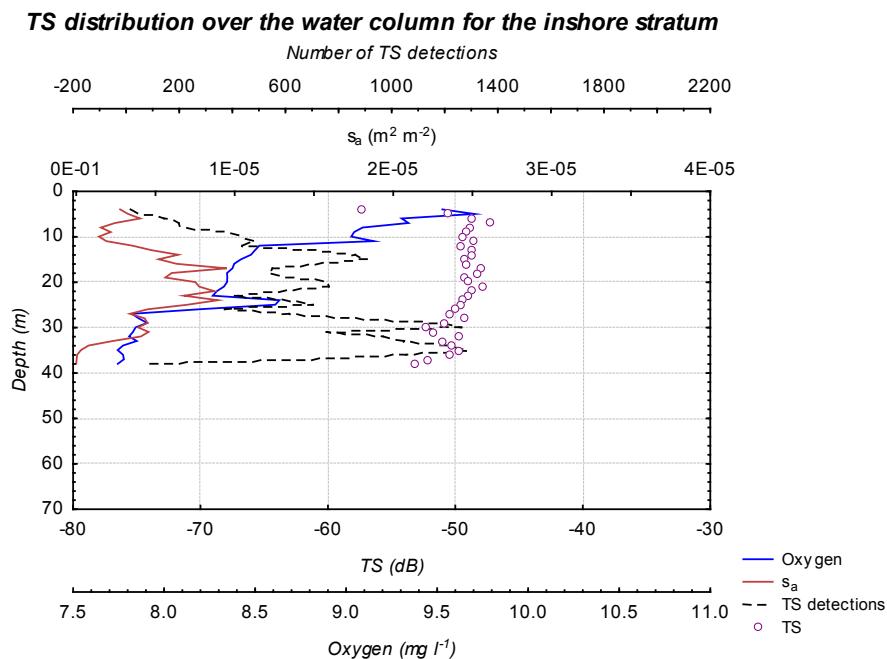


Figure 3.19 – Distribution of TS (averaged for each meter depth), dissolved oxygen, area backscattering coefficient (s_a), and TS detections over depth, for the inshore stratum.

Most of the fish scatters concentrate from 15m to 30 m deep in the inshore stratum (figure 3.19). The majority of the TS detections are found from 10 until 35 m, with two peaks at 30 and 35 m. It should be pointed out that only three stations had bottom depths over 25m, for the inshore stratum.

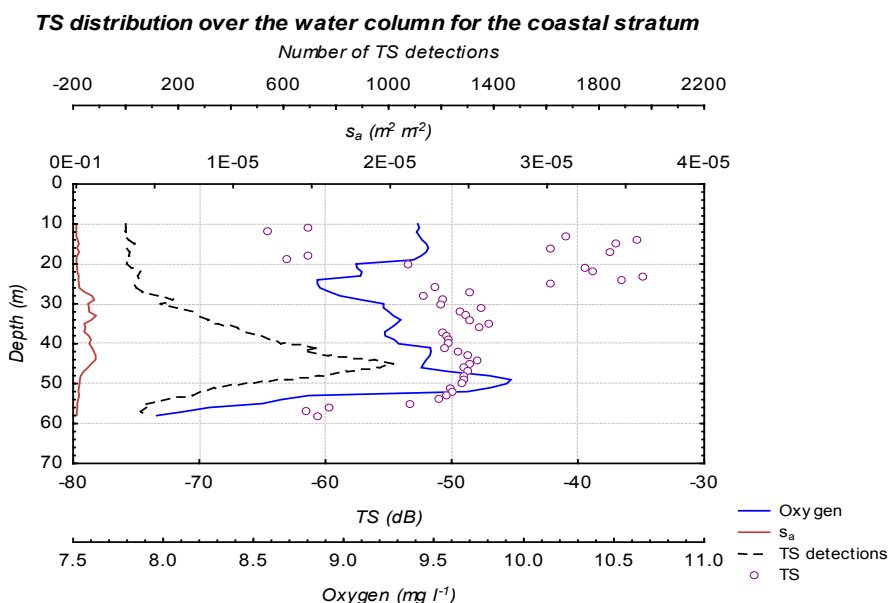


Figure 3.20 – Distribution of TS (averaged for each meter depth), dissolved oxygen, area backscattering coefficient (s_a), and TS detections over depth, for the coastal stratum.

The fish echoes in the coastal stations are distributed from 10 to 58 m, with higher values from 25 to 50 m. The peak in number of TS detections is observed between 40-46 m.

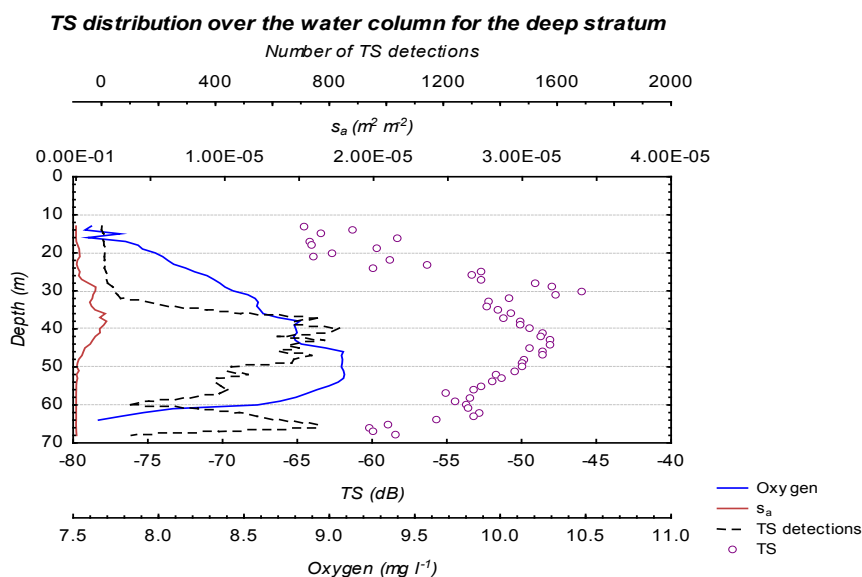


Figure 3.21 – Distribution of TS (averaged for each meter depth), dissolved oxygen, area backscattering coefficient (s_a), and TS detections over depth, for the deep stratum.

In deep stations, there are two peaks found in the fish densities, close to 30 and 38 m; while higher numbers of TS detections are found from 38 to 48 m and at 65 m.

3.4 Comparison of fish densities between the sampled stations

Total fish densities show fluctuations between the stations sampled (figure 3.22). A table showing total fish densities per unit area can be consulted in Appendix XIII (Table 1).

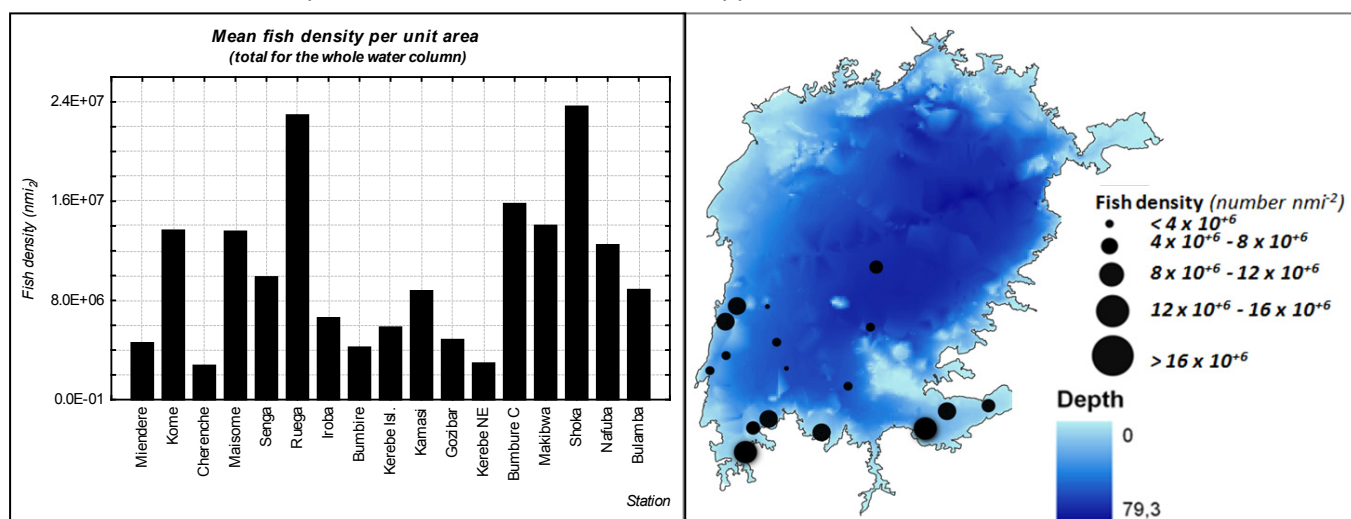


Figure 3.22 – Fish density ($n^{\circ} nmi^{-2}$) for the entire water column, for each CTD station (figure on the left), and fish density distribution according to depth (figure on the right).

The lowest fish densities are observed in Cherenche while Shoka and Ruega are the locations showing the highest fish numbers per square nautical mile. A statistical difference was found in fish densities with strata ($p=0,000$). However, the mean fish densities not show to be statistically different when comparing coastal and deep strata. This can be observed in figure 3.23.

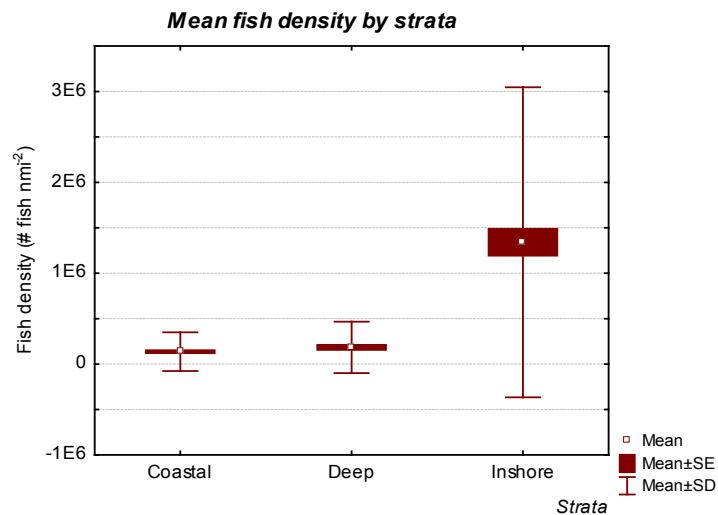


Figure 3.23 – Mean fish densities, with standard error and deviation, calculated for each stratum.

3.5 Relation between limnological variables and fish density

In figures 3.24 to 3.28 it is possible to observe mean fish densities in function of oxygen interval for all stations together, for each stratum as for Speke Gulf only. Figure 3.24 display the mean fish density for each oxygen interval ($0,5 \text{ mg l}^{-1}$ intervals), for all the strata grouped in this graph.

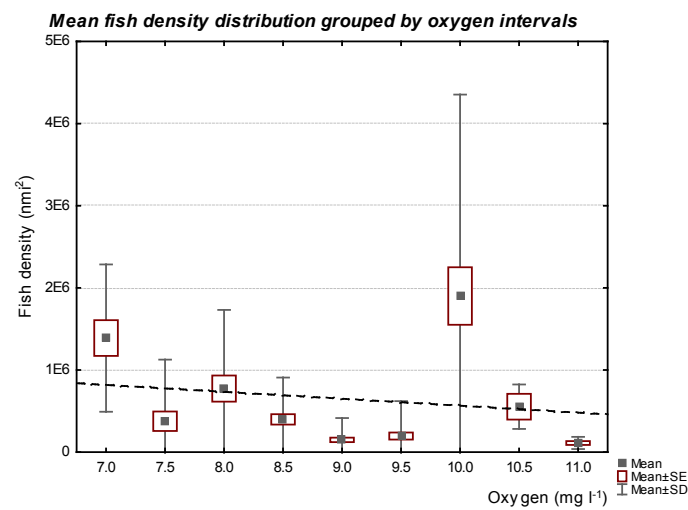


Figure 3.24 – Mean fish density (■) (with standard error [□] and standard deviation [⊥]) grouped by oxygen intervals (intervals of $0,5 \text{ mg l}^{-1}$).

A decreasing trend in fish density is observed when grouped by oxygen intervals, however with no statistical significant relation.

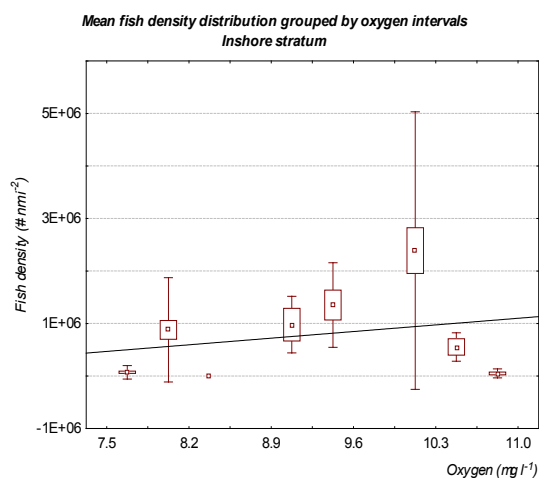


Figure 3.25

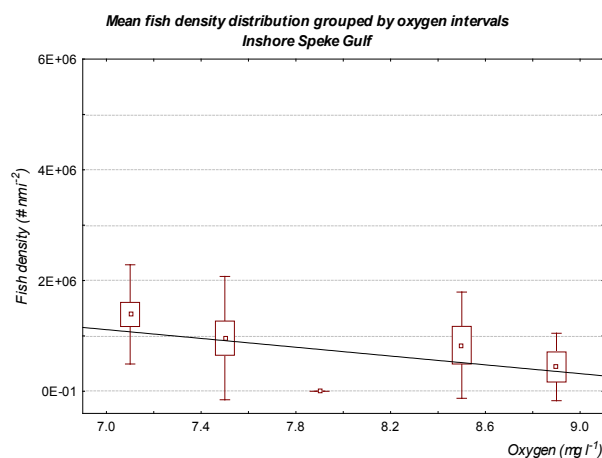


Figure 3.26

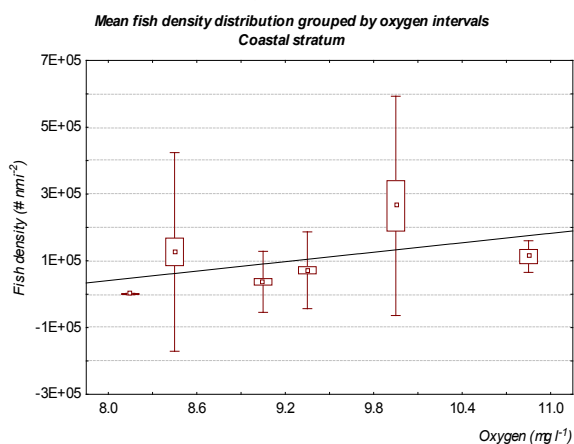


Figure 3.27

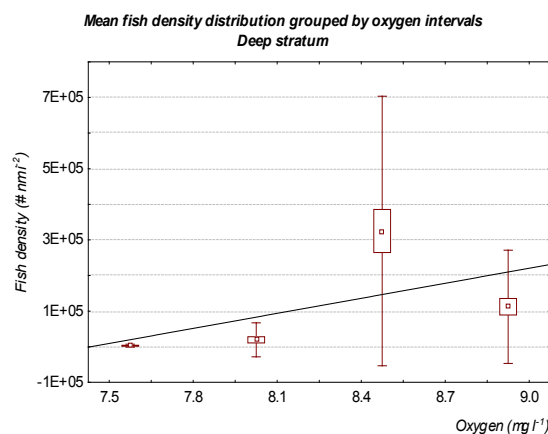


Figure 3.28

Figures 3.25 to 3.28 – Distribution of fish density, grouped by oxygen interval for all strata and Speke Gulf.. Figures show the mean (\square) with standard error (\square) and standard deviation (\perp), for the inshore stratum, Speke Gulf, coastal and deep strata. Note: graphs are not at the same scale.

With exception of data from Speke Gulf, all strata show a positive relation between oxygen and fish densities (Figures 3.25 to 3.28), being only significant for the coastal and deep strata ($p=0,007$ and $p=0,002$, respectively). In Speke Gulf (fig. 3.28), a negative trend in the influence of oxygen in fish numbers is observed. Both for the inshore and coastal strata the oxygen level varies from around 8 mg l^{-1} up to almost 11 mg l^{-1} . In these stations, the peak in fish densities is found close to 10 mg l^{-1} ; before that level, there is an increase in fish densities with oxygen level, after which there is a decrease. For the stations from Speke Gulf, as from the deep stratum, the upper limit of the oxygen level is at 9 mg l^{-1} .

A statistical significant relation between chlorophyll *a* level and fish densities was observed, for all stations together as for the deep stratum ($p=0,000$ and $p=0,050$, respectively). It is however difficult

to observe a trend in the fish density distribution against chlorophyll *a*. Temperature showed also a statistical relation with fish densities, but only for the deep stratum ($p=0,001$; see Appendix XIII, Table 2).

3.6 Echogram analysis

All echograms, from the stations sampled, can be consulted in Appendix XII (Figures 1 to 17). In most of these stations it is possible to identify a region with higher density of fish scatters (referred as fish layer). The depth at which this fish layer is found, its height, density and distance from the bottom differ for each CTD station.

For the stations from the inshore stratum, only in Kome and Bulamba fish is observed over the entire water column; in these two stations, however, several dense schools can be observed but there are less fish scatters distributed over the water column, compared to the other inshore stations. In the remaining inshore stations, fish densities found are variable; but the fish distributes near the bottom.

In the coastal stratum the fish layer distribution differ from the one observed in inshore stations; the fish distributes, in general, in the deeper half of the water column and the fish layer (the denser fish scattering layer) is seen some meters above the bottom. Moreover, the density of fish scatters observed is lower when compared to shallower stations. When analyzing the distance from the bottom of the fish layer and comparing with oxygen profile, it is possible to see that the stations where the fish scatters are concentrated far from the bottom (Miendere, Cherenche and Iroba) there is a decrease in oxygen values from the fish layer depth towards the bottom. In Kerebe Island North the fish layer is distributed up to the bottom while the oxygen level shows also an increase above 45m. In Kerebe Island and Bumbire stations it is not possible to do any comparisons since there are oxygen values missing (due to technical problems).

Some similarities can be found in the fish echoes distribution between the deep and the coastal stations. The fish layer in the deep stratum, unlike it is seen in the coastal stratum, is found in the middle of the water column. Kamasi station has a steep bottom that varies from 47 to 65 m. Here, the fish echoes are distributed at the same depth over the water column, despite the increase in depth. In Gozibar it is seen a decrease in oxygen above 50 m, which is the lower limit of the fish layer. In the other hand, in Kamasi the oxygen level is stable from 45 to 60 m; being that the CTD profile was taken at 60 m, there are not oxygen measurements above that depth.

3.7 Biological data analysis

Frequency distribution of length data collected for Nile perch, from all stations, is displayed in figure 3.29.

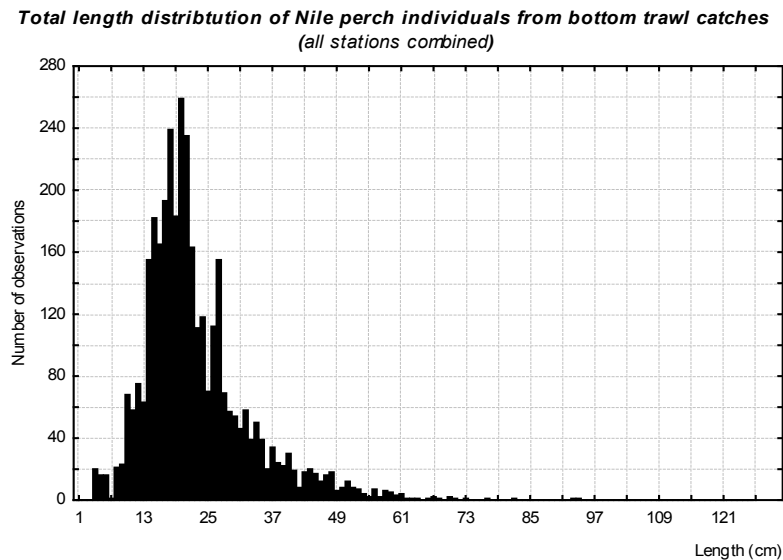


Figure 3.29 – Total length distribution of Nile perch from all net hauls (11 bottom trawl hauls).

Length distribution for Nile perch include individuals with total length ranging from 4 to 94cm. A peak in the number of observations is seen at 19cm. Root mean square length (RMSL) calculated for the Nile perch captured ranged between 16,47 and 32,83 cm (in Bulamba and Iroba Island respectively), with an overall mean of 25,79 cm for all stations. Table 3.1 shows the RMSL calculated for each station.

Table 3.1– Root mean square length calculated for Nile perch from the bottom trawl catch data. Maximum and minimum values for total length (TL) are also shown.

Station name	Station number	Number of individuals	RMS Length (cm)	Minimum TL (cm)	Maximum TL (cm)
Kome Channel	2	41	30,20	14	51
Maisome Channel	4	123	25,67	12	51
Senga (Emin Pasha Gulf)	5	0	-	-	-
Ruega Point	6	231	29,33	11	68
Iroba Isl.	7	193	32,83	11	67
Kerebe Isl.	9	310	24,65	9	77
Kerebe Isl.North	12	327	24,10	4	64
Bumbure Channel	13	665	26,08	9	93
Makibwa Isl.	14	287	34,86	12	94
Nafuba Isl.	54	727	19,78	9	70
Bulamba (Speke Gulf)	55	556	16,47	5	67
All stations	-	3460	25,79	5	94

Figure 3.32 shows the contribution of each species for the trawl catches. Additional information relating to the bottom trawl catches can be consulted in Appendix VII.

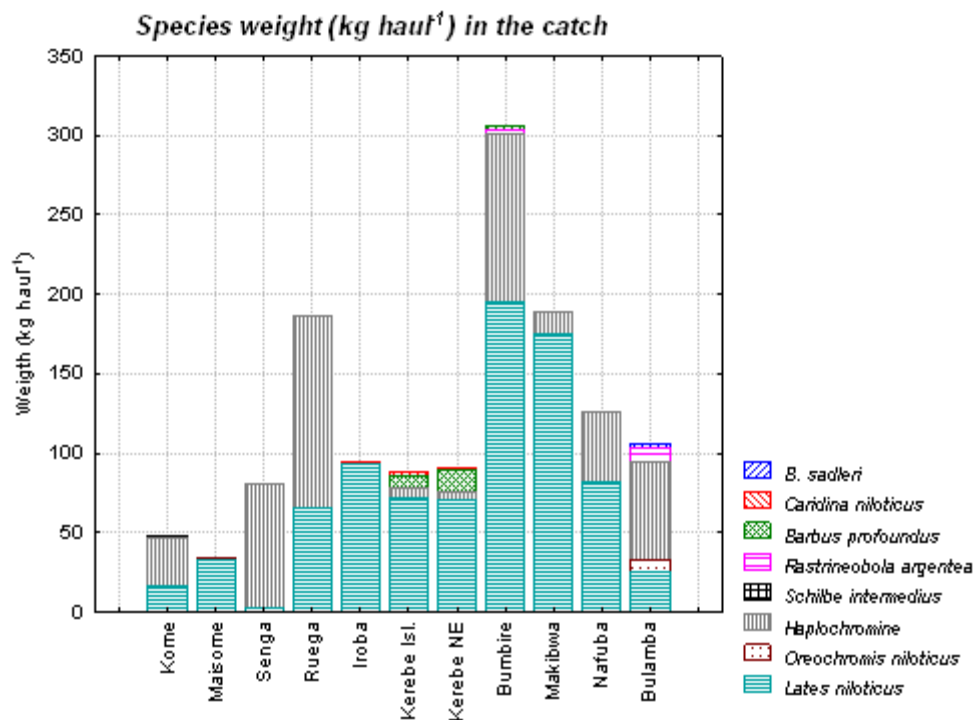


Figure 3.30 – Total weight for each specie captured from the bottom trawl catches.

Trawl catches differed between the locations sampled both in respect to the total weight per haul as in terms of species' proportions (see Tables 1 and 2, Appendix VII). Only a few groups of species were present in the bottom net hauls, which was common for all the trawled stations. The species which contributed to the bulk of the catches were Haplochromines and Nile perch (*Lates niloticus*); these two groups together comprised over 80 % of the catches in all stations. However, the proportion of each of these species varied within the sampled locations. In 4 of the 11 stations (Maisome, Iroba, Kerebe Isl. and Makibwa) the proportion of Nile perch in the catches was above 81 % (from 81,8 to 98,5 %) while in others the proportion was shared more evenly.

Other species observed in the net hauls were Nile tilapia (*Oreochromis niloticus*), dagaa (*Rastrineobola argentea*), silver catfish (*Schilbe intermedius*), *Barbus profundus* and *Brycinus sadleri*. The Decapoda *Caridina nilotica* was also found in some of the net hauls.

The following graph (Figure 3.31) shows the comparison between the estimated trawl catch (in kg haul⁻¹), calculated from the acoustic data, and the total catch from the bottom trawl haul. The values are transformed to logarithmic scale.

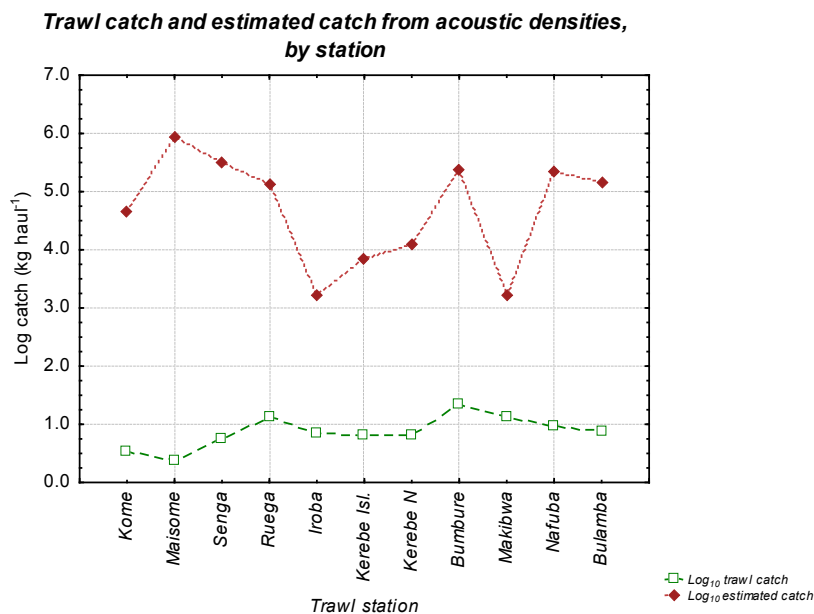


Figure 3.31 – Comparison between estimated catch, from acoustic data, and trawl catches (kg haul⁻¹). Values are in Log scale.

In the Figure 3.32, the relation between the trawl catches and the estimated catch, from the acoustic densities, is shown. From both figures, a disparity of the values from the both methods can be observed; in graph 3.32 the absence of relation between the trawl catch and the acoustic densities registered within the trawl area is reinforced.

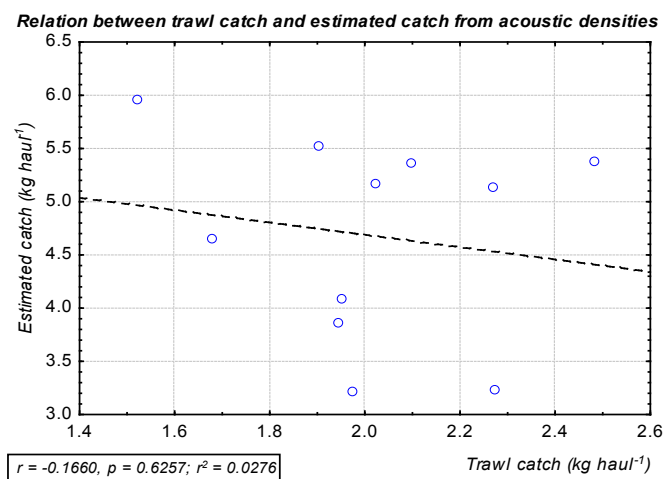


Figure 3.32 – Relation between estimated catch, from acoustic sampling, and trawl data.

Total length distribution, seen in figures 3.33 and 3.34, aims to give only an indication of the size distribution expected for Nile perch since the TS data was directly converted to TL, for these two

graphs. Given that several TS detections can be made from one fish, these figures should not be looked as the actual distribution.

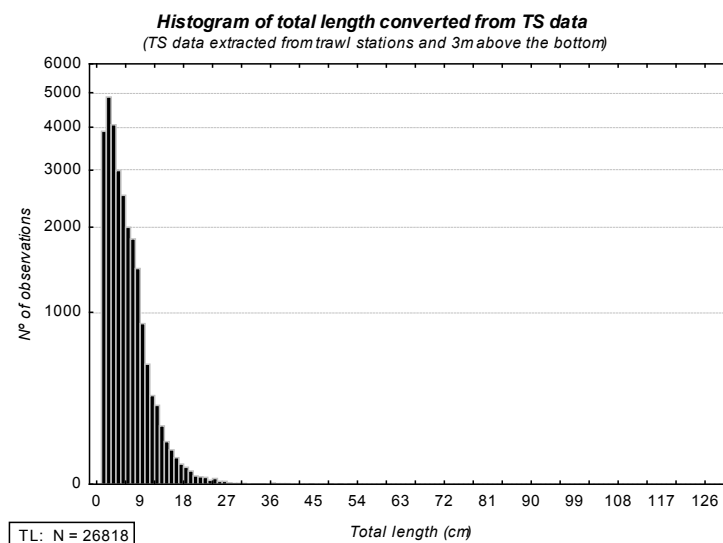


Figure 3.33 – Estimate from the frequency distribution of the expected total length from fish in the trawl area.
Note: this graph should not be interpreted as the actual fish distribution, from the acoustic data.

In figure 3.34, only data above 20 cm (corresponding to -40 dB) was plotted. The largest echo found corresponded to a 59 cm target (which is around -30 dB). It is important to recall that the acoustic data used (collected along 2 nmi), for these graphs, corresponds only to a part of the area swept by the bottom trawl, since acoustic data used was restricted to 1 nmi after the CTD profile was taken while trawling was done along 1,5 nmi after the CTD measurement.

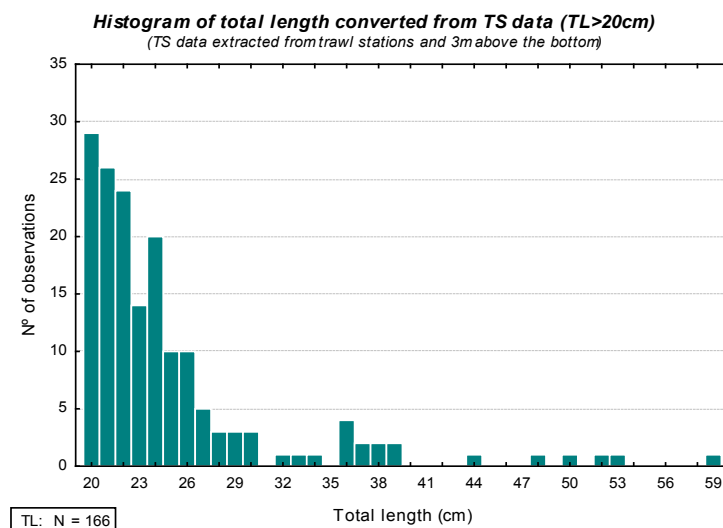


Figure 3.34 - Estimate from the frequency distribution of the expected total length from fish, above 20cm, in the trawl area. Note: this graph should not be interpreted as the actual fish distribution, from the acoustic data.

The graph 3.35 shows the comparison of TS, calculated for each CTD station, between the 70 and 120 kHz frequencies. Data at the two frequencies was compared in order to determine if it was necessary to do some correction for the TS-TL relationship.

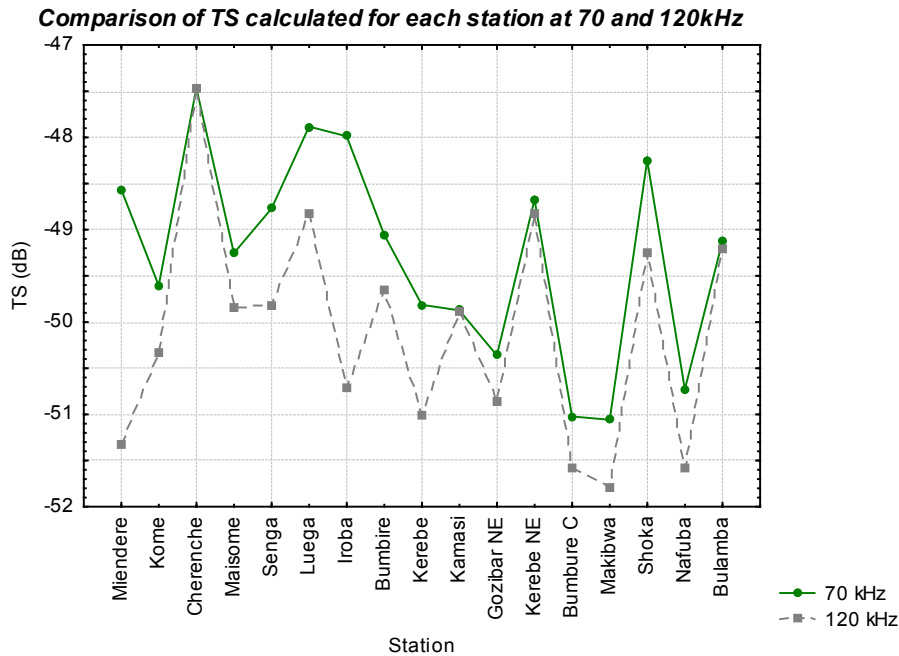


Figure 3.35 – Comparison between TS, calculated for each station, exported at 70 and 120 kHz frequencies.

The difference between TS at 70 and 120 kHz ranges from 0 (Bulamba) to 3,5 dB (Miendere). At 70 kHz frequency the TS is in average 0,9dB stronger than at 120 kHz. This corresponds to a 0,64 cm difference in the size of fish. This is within the limits found in Godlewska *et al.* (2009), thus no adjustment was made to the TS-TL relation.

4 Discussion

4.1 Limitations of this study

Several limitations which affect acoustic and trawl sampling have been described in literature. In this section, the contribution of relevant sources of bias for this study will be evaluated.

Equipment sensitivity, fish behaviour and avoidance reactions are the main sources of systematic errors (Simmonds & MacLennan 2005), which can be important for this study's results.

Equipment sensitivity relates to changes in the calibration factor during the survey period (Simmonds & MacLennan 2005). A second calibration was done in the end of the survey to test the relative contribution for this error; the small variation observed between the two calibrations indicated that the system was working properly during the survey.

Diurnal behavior rhythms are reported for some species found in Lake Victoria (Goudswaard *et al.* 2004), namely for Nile perch juveniles (<10cm) which have showed to perform diel migrations (Wanink 1988, 1992 *in* Witte & Densen 1995). Such migrations over the water column are important since they might bias target strength detections as a result of the different ambient pressures acting on the fish swimbladder, especially in deeper areas (Simmonds & MacLennan 2005). Also, vertical migrations, as a response to changes in light intensities along the day, may result in different distributions of the fish target strength due to changes in the fish tilt angle (Foote 1987). The contribution of this type of error is not possible to estimate and further acoustic studies should consider this subject.

Avoidance reactions to research vessels have been reported for several fish species (Vabø *et al.* 2002, Handegard *et al.* 2003) and are indicated as the most important error for acoustic surveys (Aglen 1994). Disturbances in fish densities and changes in the mean tilt angle of fish, and consequently in their target strength, are consequences of avoidance behavior (Aglen 1994). The importance of fish densities dilution is small in this study, since absolute abundance estimates are not the aim; however, this bias can affect fish distribution over the water column since vertical avoidance can lead fish to distribute differently in relation to limnological factors.

In stations from shallow and sheltered areas, the influence of avoidance behaviour should be more important (Simmonds & MacLennan 2005); being so, an unequal influence of bias due to avoidance is inherent to this study since bottom depth varies (from 9,32 to 67,82m) between the stations. Avoidance in freshwater result mainly from noise and visual stimuli caused from the vessel (Drăstík

& Kuběčka 2005), with a relative importance dependent on the fish species (Gunderson 1993, Fernö *et al.* 2006).

Avoidance behavior, due to the fishing gear deployment is expected to influence both acoustic as bottom trawl sampling. Different stimuli from each of bottom trawl components will result in distinct types of behavioral responses of fish (Engås 1994) leading to different avoidance reactions between species (Wardle 1993) and thus to distinct catching efficiencies between species. Herding efficiency by the trawl components decrease for species with lower swimming speeds as for smaller individuals within the same species (Ona 1999b). It is possible then that the catching efficiency for all sizes of fish as for the different species will differ, which should be quantified for later assessments.

Trophic state of the lake, with its resultant decrease in water transparency, is also suggested to influence avoidance namely for species which rely more on visual cues (Drăstík & Kuběčka 2005). The dependence of visual cues for Haplochromine species as for Nile perch has been reported for reproduction (Witte *et al.* 2005) and foraging (Mkumbo & Ligtvoet 1992), accordingly. Fish avoidance has not been extensively studied for freshwater environments (Drăstík & Kuběčka 2005) and information regarding the importance of these visual cues in gear/vessel avoidance for Lake Victoria species is essential for reaching conclusions on the contribution from this source of error.

Presence of acoustic dead zones poses a limit to the acoustic sampling, since restricts sampling in two zones (deadzones), one below the transducer face while the other just above the bottom (Aglen 1994). The importance of the surface blind-zone is negligible since areas near the surface were not included in the analysis, in most stations. On the other hand, the magnitude of bottom exclusion zones influence is dependent on the vertical distribution of the target species, becoming particularly important for demersal species (Godø & Wespestad 1993). Nile perch is described as a demersal specie (Ligtvoet & Mkumbo 1990) and higher catch rates from bottom gill nets were reported in Goudwaard *et al.* (2004), Tweedle *et al.* (1999 *in* Agnew 2005) and Asila (2000 *in* Agnew 2005), and should be considered in this discussion. These studies may not be representative from the whole population, since they were restricted to shallow areas (<16m in Goudswaard *et al.* 2004 and <25m in the two other studies). Even though, the existence of bias as a result from undetected fish due in the bottom deadzone is a possibility that should not be discarded.

TS measurements in areas with high fish densities may lead to biased higher mean TS if multiple targets are accepted as single target (Rudstam *et al.* 2003). To estimate the contribution of multiple targets in this study, Nile perch single targets were selected for comparison. In addition, the number of targets per volume was calculated using the Sawada equation (Sawada 2003 *in* Parker-Stetter *et*

al. 2009), and the correlation between fish densities and mean size of targets was examined. Results from these showed that the influence of multiple scatters for TS detections was negligible.

Diurnal variability of limnological parameters was not quantified in this study. The fluctuation on the oxygen content along the day is particularly important for waters with high primary productivity (Wetzel 2001), since photosynthetic processes are dependent on light availability; thus, increases in photosynthesis, and thus oxygen content, is expected for the mid-afternoon (Mathews 1998). It is then likely that some variation in limnological parameters might reflect the diel photosynthesis cycle; however, this was not taken into account in this study, being the CTD sampling determined previous to the beginning of the survey.

4.2 Target strength

4.2.1 Validation of TS measurements

Frequency distributions from TS extracted for the entire water column ($TS_{Station}$) as from the Nile perch selected targets ($TS_{Selected}$) were compared (see Figure 3.8). Both distributions are shown to not differ considerably. However, in Maisome, Gozibar and Kerebe Island North an increase in bigger targets could be observed. These three stations showed also a significant relation between fish density and TS (Figure 27, Appendix XI), along with some analysis cells showing $N_V > 0.1$. When observing the graphs of TS and density distribution with depth (Appendix IX, Figures 1-17), it is possible to see that the peak in the TS is not coincident with the one of fish densities in Maisome and Gozibar stations, while in Kerebe NE, the depth of TS and density peaks overlapped. Comparing the distribution (see graphs 9 and 12 in Appendix IX) of Kerebe Island with Kerebe NE, since these are close geographically, it is possible to observe that the size distribution from the targets is similar, with peaks in TS at the same depths approximately. Thus, the TS distribution is likely to increase at such depths due to habitat preference rather than due to the influence of interference of multiple echoes in single target detections.

When comparing the mean TS for the entire echogram ($TS_{Station}$) with the TS value obtained from the targets selected ($TS_{Selected}$) based on the shape of the echo traces, a discrepancy was seen between the values (Figure 3.9). Ruega was the location where the divergence was highest while for Shoka the TS calculated matched for both methods. In three of the locations (Maisome, Ruega and Shoka) the high fish densities complicated the selection of the targets within areas where the highest number of scatters was found; as a result, to select the targets in lower density areas was the only

workable option. The result was that targets in the locations with denser fish scatters were not selected for the TS calculations.

By excluding these dense areas, the biggest targets were likely being excluded as well; this is because the less dense places were generally in the upper or lower parts of the fish layer (see echograms, Appendix XII), where there is a larger variability of the mean target sizes, as seen from the TS distribution over the water column. To demonstrate this better we can have a closer look to the examples where the mean $TS_{Station}$ and $TS_{Selected}$ were similar. In Shoka, the overall variation of the TS over the water column was not very large, thus by selecting the targets in areas where these were sparsely distributed there was no divergence between the calculated TS. Bumbire and Kamasi were other locations where the TS was approximate for the two methods (approximate -1dB difference), which had to do with the low densities of scatters in these stations, allowing to select single targets in the whole water column.

It is then assumed that the higher mean size targets, found in areas with dense fish scatters, is a result of Nile perch distribution over the water column and not on the effect of multiple targets being included as single targets.

TS data extracted from the trawl area was compared with the TS for the water column to test the assumption that Nile perch is the main species contributing for the TS detections. The comparison of the $TS_{Trawl\ area}$ with the $TS_{Station}$ shows a small divergence in all the stations, except for two stations (Kome and Bulamba). In these stations, large differences from mean TS of the echoes were found close to the bottom, which should be related with the differences found. In the other stations, even if the trawl was not performed at the same depth where most of the fish scatters were found, there was no large difference between the mean TS values over the water column. The fact that there is no observable divergence in the mean $TS_{Station}$ and $TS_{Trawl\ area}$ calculated, for most of the sampled stations, show that the sizes of single targets located in the bottom is representative from the water column.

Differences in Nile perch proportions, relative to total fish biomass, in function of bottom depth have been reported. In stations less than 20 m deep, Nile perch proportion is generally lower when compared with deeper stations (Mkumbo 2002; Mlaponi 2006; Mlaponi *et al.* 2005, 2006; LVFO 2007). In accordance, acoustic survey data have shown that Nile perch constitutes 16 and 6 % of the fish biomass (excluding Dagua) in Speke and Emin Pasha Gulf, respectively (LVFO 2009); then, an increasing contribution from other fish species to single target detections, and consequently lower mean TS, would be expected in such areas. By comparing the TS from stations which had different

proportions of Nile perch in the bottom hauls, it is possible to conclude that mean TS values are not influenced by the presence of other species, being mainly Nile perch contributing for the single target detections.

Maisome, Iroba, Kerebe Island, Kerebe NE and Makibwa showed, in the trawl catches a proportion of Nile perch above 78,9 %. In opposition, Senga showed the lowest proportion (2,5 %), and in Kome, Ruega as in Bulamba the proportions of the species varied (ranged from 23,3 to 34,9 %). The small variation in $TS_{\text{Trawl area}}$ calculated between stations with such large differences in the species proportions (Senga and Iroba for e.g.) supports this deduction. Several examples of schooling behavior are described for species of the Cichlidae Family (Keenleyside 1991; Kohda & Takemon 1996; Marsh & Ribbink 1986); it is possible that the small schools observed in the echograms might be from these small fishes, preventing this species to be detected as individual targets.

4.2.2 Spatial distribution of mean target strength

Strata showed to influence significantly mean TS (Figure 3.13). The mean TS calculated (TS_{Station}) for the locations sampled fluctuated over -3 dB (corresponding to 2 cm) between the CTD locations. This is consistent with reports from bottom trawl surveys which suggest variations in the Nile perch size distribution for different depth strata (Mlaponi *et al.* 2005, 2006; Mlaponi 2006; LVFO 2007). The higher proportions of individuals above 50 cm (minimum slot size) found was between 30 and 40 m depth, followed by the 40-50 m and 20-30 m strata (Mlaponi *et al.* 2005, 2006; Mlaponi 2006; LVFO 2007). This is consistent with the highest mean TS for this study which was observed for the coastal stratum.

4.3 Fish density distribution

Fish densities from inshore stations are significantly higher than the values observed for the other two strata (Fig. 3.23). This is in agreement with reports from LVFO acoustic surveys where both Nile perch and other fish species (excluding Dagaa) which show higher fish densities (tons per km²) for inshore Tanzanian waters, compared to coastal and deep (Getabu 2003, Everson 2006, LVFO 2009).

4.4. Influence of limnological data on fish distribution

As explained in the material and methods section, separating the s_a corresponding to Nile perch from the remaining fish species proved to be impracticable. First, the fish echoes from the species present could not be separated visually since the Nile perch, the target specie for this study, has a distribution which is overlapping with Haplochromines (Goudswaard *et al.* 2004, Everson 2005).

Secondly, the dense layers of scatters that were found in most of the locations sampled hampered the visual separation based on the echo traces. The use of bottom trawl data for splitting the echoes was discarded for two main reasons. The first one was because the area swept by the trawl was not coincident with the depth where the most dense fish scatterings were observed. Secondly, there was a lack of correspondence between the acoustic and trawl data regarding both fish densities and mean size of fish. This topic will be discussed in more detail in the next section.

Since separate Nile perch densities (S_a) from the other existent fish species was not possible, the presence of oxygen effect on Nile perch densities alone could not be analyzed. Higher tolerance to low oxygen has been reported for several Lake Victoria species other than Nile perch (Fish 1956); then it is possible that a trend in fish densities, as function of oxygen level, will be masked by the different susceptibility of all fish species sampled by the echo-sounder. As such, the research question addressing the relation between oxygen and Nile perch densities cannot be answered.

On the other hand, it has been demonstrated that it was mostly Nile perch contributing for single target detections, enabling to take conclusions on the relation between limnological data and fish sizes.

Low oxygen environments are suggested to be critical for Nile perch ability of occupying areas such as swamps or other low oxygen habitats (Schofield & Chapman 2000). A higher sensitivity of Nile perch to low oxygen, compared with several indigenous species from Lake Victoria, has been shown experimentally (Fish 1956, Schofield & Chapman 1999, 2000). The fact of its metabolic rates is higher than several Haplochromine or tilapiine cichlids was demonstrated by Fish (1956) and justify the absence of Nile perch in environments with limited oxygen availability. However, no limitation was found to the fish distribution during this study since no hypoxic conditions were observed. Even so, differences in limnological data were found between strata and depth; thus, there was an attempt to understand if these differences were influential in fish distribution.

When analyzing fish density for the three strata separately, a statistical significant relation was found between fish density distribution and oxygen level, both for coastal and deep stratum. It is in these strata where there is a higher proportion of Nile perch in the demersal biomass, according to LVFO (2009) acoustic data. In the inshore stratum, where higher fish densities were found, there was no significant relationship between the same variables.

Limnological data differs considerably among inshore stations (Appendix V, Figures 1 to 9), with stations recording oxygen values close to 10 mg l^{-1} (10.03 and 10.23 mg l^{-1} were observed in Kome and Maisome) while others around $7,5 \text{ mg l}^{-1}$ ($7,24$ and $7,75 \text{ mg l}^{-1}$ in Shoka and Nafuba); this large

variability might explain the absence of relationship between fish density and oxygen in inshore stations.

A positive and statistical significant relation was observed between oxygen and fish size, both for each strata as for all data together. Since Nile perch is the main species contributing for the single target detections it was possible to identify a pattern in the species' size distribution. The data from this study shows that there is a tendency of Nile perch individuals to distribute differently according to type of strata, and with larger fishes distributing according to increases in oxygen availability (Figure 3.14). Observations showed that a high mean size of fish was found in areas with low dissolved oxygen. In fact, the data from Speke Gulf showed a contrasting pattern in the fish size distribution with oxygen, compared with data from the other strata. Since no limitation to Nile perch distribution was found, according to the levels referenced in literature (Fish 1956), nothing suggests that there should exist a limit to the distribution on large Nile perch.

A significant correlation between chlorophyll *a* and fish density could be identified, both for the deep stratum as for all stations together. Mkumbo (2002) suggested that Nile perch catch rates from bottom trawl surveys increased with peaks in chlorophyll *a* levels. Since there is no separation of fish species, it is possible that a relation with chlorophyll *a* might be related with the contribution of zooplanctivores and algae feeding fish species for the measured acoustic densities.

A significant relation was also found between chlorophyll *a* and fish size, except for the coastal stratum. A particular trend is however difficult to identify; in deep stations, a peak in the size of individuals can thus be found at chlorophyll level close to $3,2 \mu\text{g l}^{-1}$, while in inshore stratum most of the observations are seen below $13 \mu\text{g l}^{-1}$, being the peak in mean size close to $23 \mu\text{g l}^{-1}$. Nile perch depends on visual cues for feeding (Mkumbo & Ligetvoet 1992) which can explain the decrease seen in the inshore stratum of mean TS after $23 \mu\text{g l}^{-1}$. However, the same is not likely to apply to deep stations since chlorophyll *a* concentrations found are much lower. In this deep stratum, the distribution of sizes of individuals might be following the distribution of prey. Thus, the relation found between chlorophyll *a* and fish size might reflect changes in prey preferences according to fish size, since diet shifts have been described for Nile perch influenced by the individual sizes (Katunzi *et al.* 2006).

4.4 Bottom trawl and acoustic fish densities

As mentioned, bottom trawl data was not used in the partition of fish echoes. However, it is important to discuss the absence of correspondence between the two methods.

Collection of biological information is fundamental for supporting acoustic survey sampling; yet in this study, bottom trawl sampling did not seem to reflect the actual fish abundance or size distribution of Nile perch stock. Trawl data was considered non representative due to a negative relation observed between densities from acoustic and catch data (Figure 3.32); and because of a disparity in the mean length for Nile perch calculated from the two sampling methods (6,97 and 25,79 cm, acoustic and trawl data; see Figure 3.8).

Based on the little information available relating to the bottom trawl and its performance during the hauls, the grounds for the divergence between sampling methods found, can only be speculative. Still, the most likely factors that can explain the divergence between the two methods will be described.

According to Ona & Mitson (1996), higher avoidance behavior is likely to occur in shallower waters and lower fish densities are likely to be observed within the acoustic beam whereas it would still be available in the trawl path. In accordance, the effective fishing height from a bottom trawl is not limited to the height of its floatline (Hjellvik *et al.* 2003), since an increase in fish availability, for the trawl, occurs due to a downwards avoidance from fish (Godø & Wespestad 1993); however this vertical herding is more effective for large fish (Hjellvik *et al.* 2003). These findings can explain the observed disparity between mean sizes of fish calculated by the two methods; since by herding more effectively large fish, it will lead to a bias towards larger individuals in the trawl swept area, as seen.

An influence of the bottom acoustic deadzone can explain also some of the divergence between the acoustic and catch data found. Findings from Engås & Godø (1989) support this supposition, since a lack of a significant relation between the two sampling methods was observed in demersal stocks due to the effect of the bottom deadzone. The influence of the deadzone for Nile perch should be small since its detections, reported from acoustic surveys, are mostly pelagic (Everson 2006). However, the vertical avoidance caused both by the gear and the vessel might enhance the effect of the bottom acoustic deadzone since it will “push” fish down.

Another possible cause for the inconsistency between the methods could be the small mesh size incorporated into the codend. An increase in the drag effect may result from this small mesh codend since the water flow may be affected in the case too small meshes are incorporated (Wileman *et al.* 1996). Excessive drag effect may lead to changes in the geometry of the net, reducing the net mouth opening, with a consequent decrease in catchability (Wileman *et al.* 1996). However, this is not the most likely explanation since it would lead to a constant selectivity during the net hauls, and thus a correlation between the two methods.

Catching efficiency differs according to fish size, since small fish is usually herded more effectively by the sand clouds generated by the trawl doors, while for large fishes there is an increase in herding stimulus by the trawl doors or by the sweep wires (Engås & Godø 1989). Moreover, mesh selection can occur before fish enter the codend (Walsh 1996). It is then possible that a difference in the gear efficiency exist for the different type of species present in Lake Victoria, leading to divergences in catching efficiency such as the ones found in this study, being likely to be the major cause for the negative correlation between trawl and acoustic data as for the high proportion of large individuals found in this study.

Several possibilities have been suggested to explain the inconsistency from data of the two sampling methods. However, there is insufficient data available from this or from previous studies conducted in Lake Victoria, that allow a conclusion on the relative influence of the above stated possibilities.

5 Conclusions

A relation between Nile perch size and oxygen level was demonstrated in this study, with higher individuals being observed along increasing oxygen levels. A relation, between fish size and chlorophyll *a* level was demonstrated for the three strata combined, as for the deep and inshore strata. No significant relation was observed between temperature and Nile perch size. Seasonality has been described in literature, such as in Mkumbo (2002), as an influential for fish stocks dynamics, which is important to be explored in further studies.

This thesis failed to address one of the research questions proposed, aiming to investigate the correlation of Nile perch density and limnological data collected, since it was not possible to isolate the target specie's echoes from the remaining fish species.

Further research on the relation between Nile perch and environmental data, covering some of the limitations from this study, is fundamental for Lake Victoria fishery as for understanding the actual impacts of enhanced eutrophication on Nile perch stocks. This study can thus serve as a platform for future work focusing Nile perch distribution. As such, complementing the acoustic data with additional information would enable to have a more comprehensive perspective. This could be achieved through:

- Complementing the acoustics with Nile perch feeding information;
- Evaluate the relative contribution of the diel cycle on the limnological data;
- Assessing the contribution of errors in TS both due to influence of diurnal fish behaviour, as from vessel/gear avoidance, by using stationary methods;
- Investigate gear efficiency and selectivity, considering not only Nile perch but also the other fish stocks.

6 References

- Aglen. 1994. Sources of error in acoustic estimation of fish abundance. Pp 107-133. *In: Fernø and Olson (Eds). Marine fish behaviour in capture and abundance estimation.* Oxford: Fishing News Books.
- Agnew, D. J. 2005. *Consultancy Report No 7 – Completion of Standard Operating Procedures for trawl Surveys.* [Available online: <http://www.lvfo.org/downloads/CR7%20Trawl%20Survey%20SOP.pdf>].
- Allison, E. H. 2004. The fisheries sector, livelihoods and poverty reduction in Eastern and Southern Africa: 256-273. *In: Ellis, Frank and Freeman, H. Ade (2005) (eds.) Rural livelihoods and poverty reduction policies,* London: Routledge.
- Bootsma, H. and Hecky, R. 1993. Conservation of the African Great Lakes: A Limnological perspective. *Conservation Biology. Vol. 7, №3:* 644-655.
- Brönmark & Hansson 2005. *The biology of lakes and ponds.* Oxford : Oxford University Press.
- Chapman, L.J., C.A. Chapman, F. Witte, L. Kaufman, and J. Balirwa. 2008. Biodiversity Conservation in African Inland Waters: Lessons of the Lake Victoria Basin. Plenary Paper: *Verhandlungen Internationale Vereinigung Limnologie 30 (Part I):*16-34.
- Chapman, L.J.; Chapman, C.A.; Nordlie, F.G; Rosenberger, A.E. 2002. Physiological refugia: swamps, hypoxia tolerance and maintenance of fish diversity in the Lake Victoria region. *Comparative Biochemistry and Physiology (Part A). 133:* 421–437.
- Cowx, I.G, van der Knaap, M., Muhoozi, L.I., and Othina, A. 2003. Improving fishery catch statistics for Lake Victoria. *Aquatic Ecosystem Health & Management* 6(3):299-310.
- Doudoroff, P.; Shumway, D.L. 1970. *Dissolved oxygen requirements of freshwater fishes.* FAO Technical Paper 86. Rome: FAO.
- Drastik, V.; Kubecka, J. 2005. Fish avoidance of acoustic survey boat in shallow waters. *Fisheries Resources* 72: 219–228.

- Engås, A. 1994. The effects of trawl performance and fish behaviour on the catching efficiency of demersal sampling trawls: 45–68. *In: A. Fernö and S. Olsen [eds.]. Marine Fish Behaviour in Capture and Abundance Estimation*. Fishing News Books. Oxford.
- Engås, A.; Godø, O. 1989. The effect of different sweep lengths on the length composition of bottom-sampling trawl catches. *ICES Journal of Maritime Science* 45: 263-268.
- Everson, I. 2005. *Consultancy report N. 8. Completion of Standard Operating procedures for Hydro-acoustic Fisheries surveys*. [Available online: <http://www.lvfo.org/downloads/CR8%20Acoustic%20Survey%20SOP.pdf>]
- Everson, I. 2006. *Consultancy Report N. 24. Acoustic Survey Mission Report: 4 February to 31 March 2006*. [Available online: <http://www.lvfo.org/downloads/CR24%20Acoustics%20survey%20Feb%202006.pdf>]
- FAO. 2007. *United Republic of Tanzania: National Fishery Sector Overview*. [Available online: ftp://ftp.fao.org/fi/document/fcp/en/FI_CP_TZ.pdf]
- Fernö A, Huse G, Jakobssen PJ, Kristiansen TS (2006) The role of fish learning skills in fisheries and aquaculture: 278-309. *In: Brown C, Laland KN, Krause J (eds), Fish cognition and behaviour*. Oxford: Blackwell Publishing.
- Fish G. R. (1956) Some aspects of the *respiration* of six species of *fish* from Uganda. *Journal of Experimental Biology*. 33: 186-195.
- Foote, K. G., 1987. Fish target strengths for use in echo-integrator surveys. *Journal of the Acoustical Society of America* 82: 981–987.
- Geheb, K.; Medard, M.; Kyangwa, M.; Lwenya, C. 2007. The future of change: Roles, dynamics and functions for fishing communities in the management of Lake Victoria's fisheries. *Aquatic Ecosystem Health & Management*. 10 (4):467–480.
- Getabu, A., Tumwebaze, R. and MacLennan, D.N. 2003. Spatial distribution and temporal changes in the fish populations of Lake Victoria. *Aquatic Living Resources*. 16: 159- 165.
- Godlewska, M. Colon, L. Doroszczyk, B. Długoszewski, C. Verges, J. Guillard. 2009. Hydroacoustic measurements at two frequencies: 70 and 120 kHz – consequences for fish stock estimation. *Fisheries Research*. 96: 11–16.

- Godø, O. R. and Wespestad V. G. 1993. Monitoring changes of abundance of gadoids with varying availability to trawl and acoustic surveys. *ICES Journal of Marine Science*. 50: 39–51.
- Goudswaard, K.; Wanink, J.; Witte, F.; Katunzi, E.; Berger, M.; Postma, D. 2004. Diel vertical migration of major fish-species in Lake Victoria, East Africa. *Hydrobiologia*. 513: 141–152.
- Grosslein & Laurec. 1982. *Bottom Trawl surveys design, operation and analysis*. Interregional Fisheries development and management programme. [Available online: <http://www.fao.org/DOCREP/003/P7841E/p7841E00.htm#TOC>]
- Gunderson D. R. 1993. *Surveys of Fisheries Resources*. New York: John Wiley and Sons, Inc.
- Ha, V. 2008. *Separating blue whiting (Micromesistius poutassou Risso, 1826) from myctophid targets using multi-frequency methods*. Department of Biology, University of Bergen. Msc thesis. 54pp.
- Handegard, N.; Michalsen, K.; Tjøstheim, D. 2003. Avoidance behaviour in cod (*Gadus morhua*) to a bottom-trawling vessel. *Aquatic Living Resources*. 16: 265–270.
- Hecky, R.; Bugenyi, F.; Ochumba, P.; Talling, J.; Mugidde, R.; Gophen, M.; Kaufman, L. 1994. Deoxygenation of the Deep Water of Lake Victoria, East Africa. *Limnology and Oceanography*, Vol. 39, No. 6: 1476-1481.
- Hecky, R.E. 1993. The eutrophication of Lake Victoria. *Verhandlungen Internationale Vereinigung für Theoretische und Angewandte Limnologie*. 25:39-48.
- Hjellvik, V., Michalsen, K., Aglen, A., and Nakken, O. 2003. An attempt at estimating the effective fishing height of the bottom trawl using acoustic survey recordings. *ICES Journal of Marine Science*, 60: 967–979.
- Horne, J.K. 2000. Acoustic approaches to remote species identification: a review. *Fisheries Oceanography*. 9(4): 356-371.
- Hughes, N.F. (a) 1992. Growth and reproduction of the Nile perch, *Lates niloticus*, an introduced predator, in the Nyanza Gulf, Lake Victoria, East Africa. *Environmental Biology of Fishes* 33: 299-305.

Hughes, N.F. (b) 1992. Nile perch, *Lates niloticus*, predation on the freshwater prawn, *Caridina nilotica*, in the Nyanza Gulf, Lake Victoria, East Africa. *Environmental Biology of Fishes* 33: 307-309.

[Johnson](#), T.; [Odada](#), E. (Ed.) 1996. *Limnology, Climatology and Paleoclimatology of the East African Lakes*. Amsterdam: Gordon and Breach Publishers.

Katunzi, E.; Van Densen, W.; Wanink, J.; Witte, F. 2006. Spatial and temporal patterns in the feeding habits of juvenile Nile perch in the Mwanza Gulf of Lake Victoria. *Hydrobiologia* 256:121–133.

Kayombo, S.; Jorgensen, S. 2005. *Lake Victoria: Experience and Lessons learned brief*: 432-446
[Available online: http://www.iwlearn.net/publications/II/lakevictoria_2005.pdf]

Keenleyside, M.A. 1991. *Cichlid fishes: behavior, ecology and evolution*. London: Chapman & Hall.

Kohda, M.; Takemon, Y. 1996. Group foraging by the herbivorous cichlid fish, *Petrochromis fasciolatus*, in Lake Tanganyika. *Ichthyological Research* 43: 55-63.

Kendall, R.L. 1969. An Ecological History of the Lake Victoria Basin. *Ecological Monographs*, Vol. 39, No. 2, pp. 121-176.

Kitchell, J. F., D. E. Schindler, P. M. Reinthal, and R. Ogutu-Ohwayo. 1997. The Nile perch in Lake Victoria: strong interactions between fishes and fisheries. *Ecological Applications* 7: 653–664.

Klohn, W.; Andjelic, M. (n.d.). *Lake Victoria: A Case in International Cooperation*. Rome: FAO
[Available online:
<http://www.fao.org/waicent/faoinfo/agricult/agl/aglw/webpub/lakevic/lakevic4.htm>]

Kolding, J., Haug, L. and Stefansson, S. 2008 (a). Effect of oxygen on growth and reproduction in Nile tilapia (*Oreochromis niloticus*). *Canadian Journal of Fisheries and Aquatic Sciences* Vol. 65: 1413-1424.

Kolding, J.; van Zwieten, P.; Mkumbo, O.; Silsbe, G.; Hecky, R. 2008 (b). Are the Lake Victoria fisheries threatened by exploitation or eutrophication? Towards an ecosystem based approach to management :309-350 In: Bianchi, G., Skjoldal, H.R. (eds) 2008. *The Ecosystem Approach to Fisheries*. Rome: FAO.

- Korneliussen, R. J., and Ona, E. 2003. Synthetic echograms generated from the relative frequency response. *ICES Journal of Marine Science*, 60: 636–640.
- Ligtvoet W & Mkumbo O.C. (1990) Synopsis of ecological and fishery research on Nile perch (*Lates niloticus*) in Lake Victoria, conducted by HEST/TAFIRI. In: *CIFA Report of the fifth session of the sub-committee for the development and management of the fisheries in Lake Victoria, 12-14 September 1989, Mwanza, Tanzania. FAO Fisheries Report 430: 35-74.*
- Ligtvoet, W.; Mkumbo, O.; Mous, P.; Goudswaard, P. 1995. Monitoring fish stocks from survey data. Chapter 5. in: Witte, F. and Van Densen, W.L.T. (eds.). 1995. *Fish stocks and fisheries of Lake Victoria. A handbook for field observations.* Dyfed: Samara Publishing Limited.
- LVFO 2007. Technical report on Bottom trawl, biological and environmental monitoring survey in Lake Victoria – October 2007 (Tanzania). Implementation of a Fisheries Management Plan Report, Jinja: Lake Victoria Fisheries Organization.
- LVFO 2008. Technical Report: Stock assessment task force. Implementation of a Fisheries Management Plan, Jinja: Lake Victoria Fisheries Organization.
- LVFO 2009. Report of the lake-wide acoustic survey, 16 August-11 September 2009. Implementation of a Fisheries Management Plan Report, Jinja: Lake Victoria Fisheries Organization.
- LVFO website [Consulted in March 2009] <http://www.lvfo.org/>
- MacLennan, D.N. 1990. Acoustical measurement of fish abundance. *Journal of Acoustical Society of America*. 87 (1): 1-15.
- Manyala, J.O. 2005 Chapter 1 in: *Synthesis Report on Fisheries Research and Management.* Lake Victoria Environment Management Project (LVEMP). Draft Report.
- Mathews, W. 1998. *Patterns in freshwater fish ecology.* New York : Chapman & Hall.
- Matsuishi, T, Muhoozi, L., Mkumbo, O.C., Budeba, Y., Njiru, M., Asila, A., Othina, A. and Cowx, I.G. 2006. Are the exploitation pressures on the Nile perch fisheries resources of Lake Victoria a cause for concern? *Fisheries Management and Ecology* 13:53-71.
- Marsh, A.; Ribbink, A. 1986. Feeding schools among Lake Malawi cichlid fishes. *Environmental Biology of Fishes* 15: (1) 75-79.

- Mkumbo, O.; Ligtvoet, W. 1992. Changes in the diet of Nile Perch, *Lates niloticus* (L), in the Mwanza Gulf, Lake Victoria. *Hydrobiologia* 232 : 79-83.
- Mkumbo, O.C. 2002. *Assessment and management of Nile perch (Lates niloticus L.) stocks in the Tanzanian waters of Lake Victoria*. PhD Thesis, University of Hull.
- Mlaponi, E. 2006. *Technical report on Bottom trawl, biological and environmental monitoring survey in Lake Victoria – December 2006 (Tanzania)*. Implementation of a Fisheries Management Plan Report, Mwanza: Lake Victoria Fisheries Organization.
- Mlaponi, E., A. S. E. Mbonde, R. Waya and Y.L. Budeba. 2006. *Technical report on Bottom trawl, biological and environmental monitoring survey in Lake Victoria – March 2006 (Tanzania)*. Implementation of a Fisheries Management Plan Report, Mwanza: Lake Victoria Fisheries Organization.
- Mlaponi, E.; Ezekiel, C.N.; Mbonde, A.S.E.; and Waya, R. 2005. *Technical report on Bottom trawl, biological and environmental monitoring survey in Lake Victoria – November 2005 (Tanzania)*. Implementation of a Fisheries Management Plan Report, Mwanza: Lake Victoria Fisheries Organization.
- Mlaponi, E.; Mbonde, A.; Waya, R.; and Budeba, Y. 2006. *Technical report on Bottom trawl, biological and environmental monitoring survey in Lake Victoria – March 2006 (Tanzania)*. Implementation of a Fisheries Management Plan Report, Mwanza: Lake Victoria Fisheries Organization.
- Moyle, P.B. and J.J. Cech, Jr. 2004 *Fishes: an introduction to ichthyology*. Upper Saddle River: Prentice Hall.
- Mwakosya, C.; Mgaya, Y.D.; and Mahongo, S. 2005. Environmental quality. Chapter 3. 23-39. In: Mgaya, Y. D. (Ed.). 2005. *Synthesis Report on Fisheries Research and Management. Lake Victoria Environment Management Project (LVEMP). Final Report. Tanzania*.
- Odada, E. and Olago, D. 2006. Challenges of an ecosystem approach to water monitoring and management of the African Great Lakes. *Aquatic Ecosystem Health & Management* 9 (4): 433 – 446.

- Odada, E.O.; Olago, D.; Kulindwa, K.A.A.; Bugenyi, F.; West, K.; Ntiba, M.; Wandiga, S.; Karimumuryango, J. 2004. *East African Rift Valley Lakes, GIWA Regional assessment 47*. UNEP, University of Kalmar, Sweden.
- Ogutu-Ohwayo, R.; Twongo, T.; Wandera, S.B.; Balirwa, J.B. 1991. *Suggestion to set mesh size limits and restrict the fishing methods and the types of fishing gears on the Lakes Victoria and Kyoga*. [Available online: <http://www.oceandocs.org/bitstream/1834/1278/1/9290640789-P139152.pdf>]
- Ogutu-Ohwayo, R. 1988 Reproductive potential of the Nile perch, *Lates niloticus* L. and the establishment of the species in Lakes Kyoga and Victoria (East Africa). *Hydrobiologia* 162:193-200.
- Ogutu-Ohwayo, R. 2004. Management of the Nile perch, *Lates niloticus* fishery in Lake Victoria in light of the changes in its life history characteristics. *African Journal of Ecology*, 42, 306–314.
- Okemwa, E. N. 1984. Potential fishery of Nile perch *Lates niloticus* Linne (Pisces: Centropomidae) in Nyanza Gulf of Lake Victoria, East Africa. *Hydrobiologia* 108: 121-126.
- Ona E.; Mitson R. B. 1996. Acoustic sampling and signal processing near the seabed: the deadzone revisited. *ICES Journal of Marine Science*, 53: 677–690.
- Ona, E. (ed.) 1999a. Methodology for Target Strength Measurements. International Council for the Exploration of the Sea. *Cooperative Research Report*, 235: 1–58.
- Ona, E. 1999b. Determining the entrance position of fish in trawls. *International Council for the Exploration of the Sea*. 13: 1-10.
- Ona, E. 2009. *Introduction to acoustics* (course material). University of Bergen.
- Parker-Stetter, S.L., Rudstam, L.G., Sullivan, P.J., and Warner, D.M. 2009. Standard operating procedures for fisheries acoustic surveys in the Great Lakes. In: *Great Lakes Fisheries Commission Special Publication 09-01*. [Available online: http://www.glfc.org/pubs/SpecialPubs/Sp09_1.pdf]
- Pfliegner, K. 2008. Harnessing natural resources for sustainable growth. In: Utz, R.J. (Ed.) *Sustaining and sharing economic growth in Tanzania*. Washington, D.C.: World Bank. 341p.

- Reynisson 1999. Split beam method: 19-27 in Ona, E. (ed.) 1999a. Methodology for Target Strength Measurements. *International Council for the Exploration of the Sea. Cooperative Research Report*, 235: 1–58.
- Salehe, M.A. 2008. *Capability and legitimacy of Beach Management Units (BMU's) to improve fisher's income through management of first-hand sales system in Lake Victoria – Tanzania*. Master thesis in International Fisheries Management, University of Tromsø. 107p.
- Schofield, P. J. & Chapman, L. J. 2000. Hypoxia tolerance of introduced Nile perch: Implications for survival of indigenous fishes in the Lake Victoria basin. *African Zoology* 35, 35–42.
- Schofield, P.J.; Chapman, L.J. 1999. Interactions between Nile perch, *Lates niloticus*, and other fishes in Lake Nabugabo, Uganda. *Environmental Biology of Fishes* 55: 343–358.
- Scullion, J. 2005. *Inland fisheries Co-Management in East Africa*. Jinja: Lake Victoria Fisheries Organization.
- Seabird 2009. *SBE 19 SEACAT profiler operator manual*. [Consulted in May 2010, available online: <http://www.seabird.com/products/profilers.htm>].
- Silsbe, G.M. 2004. *Phytoplankton production in Lake Victoria, East Africa*. MSc. Thesis University of Waterloo, Ontario, Canada.
- Simmonds E. J., MacLennan D. N. 2005. *Fisheries Acoustics: Theory and Practice*. Oxford: Blackwell.
- Smith, V.; Joye, S.; Howarth, R. 2006. Eutrophication of freshwater and marine ecosystems. *Limnology & Oceanography*, Vol. 51 No. 1:351 - 355.
- Tamatamah, R.; Hecky, R.; Duthie, H. 2005. The atmospheric deposition of phosphorus in Lake Victoria (East Africa). *Biogeochemistry*, 73: 325–34
- Vabø, R.; Olsen, K.; Huse, I. 2002. The effect of vessel avoidance of wintering Norwegian spring spawning herring. *Fisheries Research* 58: 59–77.
- Van der Knaap, M., Roest, F. C. and Munawar, M.(2007)'Great Lake Victoria fisheries: Changes and sustainability, and Building Blocks for Management, *Aquatic Ecosystem Health & Management*, 10(4) : 481- 483.

- Verreth, J.; van Zwieten, P.; Nagelkerke, L. (2007). *Exploitation or eutrophication as threats for fisheries? Disentangling social and ecological drivers of ecosystem changes in Lake Victoria, Tanzania (SEDEC)*. Project proposal for the WOTRO/DGIS Science for Global Development Programme. 2007. Wageningen University, Aquaculture and Fisheries Group. Netherlands. [Available online: http://www.afi.wur.nl/UK/Research/Projects_SEDEC/]
- Walsh, S. 1996. Efficiency of Bottom Sampling Trawls in Deriving Survey Abundance Indices. *NAFO Science Council Studies*, 28: 9–24.
- Wanink, J. and Joordens, J. 2007. Dietary shifts in *Brycinus sadleri* (Pisces: Characidae) from southern Lake Victoria, *Aquatic Ecosystem Health & Management*, 10(4) : 392 - 397.
- Wardle C.S. 1993. Fish behaviour and fishing gear: 609–643. In Pitcher T.J. (Ed.). *Behaviour of Teleost Fishes*. London: Chapman and Hall.
- [Wetzel, R.](#) 2001. *Limnology: lake and river ecosystems*. San Diego: Academic Press. 3rd ed.
- Wileman, D.; Ferro, R.; Fonteyne, R.; Myllar, R. (Ed). 1996. *Manual of methods of measuring the selectivity of towed fishing gears*. ICES Cooperative research report. N. 215. Copenhagen: ICES.
- Witte, F. and Van Densen, W.L.T. (eds.). 1995. *Fish stocks and fisheries of Lake Victoria. A handbook for field observations*. Dyfed: Samara Publishing Limited.
- Witte, F., J. H. Wanink, H. A. Rutjes, H. J. van der Meer, and G. E. E. J. M. van den Thillart. 2005. Eutrophication and its influences on the fish fauna of Lake Victoria: 301–338 in M. V. Reddy, editor. *Restoration and management of tropical eutrophic lakes*. Enfield: Science Publishers.
- Witte, F., J. H. Wanink, M. A. Kische, O. C. Mkumbo, P. C. Goudswaard, and O. Seehausen. 2007. Differential decline and recovery of haplochromine trophic groups in the Mwanza Gulf of Lake Victoria. *Aquatic Ecosystem Health and Management*. 10(4): 416–433.
- Wootton, R. 1998. *Ecology of teleost fishes*. Chapman & Hall fish and fisheries series; 24. Dordrecht: Chapman & Hall. 2nd edition.
- Yin, X.; Nicholson, S. 1998. The water balance of Lake Victoria. *Hydrological Sciences Journal*, 43(5): 789-811.

7 Appendixes

Appendix I – Terminology

Appendix II – Survey details

Appendix III – Acoustic equipment calibration

Appendix IV – CTD and trawl sampling stations

Appendix V – CDT results

Appendix VI – Relation between the limnological variables

Appendix VII – Biological data analysis results

Appendix VIII – Target strength analysis results

Appendix IX – Graphs of TS and fish density distribution

Appendix X – Relation between TS and the limnological data

Appendix XI – Validation of the TS measurements

Appendix XII – Echograms

Appendix XIII – Fish density results

Appendix XIV – List of equations used

Appendix I – Terminology

Acoustic deadzones - region of the water column where no fish detection is possible (Ona & Mitson 1996). The acoustic sampling of the entire water column is limited by the existence of two acoustic deadzones. One of them is found below the transducer face, while the other zone is located at the bottom (0.5m typically for flat bottom less than 100m depth) (Aglen 1994).

Acoustic blindzone – one of the regions where there is no fish detection, referring usually to the surface exclusion zone. The blindzone is formed by the surface deadzone plus the depth of the transducer relative to surface (Ona 2009).

Area scattering coefficient (s_a [$m^2 m^{-2}$]) – measure of energy returned from a layer in the water column, in meters (Simmonds & MacLennan 2005).

Backscattering cross section (σ) – The backscattering cross section (σ) relates to the acoustic properties of the target reflected at a certain frequency, while the target strength (TS) is the logarithmic conversion of the backscattering cross section (Simmonds & MacLennan 2005; Horne 2000). The relation between σ and TS is described by the equation: $\sigma = 4\pi 10^{TS/0,1}$.

Beam pattern – expresses the change in sensitivity of the transducer on the different directions (both in transmission and reception of the sound) (Simmonds & MacLennan 2005).

Beam width – describe the angles, measured in degrees, between the lines that represent the half intensity (or 3dB less) than the acoustic axis. These angles can be measured both along and athwardship, in the case of elliptical beams (Parker-Stetter *et al.* 2009, Simmonds & MacLennan 2005).

Catchability – refers to the number of fish that is in the area swept by the trawl and is captured by the gear (Grosslein & Laurec 1982).

Equivalent beam angle – also expresses the beam pattern, although it is expressed in steradians. This measures all the insonified volume, including the side lobes, of the transducer.

Far field – within this region, the beam spreads in accordance to the inverse square law, being described by the equation $I = \frac{I_0}{R^2}$ (Simmonds & MacLennan 2005).

Appendix I - Terminology

Frequency response – defined as the ratio between the volume backscattering coefficient at two frequencies. It is described by the equation $r(f) = \frac{s_v(f)}{s_v}$ (Korneliussen & Ona 2002), where $s_v(f)$ is the volume backscattering coefficient at a reference frequency.

Lobe – area of the beam with higher sensitivity (Simmonds & MacLennan 2005).

Nautical area scattering coefficient (s_A [$m^2 \text{ nmi}^{-2}$]) - measure of the energy returned from a layer of the water column (Simmonds & MacLennan 2005).

Near field – region below the transducer where the intensity of the acoustic signal cannot be predicted, as in the far field region. This region does not follow the same mathematical expression (Simmonds & MacLennan 2005).

Scope ratio – defined by the warp length divided by towing depth (Engås 1994).

Split beam transducer – the beam is divided into four quadrants, which transmit and receive signals simultaneously. The signals from these four quadrants are then combined to form the full beam, as to give the position of the target in relation to the transducer (Reynisson 1999).

Sweeps – cables connecting the otter doors to the bridles (Walsh 1996).

Swept area – area calculated by the distance of the wing spread along the tow distance (Walsh 1996).

Target strength – is the logarithmic conversion of the backscattering cross section. Express the size of the echo, in dB, and be converted mathematically to fish length (Simmonds & MacLennan 2005; Horne 2000).

Tilt angle – orientation of the fish in relation to the horizontal plane. This orientation is determinant to the intensity of the target backscattered echo and the highest echo is obtained when fish's swimbladder (its longitudinal axis) is perpendicular to the sound beam axis (Aglen 1994).

Trawl doors (same as otter boards) – Devices that allow the horizontal opening of the trawl opening (referred as trawl mouth) (Wileman *et al.* 1996).

Volume scattering coefficient (s_v [$m^3 \text{ m}^{-3}$]) – measure of energy returned from a layer in the water column, in meters (Simmonds & MacLennan 2005).

Warps – steel cables which connect the trawl doors to the vessel (Wileman *et al.* 1996).

Appendix II – Survey details

The survey Event Log shows a record of all the events occurred during the survey. These events are numbered, the type of event is described (in Activt column), the time is recorded and are located in terms its quadrant location as well the type of strata where these are.

DH – Code to deadhead transect which is the interval between two transects.

TI – Code to Inshore transect.

TC – Code for coastal transect.

TD – Code for deep transect.

CTD – Environmental data sampling.

DR – Code to the drift station.

NB – Code for bottom trawl sampling.

The type of strata where the survey event is taking place is also recorded (Strat column).

Table 1 - EVENT LOGSHEET, IFMP August 2009 ACOUSTIC SURVEY

Date	Event No.	Activt	Stn	Quadrant	Strata	Time Start GMT +3	Time End GMT +3	Remarks
16/08/09	1	DH		SW	I	0951	1013	Left Ilemera
	2	TI		SW	I	1013	1123	
	3	DH		SW	I	1123	1150	
	4	TC		SW	C	1150	1319	
	5	CTD	1	SW	C	1321	1331	
	6	DR	1	SW	C	1331	1346	
	7	DH		SW	C	1348	1440	
	8	TC		SW	C	1440	1609	
	9	TI		SW	I	1609	1720	
	10	CTD	2	SW	I	1720	1728	
	11	DR	2	SW	I	1728	1738	
	12	NB	2	SW	I	1745	1816	
	13	DH		SW	I	1826	1850	
17/08/09	14	TI		SW	I	0629	0743	Couldn't fish due to rough ground
	15	TC		SW	C	0743	0927	
	16	DH		SW	C	0927	1024	
	17	CTD	3	SW	C	1026	1033	
	18	DR	3	SW	C	1033	1048	
	19	TC		SW	C	1049	1242	
	20	TI		SW	I	1242	1345	
	21	CTD	4	SW	I	1347	1354	
	22	DR	4	SW	I	1354	1409	
	23	DH		SW	I	1425	1505	
	24	NB	4	SW	I	1511	1542	
	25	DH		SW	I	1554	1616	
18/08/09	26	DH		SW	I	0629	0636	
	27	TI		SW	EP	0636	0723	
	28	TI		SW	EP	0723	0804	
	29	CTD	5	SW	EP	0805	0814	
	30	DR	5	SW	EP	0814	0830	
	31	NB	5	SW	EP	0836	0905	

Appendix II – Survey Details

	32	TI		SW	EP	0916	1017	
	33	TI		SW	EP	1017	1133	
	34	TI		SW	EP	1133	1250	
	35	TI		SW	I	1250	1420	
	36	CTD	6	SW	I	1422	1431	
	37	DR	6	SW	I	1431	1446	
	38	NB	6	SW	I	1452	1522	
	39	DH		SW	I	1540	1555	End of the day Ruega Point
19/08/09	40	DH		SW	I	0650	0710	
	41	TI		SW	I	0710	0816	
	42	CTD	7	SW	C	0817	0823	
	43	DR	7	SW	C	0823	0838	
	44	NB	7	SW	C	0846	0916	
	45	DH		SW	C	0936	1041	
	46	TC		SW	C	1041	1256	
	47	CTD	8	SW	C	1258	1305	
	48	DR	8	SW	C	1305	1320	
	49	DH		SW	C	1321	1348	
	50	TC		SW	C	1348	1518	
	51	DH		SW	C	1518	1548	
	52	CTD	9	SW	C	1550	1556	
	53	DR	9	SW	C	1556	1611	
	54	NB	9	SW	C	1618	1649	
	55	DH		SW	C	1704	1721	End of day Kerebe Is.
20/08/09	56	DH		SW	C	0331	0506	
	57	TD		SW	D	0506	0849	
	58	CTD	10	SW	D	0849	0857	
	59	DR	10	SW	D	0857	0907	
	60	DH		SW	D	0908	1002	
	61	TD		SE	D	1002	1401	
	62	TC		SE	C	1401	1540	
	63	TI		SE	I	1540	1651	
	64	DH		SE	I	1651	1700	End of Day Musoma
21/08/09	65	DH		SE	C	0340	0444	
	66	DH		SE	D	0444	0648	
	67	TD		SE	D	0648	1056	
	68	CTD	11	SE	D	1057	1105	
	69	DR	11	SE	D	1105	1120	
	70	DH		SE	D	1121	1200	
	71	TD		SW	D	1200	1539	
	72	DH		SW	C	1539	1542	
	73	CTD	12	SW	C	1542	1551	
	74	DR	12	SW	C	1551	1601	
	75	NB	12	SW	C	1608	1641	
	76	DH		SW	C	1655	1750	End of Day Kerebe Is.
22/08/09	77	DH		SW	C	0639	0659	
	78	TC		SW	C	0659	0937	
	79	DH		SW	I	0937	1007	
	80	TI		SW	I	1007	1059	
	81	CTD	13	SW	I	1101	1107	
	82	DR	13	SW	I	1107	1123	
	83	NB	13	SW	I	1130	1200	
	84	TI		SW	I	1213	1314	
	85	CTD	14	SW	I	1315	1323	
	86	DR	14	SW	I	1323	1333	

Appendix II – Survey Details

	87	NB	14	SW	I	1345	1416	
	88	TI		SW	I	1434	1521	End of Day Bukoba
11/09/09	328	DH		SE	I	0559	0602	
	329	TI		SE	SG	0602	0733	
	330	DH		SE	SG	0733	0844	
	331	CTD	53	SE	SG	0845	0850	
	332	DR	53	SE	SG	0850	0900	
	333	TI		SE	SG	0901	1014	
	334	DH		SE	SG	1014	1102	
	335	CTD	54	SE	SG	1103	1108	
	336	DR	54	SE	SG	1108	1121	
	337	NB	54	SE	SG	1128	1200	
	338	TI		SE	SG	1212	1318	
	339	DH		SE	SG	1318	1423	
	340	TI		SE	SG	1423	1502	
	341	DH		SE	SG	1502	1540	
	342	CTD	55	SE	SG	1541	1547	
	343	DR	55	SE	SG	1547	1603	
	344	NB	55	SE	SG	1611	1641	
	345	TI		SE	SG	1652	1738	End of survey Nyamikoma

Appendix III – Acoustic equipment calibration

2.1. Calibration settings

2.1.1. 70 kHz transducer, First calibration results

Calibration Version 2.1.0.11

Date: 8/14/2009

Comments:

Reference Target:

TS	-39.10 dB	Min. Distance	7.00 m
TS Deviation	5.0 dB	Max. Distance	8.50 m

Transducer:	ES70-7C	Serial No.	70140809
Frequency	70000 Hz	Beamtype	Split
Gain	26.41 dB	Two Way Beam Angle	-21.0 dB
Athw. Angle Sens.	23.00	Along. Angle Sens.	23.00
Athw. Beam Angle	6.57 deg	Along. Beam Angle	6.65 deg
Athw. Offset Angle	-0.02 deg	Along. Offset Angle	-0.07 deg
SaCorrection	-0.78 dB	Depth	1.80 m

Transceiver:	GPT 70 KHz 00907205aebd 3-1 ES70-7C		
Pulse Duration	0.256 ms	Sample Interval	0.048 m
Power	200 W	Receiver Bandwidth	6.16 KHz

Sounder Type:

EK60 Version 2.2.0

TS Detection:

Min. Value	-60.0 dB	Min. Spacing	100 %
Max. Beam Comp.	6.0 dB	Min. Echolength	80 %
Max. Phase Dev.	8.0	Max. Echolength	180 %

Environment:

Absorption Coeff.	0.8 dB/km	Sound Velocity	1499.3 m/s
-------------------	-----------	----------------	------------

Beam Model results:

Transducer Gain	= 26.30 dB	SaCorrection	= -0.80 dB
Athw. Beam Angle	= 6.64 deg	Along. Beam Angle	= 6.65 deg
Athw. Offset Angle	= -0.02 deg	Along. Offset Angle	= -0.06 deg

Data deviation from beam model:

RMS	= 0.14 dB
Max	= 0.28 dB No. = 56 Athw. = -2.8 deg Along = -2.2 deg
Min	= -0.47 dB No. = 391 Athw. = 1.1 deg Along = -4.6 deg

Data deviation from polynomial model:

RMS	= 0.08 dB
Max	= 0.34 dB No. = 376 Athw. = 0.5 deg Along = -1.1 deg
Min	= -0.22 dB No. = 126 Athw. = -2.1 deg Along = -0.2 deg

Appendix III – Acoustic Equipment Calibration

2.1.2. 70 kHz transducer, second calibration results (09-09-2009)

Calibration Version 2.1.0.11

Date: 9/9/2009

Comments:

Reference Target:

TS	-39.10 dB	Min. Distance	8.60 m
TS Deviation	5.0 dB	Max. Distance	9.60 m

Transducer: ES70-7C	Serial No.	70090909	
Frequency	70000 Hz	Beamtype	Split
Gain	26.30 dB	Two Way Beam Angle	-21.0 dB
Athw. Angle Sens.	23.00	Along. Angle Sens.	23.00
Athw. Beam Angle	6.64 deg	Along. Beam Angle	6.65 deg
Athw. Offset Angle	-0.02 deg	Along. Offset Angle	-0.06 deg
SaCorrection	-0.80 dB	Depth	1.80 m

Transceiver: GPT 70 kHz 00907205aebd 3-1 ES70-7C			
Pulse Duration	0.256 ms	Sample Interval	0.048 m
Power	200 W	Receiver Bandwidth	6.16 kHz

Sounder Type:

EK60 Version 2.2.0

TS Detection:

Min. Value	-50.0 dB	Min. Spacing	100 %
Max. Beam Comp.	6.0 dB	Min. Echolength	80 %
Max. Phase Dev.	8.0	Max. Echolength	180 %

Environment:

Absorption Coeff.	0.8 dB/km	Sound Velocity	1499.3 m/s
-------------------	-----------	----------------	------------

Beam Model results:

Transducer Gain	= 26.45 dB	SaCorrection	= -0.72 dB
Athw. Beam Angle	= 6.56 deg	Along. Beam Angle	= 6.57 deg
Athw. Offset Angle	= -0.02 deg	Along. Offset Angle	= -0.08 deg

Data deviation from beam model:

RMS	= 0.15 dB		
Max	= 0.83 dB	No. = 180	Athw. = 2.5 deg Along = -4.0 deg
Min	= -0.75 dB	No. = 319	Athw. = -3.9 deg Along = 0.2 deg

Data deviation from polynomial model:

RMS	= 0.11 dB		
Max	= 0.91 dB	No. = 180	Athw. = 2.5 deg Along = -4.0 deg
Min	= -0.67 dB	No. = 319	Athw. = -3.9 deg Along = 0.2 deg

Appendix III – Acoustic Equipment Calibration

2.1.3. 120 kHz transducer, second calibration results (09-09-2009)

Calibration Version 2.1.0.11

Date: 9/9/2009

Comments:

Reference Target:

TS	-40.40 dB	Min. Distance	8.00 m
TS Deviation	5.0 dB	Max. Distance	9.00 m

Transducer: ES120-7C	Serial No.	120090909	
Frequency	120000 Hz	Beamtype	Split
Gain	25.93 dB	Two Way Beam Angle	-21.0 dB
Athw. Angle Sens.	23.00	Along. Angle Sens.	23.00
Athw. Beam Angle	6.53 deg	Along. Beam Angle	6.48 deg
Athw. Offset Angle	0.04 deg	Along. Offset Angle	0.06 deg
SaCorrection	-0.58 dB	Depth	1.80 m

Transceiver: GPT 120 KHz 00907205b606 1-1 ES120-7C			
Pulse Duration	0.256 ms	Sample Interval	0.048 m
Power	200 W	Receiver Bandwidth	8.71 kHz

Sounder Type:

EK60 Version 2.2.0

TS Detection:

Min. Value	-50.0 dB	Min. Spacing	100 %
Max. Beam Comp.	6.0 dB	Min. Echolength	80 %
Max. Phase Dev.	8.0	Max. Echolength	180 %

Environment:

Absorption Coeff.	2.5 dB/km	Sound Velocity	1499.3 m/s
-------------------	-----------	----------------	------------

Beam Model results:

Transducer Gain	= 25.69 dB	SaCorrection	= -0.60 dB
Athw. Beam Angle	= 6.51 deg	Along. Beam Angle	= 6.48 deg
Athw. Offset Angle	= 0.01 deg	Along. Offset Angle	= 0.07 deg

Data deviation from beam model:

RMS	= 0.19 dB				
Max	= 0.65 dB	No. = 231	Athw. = 0.3 deg	Along = -4.2 deg	
Min	= -0.77 dB	No. = 208	Athw. = -3.3 deg	Along = -2.6 deg	

Data deviation from polynomial model:

RMS	= 0.16 dB				
Max	= 0.57 dB	No. = 173	Athw. = -2.8 deg	Along = -0.6 deg	
Min	= -0.49 dB	No. = 225	Athw. = 0.8 deg	Along = -2.1 deg	

Appendix IV – CTD and trawl sampling stations

4.1. Limnological sampling

4.1.1. CTD stations' details

Table 1 – Information on the CTD sampling locations

<i>Station</i>	<i>Station Number</i>	<i>Date</i>	<i>Time (GMT +3)</i>	<i>Latitude</i>	<i>Longitude</i>	<i>Quadrant</i>	<i>Strata</i>
Miendere	1	16.08.2009	13:20	-2,07940	32,63628	SW	C
Kome	2	16.08.2009	17:20	-2,43487	32,48628	SW	I
Cherenche	3	17.08.2009	10:25	-1,95690	32,25230	SW	C
Maisome	4	17.08.2009	13:45	-2,33373	32,13738	SW	I
Senga	5	18.08.2009	8:05	-1,95690	32,25230	SW	IEP
Ruega	6	18.08.2009	14:20	-1,99848	31,71827	SW	I
Iroba	7	19.08.2009	8:15	-1,87062	31,82970	SW	C
Bumbire	8	19.08.2009	12:55	-1,73493	32,23423	SW	C
Kerebe Isl.	9	19.08.2009	15:48	-1,47870	32,19448	SW	C
Kamasi	10	20.08.2009	8:50	-1,65817	32,80125	SW	D
Gozibar NE	11	21.08.2009	11:00	-1,22615	32,79925	SE	D
Kerebe NE	12	21.08.2009	15:45	-1,33672	32,24295	SW	C
Bumbure C	13	22.08.2009	11:00	-1,61488	31,79615	SW	I
Makibwa	14	22.08.2009	13:15	-1,47258	31,92005	SW	I
Shoka	53	11.09.2009	8:48	-2,41333	33,24072	SE	ISG
Nafuba	54	11.09.2009	11:08	-2,23602	33,36620	SE	ISG
Bulamba	55	11.09.2009	15:46	-2,21258	33,63483	SE	ISG

4.2. Biological sampling

4.2.1. Trawl stations' details

Table 2 - Information on the trawl sampling locations

Date	Location	Strata	Longitude Start	Latitude Start	Longitude Start	Longitude Start
16/08	Kome	Inshore	2°26'213 S	32° 29'018 E	2° 26'394 S	32° 27'572 E
17/08	Maisome	Inshore	2° 22'483 S	32° 1'777 E	2° 22'660 S	32° 0'277 E
18/08	Senga	Inshore (Emin Pasha Gulf)	2° 33'248 S	31° 58'148 E	2° 33'547 S	31° 56'615 E
18/08	Ruega Point	Inshore	1° 59'472 S	31° 42'980 E	1° 57'494 S	31° 42'350 E
19/08	Iroba Isl.	Coastal	1° 52'367 S	31° 49'972 E	1° 53'178 S	31° 51'046 E
19/08	Kerebe Isl.	Coastal	1° 28'535 S	32° 11'440 E	1° 28'107 S	32° 10'027 E
21/08	Kerebe Isl. North	Coastal	1° 20'340 S	32° 14'119 E	1° 21'735 S	32° 13'256 E
22/08	Bumbire	Inshore	1° 36'632 S	31° 47'994 E	1° 36'108 S	31° 49'360 E
22/08	Makibwa Isl.	Inshore	1° 28'996 S	31° 54'744 E	1° 26'817 S	31° 53'760 E
09/11	Nafuba Isl.	Inshore (Speke Gulf)	2° 14'195 S	33° 21'478 E	2° 14'205 S	33° 22'983 E
09/11	Bulamba	Inshore (Speke Gulf)	2° 12'633 S	33° 38'441 E	2° 11'930 S	33° 39'948 E

Table 3 – Details from the bottom trawl hauls. Details on duration, time (at start and end), depth (refers to the floatline depth) and distance of the haul is detailed.

Location	Time Start	Time End	Duration (min)	Depth Start (m)	Depth End (m)	Mean Depth (m)	Distance (nmi)
Kome	17.46	18.16	30	8.5	8.5	8.5	1.55
Maisome	15.11	15.42	30	17	14	15.5	1.57
Senga	8.35	9.05	30	8.2	9	8.6	1.52
Ruega Point	14.52	15.22	30	23	22.9	22.95	1.45
Iroba	8.46	9.16	30	38	40	39	1.39
Kerebe Isl.	16.18	16.48	30	50	50	50	1.5
Kerebe NE	16.10	16.40	30	50	50	50	1.58
Bumbire	11.30	12.00	30	28.2	30.2	29.2	1.51
Makibwa	13.45	14.15	30	35	33	34	1.59
Nafuba	13.20	11.58	30	13.8	13.3	13.55	1.58
Bulamba	16.10	16.40	30	7.6	7.3	7.45	1.57

4.2.2. Bottom trawl specifications

Bottom Trawl net diagram

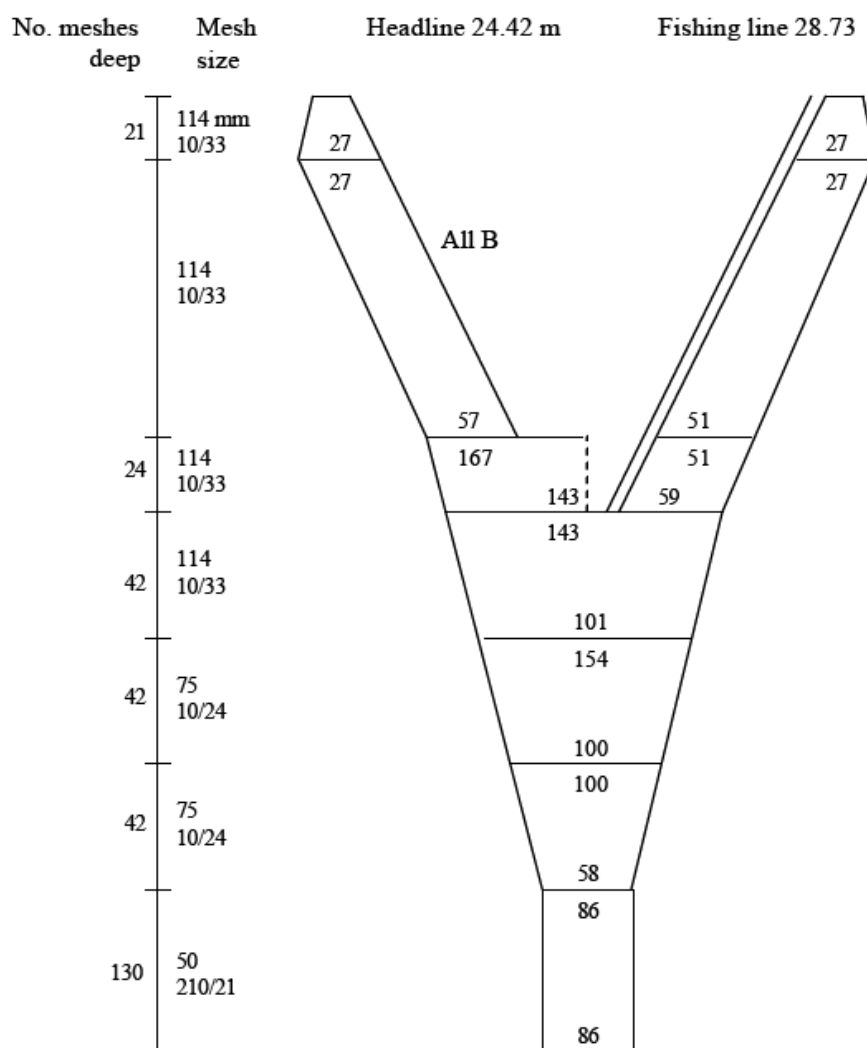


Figure 1 – Bottom trawl net diagram (source: Agnew 2005)

Table 4 – Specifications for bottom trawls from LVFO. Details from the R.V. Victoria Explorer are highlighted in green (source: Agnew 2005).

Vessel	Before November 1998			(LVFRP II)
	<i>R.V. Ibis</i> (Uganda)	<i>R.V. Utafti</i> (Kenya)	<i>R.V. Victoria Explorer</i> (Tanzania)	All
Otterboards	V-type	Flat wooden	V-type	V-type
Backstrops (m)	2.3	3.4	3.0	3.0
Sweep length (m)	15.6	None	15.0	15.0
Bridle length (m)	20.1	13.7	20.0	20.0
Headline length (m)	24.0	21.0	24.0	24.0
Headline height (m)	Not known	Not known	3.0	3.0
Footrope (m)	24.9	Not known	27.6	27.6
Codend mesh (mm)	25.0	25.0	30.0	25.0

Appendix V – CDT results

5.1. Limnological data averaged for each station

Values for each station were calculated by averaging all measurements (app. 3 measurements per meter were taken).

Table 1 – Results from CTD measurements and bottom depth for each station. Oxygen, temperature and chlorophyll a, averaged for the water column.

<i>Name</i>	<i>Strata</i>	<i>Station Number</i>	<i>Bottom depth (m)</i>	<i>Mean temperature (°C)</i>	<i>Mean chlorophyll a ($\mu\text{g l}^{-1}$)</i>	<i>Mean Oxygen (mg l^{-1})</i>
Miendere	C	1	54,55	24,76	4,48	9,30
Kome	I	2	10,22	25,01	25,99	10,23
Cherenche	C	3	57,81	24,83	4,14	9,47
Maisome	I	4	24,76	25,03	9,66	10,03
Senga	IEP	5	10,73	24,76	38,40	9,78
Ruega	I	6	25,03	25,18	11,23	10,21
Iroba	C	7	39,34	24,93	6,93	8,48
Bumbire	C	8	56,31	24,83	4,18	9,28
Kerebe	C	9	51,50	24,88	4,32	9,48
Kamasi	D	10	59,70	25,03	3,53	8,30
Gozibar NE	D	11	67,82	24,92	3,51	8,47
Kerebe NE	C	12	51,79	24,88	3,77	8,71
Bumbure C	I	13	29,44	24,91	5,97	7,72
Makibwa	I	14	37,71	24,87	4,83	7,60
Shoka	ISG	53	22,32	24,63	7,74	7,24
Nafuba	ISG	54	15,44	24,56	18,60	7,75
Bulamba	ISG	55	9,32	25,16	14,16	8,59

5.2. CTD profiles for each station grouped by strata

5.2.1. CTD profiles for the stations in the inshore stratum

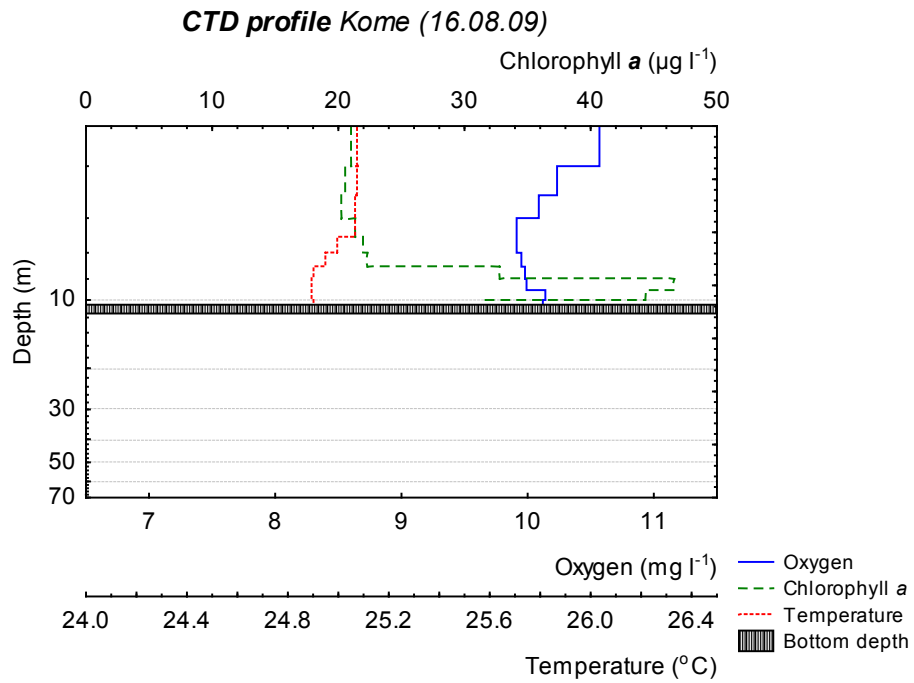


Figure 1 – CTD profiles from Kome station. Oxygen, chlorophyll *a* and temperature values were averaged for each meter.

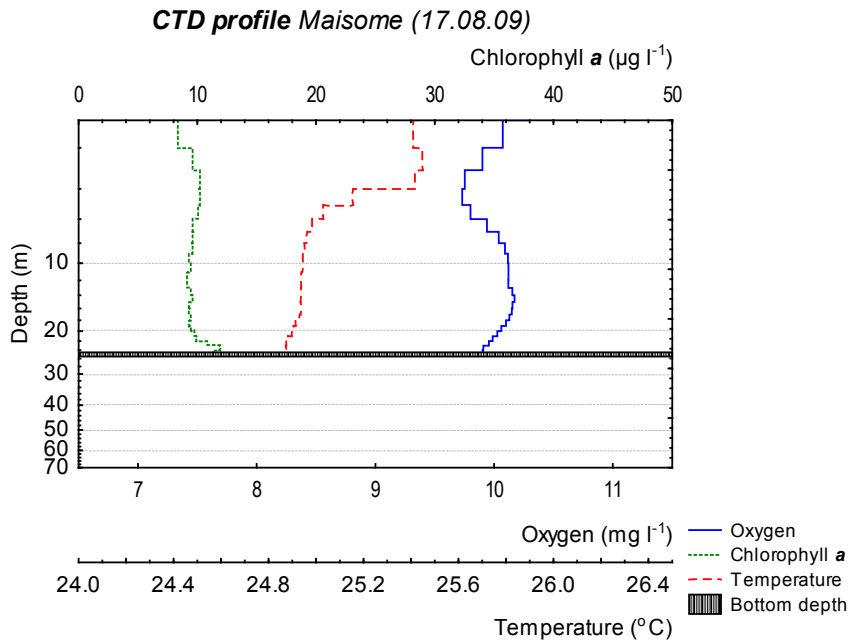


Figure 2 – CTD profiles from Maisome station. Oxygen, chlorophyll *a* and temperature values were averaged for each meter.

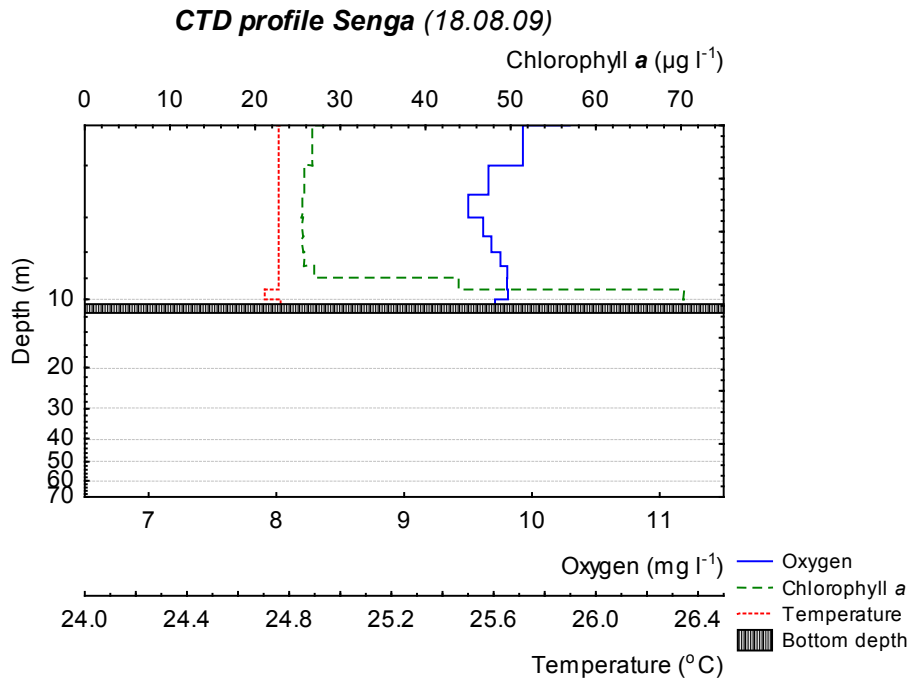


Figure 3 – CTD profiles from Senga station. Oxygen, chlorophyll *a* and temperature values were averaged for each meter (Chlorophyll *a* values are in a different scale from the other graphs).

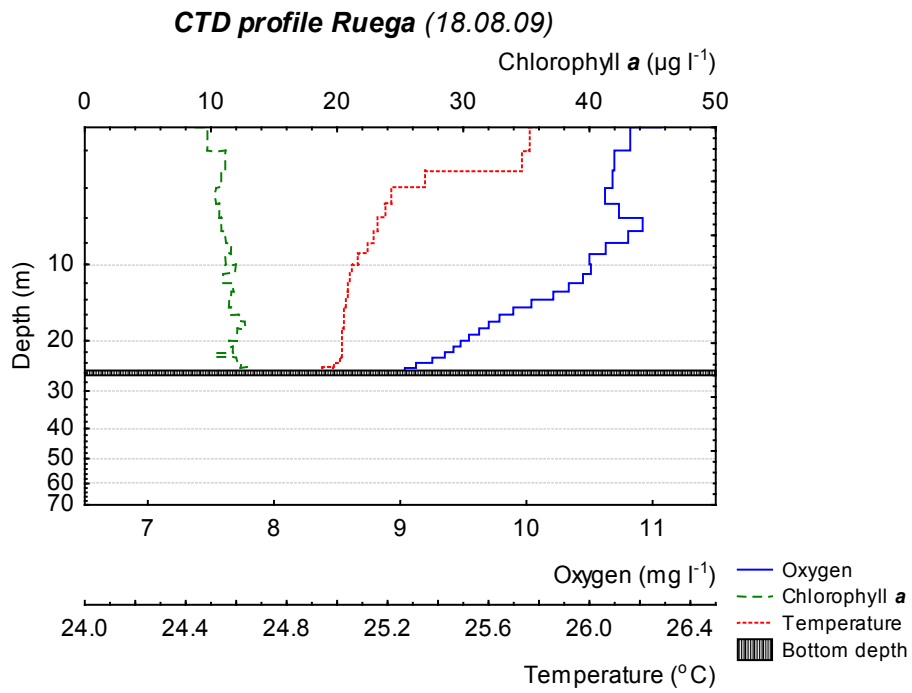


Figure 4 – CTD profiles from Ruega station. Oxygen, chlorophyll *a* and temperature values were averaged for each meter.

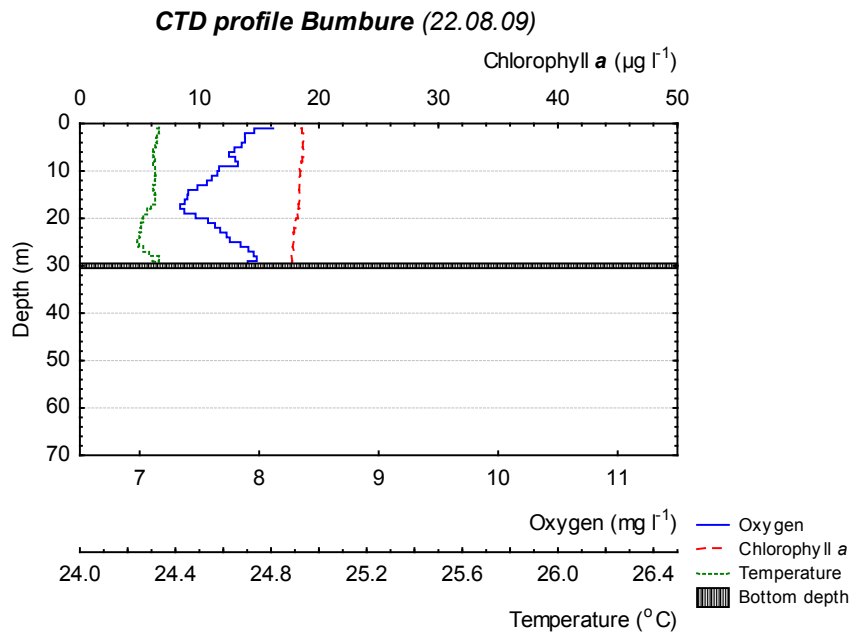


Figure 5 – CTD profiles from Bumbure station. Oxygen, chlorophyll *a* and temperature values were averaged for each meter.

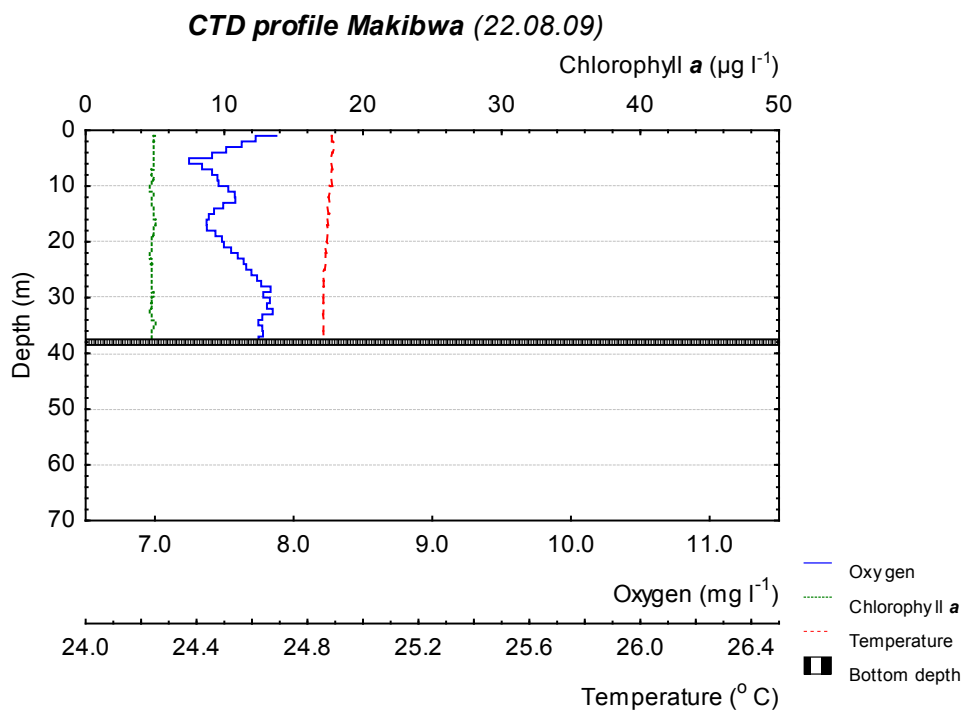


Figure 6 – CTD profiles from Makibwa station. Oxygen, chlorophyll *a* and temperature values were averaged for each meter.

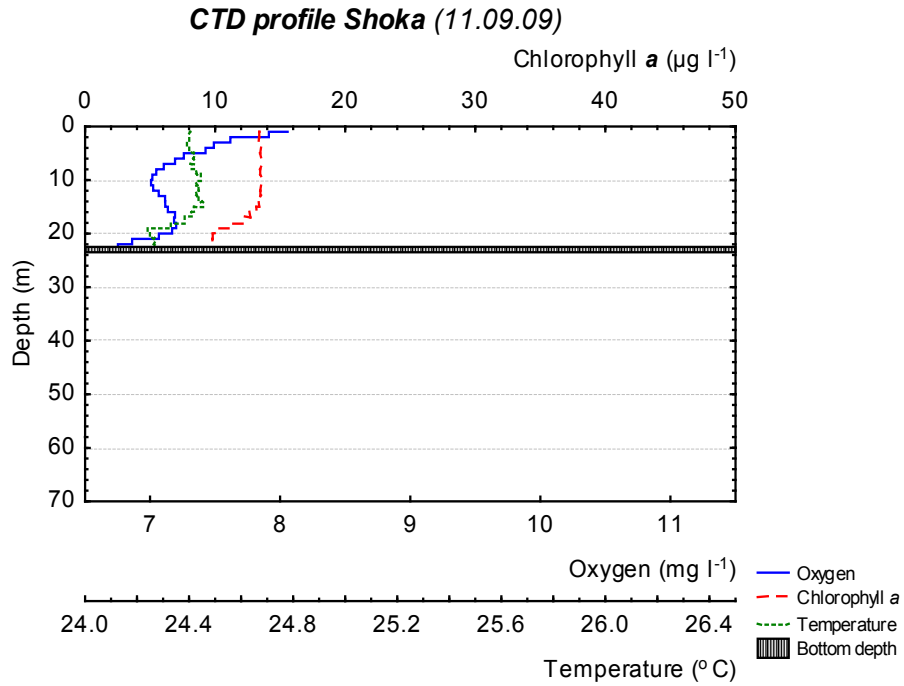


Figure 7 – CTD profiles from Shoka station. Oxygen, chlorophyll *a* and temperature values were averaged for each meter.

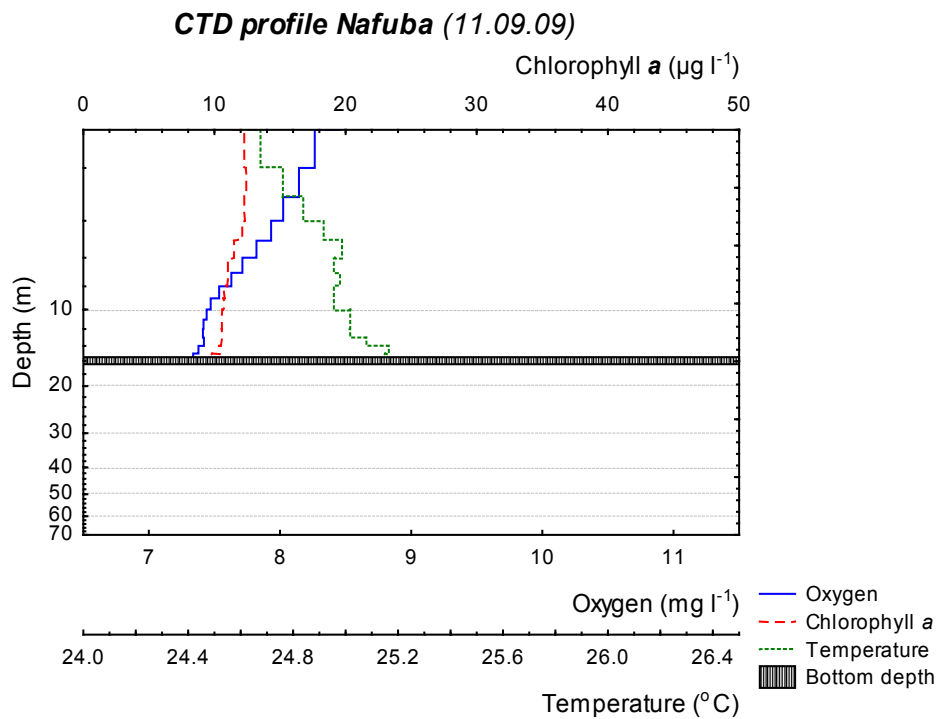


Figure 8 – CTD profiles from Nafuba station. Oxygen, chlorophyll *a* and temperature values were averaged for each meter.

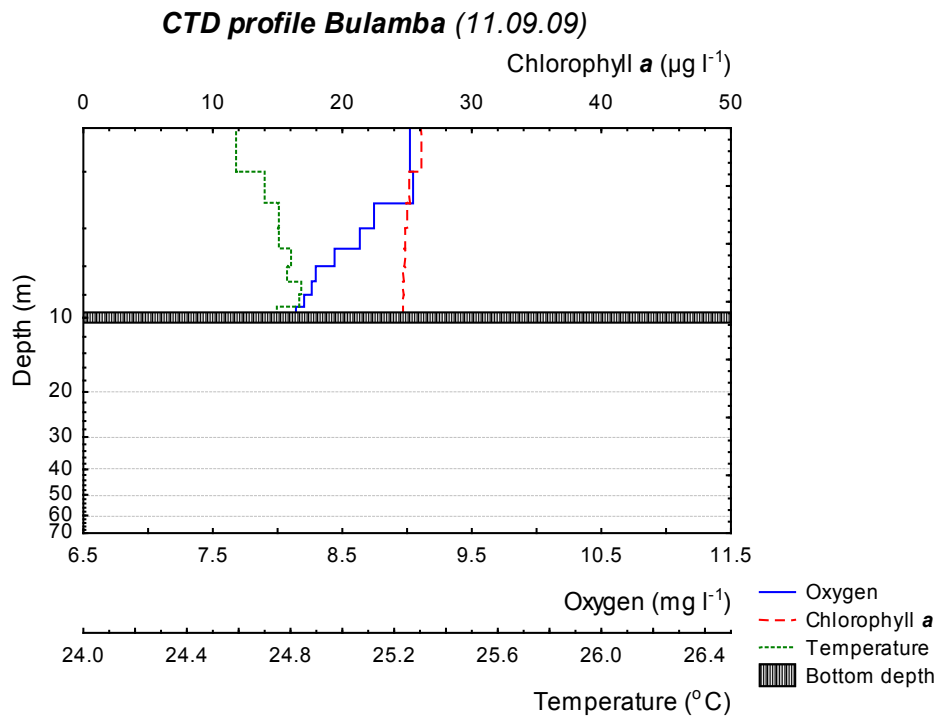


Figure 9 – CTD profiles from Bulamba station. Oxygen, chlorophyll *a* and temperature values were averaged for each meter.

5.2.2. CTD profiles for the stations in the coastal stratum

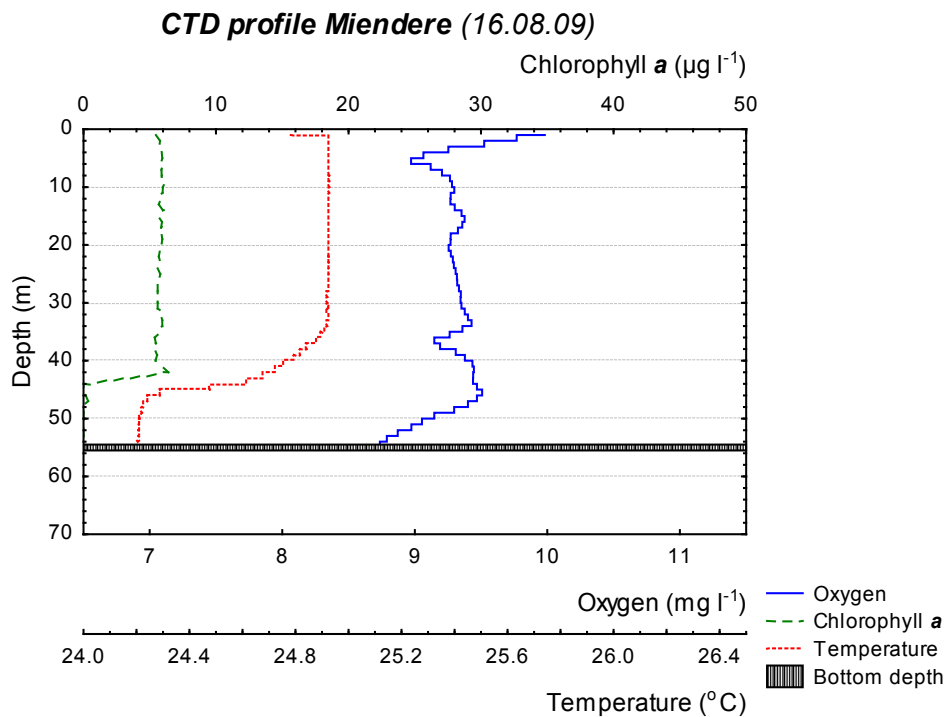


Figure 10 – CTD profiles from Miendere station. Oxygen, chlorophyll *a* and temperature values were averaged for each meter.

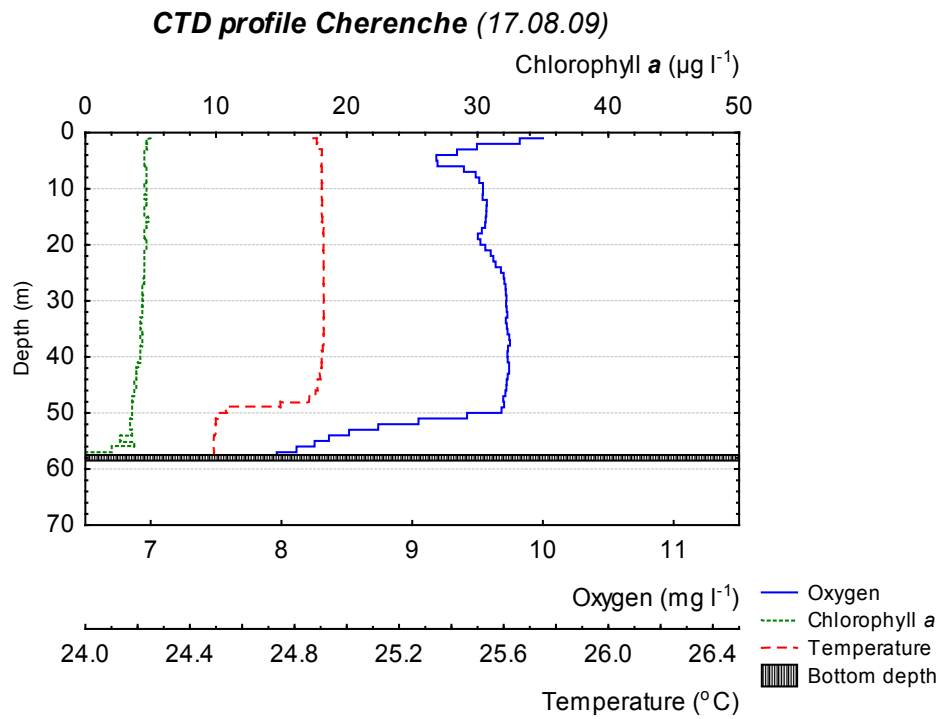


Figure 11 – CTD profiles from Cherenche station. Oxygen, chlorophyll *a* and temperature values were averaged for each meter.

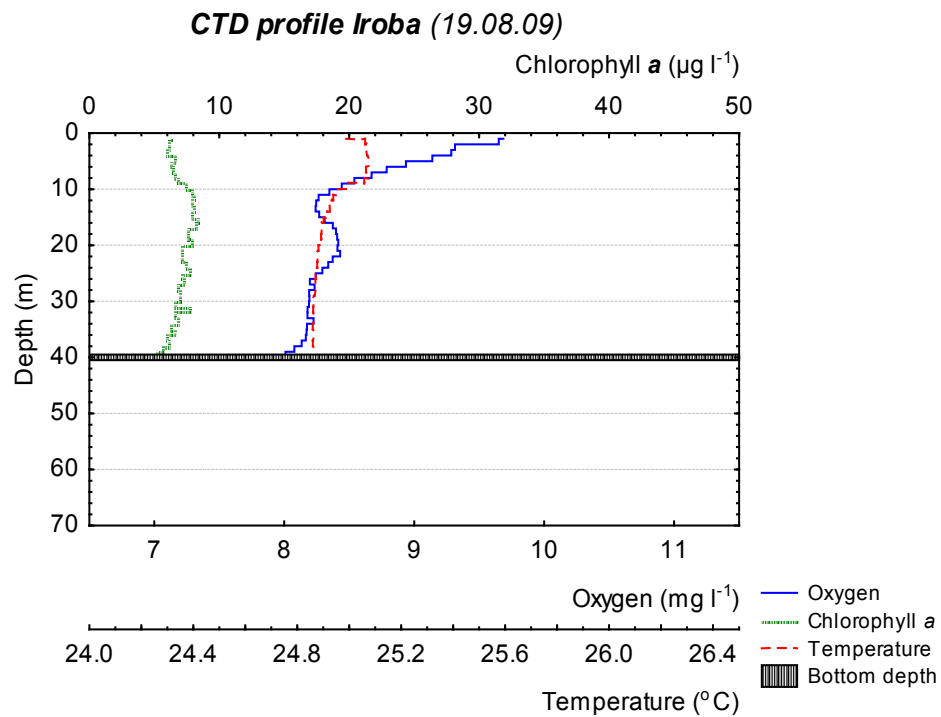


Figure 12 – CTD profiles from Iroba station. Oxygen, chlorophyll *a* and temperature values were averaged for each meter.

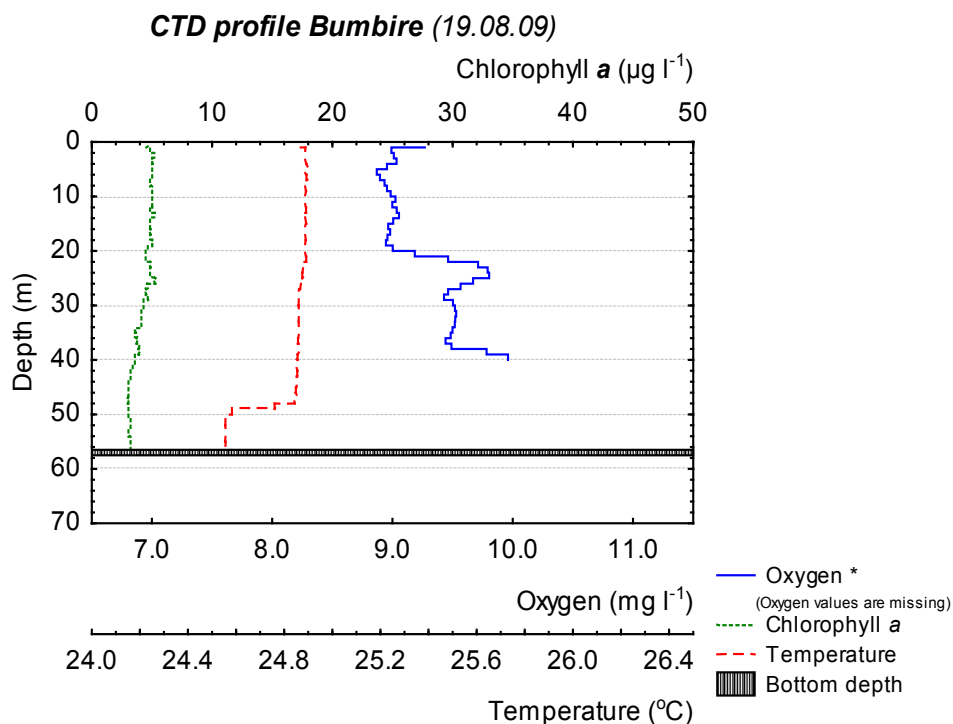


Figure 13 – CTD profiles from Bumbire station. Oxygen, chlorophyll *a* and temperature values were averaged for each meter. Note: some oxygen values are missing due to technical problems with the oxygen sensor.

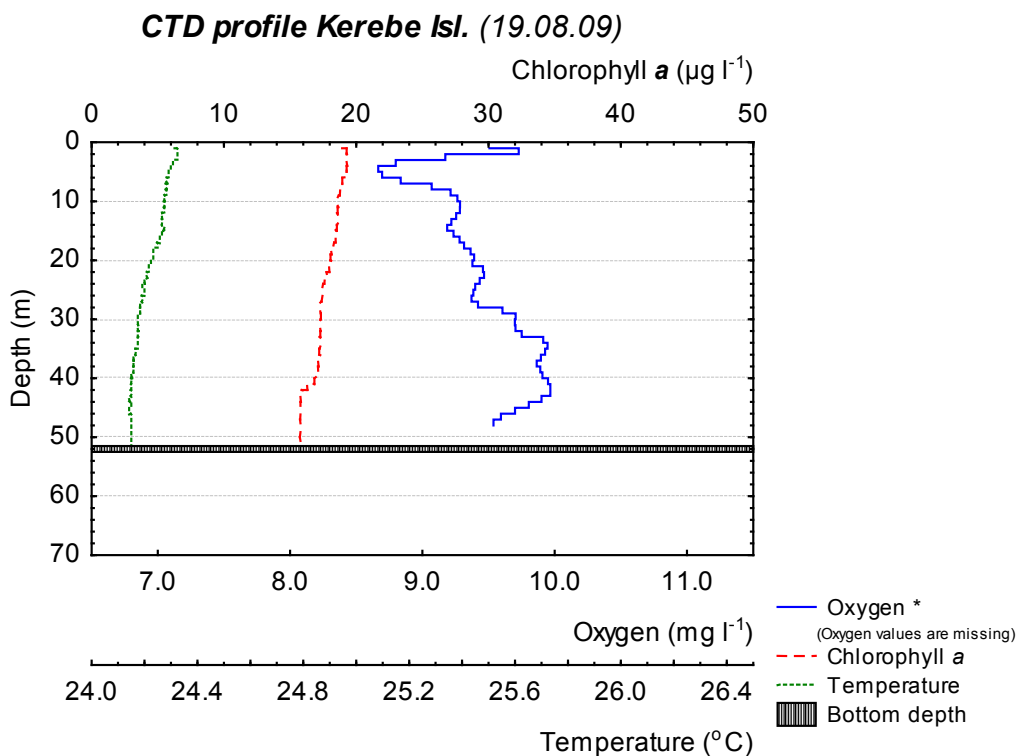


Figure 14 – CTD profiles from Kerebe Island station. Oxygen, chlorophyll *a* and temperature values were averaged for each meter. Note: some oxygen values are missing due to technical problems with the oxygen sensor.

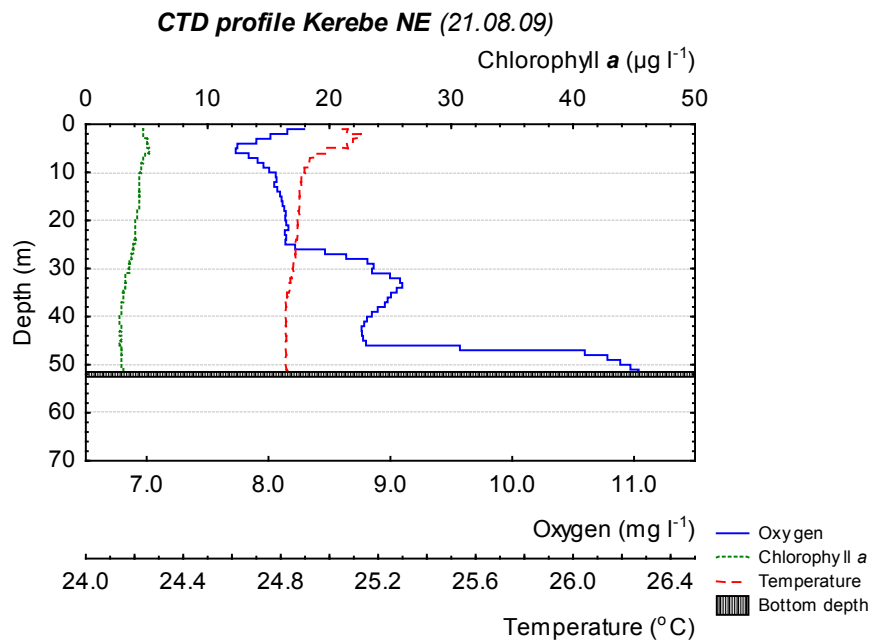


Figure 15 – CTD profiles from Kerebe NE station. Oxygen, chlorophyll *a* and temperature values were averaged for each meter.

5.2.3. CTD profiles for the stations in the deep stratum

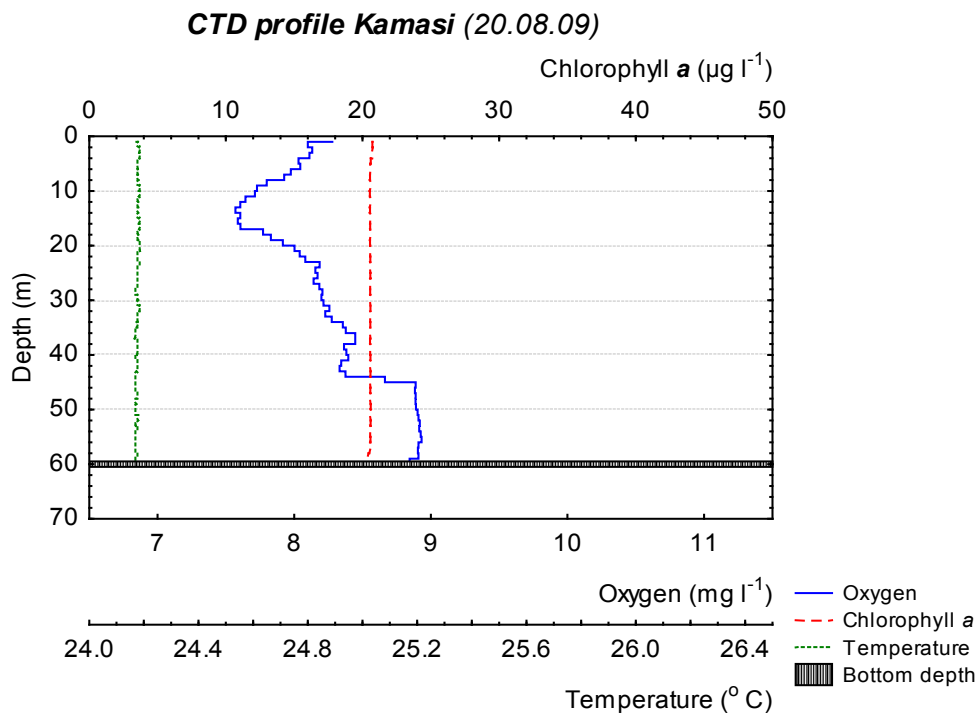


Figure 16 – CTD profiles from Kamasi station. Oxygen, chlorophyll *a* and temperature values were averaged for each meter.

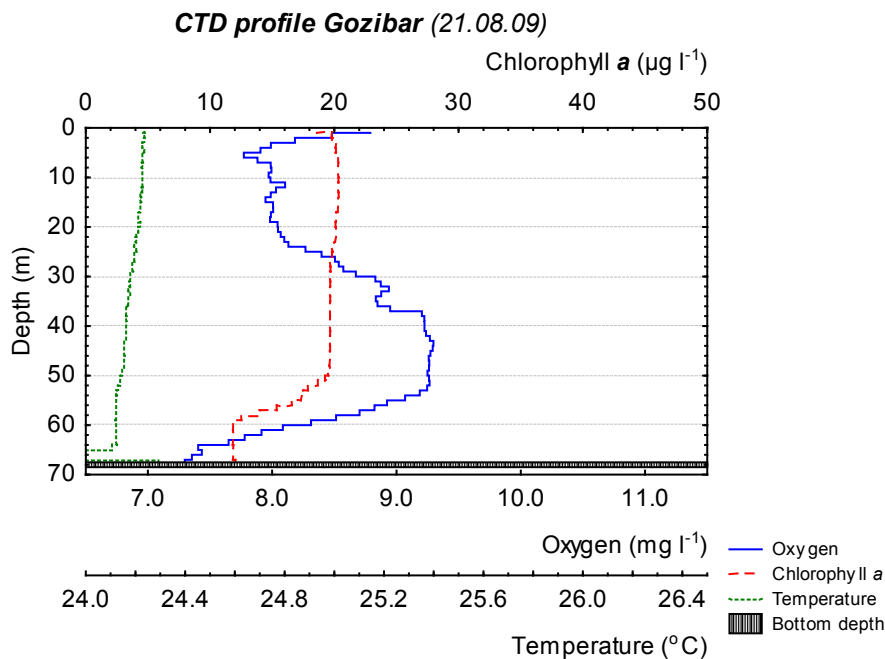


Figure 17 – CTD profiles from Gozibar station. Oxygen, chlorophyll *a* and temperature values were averaged for each meter.

5.3. Coefficient of variation (CV, in %), mean, maximum and minimum values for Oxygen, chlorophyll *a* and temperature.

The values showed in tables 7 to 9 are averaged for 10m interval and by strata (calculated from PASGERAR).

Table 2 – Dissolved oxygen level by strata (inshore, coastal, deep and all strata). Summary of coefficients of variation (CV), mean, maximum and minimum oxygen for 10m intervals.

Dissolved oxygen level by stratum (mg l^{-1})												
Depth	Inshore				Coastal				Deep			
	CV (%)	Mean	Max	Min	CV (%)	Mean	Max	Min	CV (%)	Mean	Max	Min
0	13.9	8.9	11.1	7.1	6.4	9.0	10.0	7.7	3.0	8.1	8.8	7.8
10	16.0	8.4	10.5	7.0	6.1	8.9	9.6	8.0	2.4	7.8	8.1	7.6
20	12.6	8.3	10.1	6.8	6.4	9.1	9.8	8.1	2.2	8.2	8.6	7.9
30	0.6	7.8	7.9	7.8	6.2	9.3	10.0	8.1	3.9	8.6	9.2	8.2
40					5.4	9.5	10.8	8.0	4.3	8.9	9.3	8.3
50					10.3	9.1	11.0	8.0	2.2	9.0	9.3	8.5
60									6.4	7.8	8.8	7.3
Total	14.5	8.6	11.1	6.8	6.7	9.1	11.0	7.7	6.3	8.4	9.3	7.3

Table 3 – Chlorophyll *a* level by strata (inshore, coastal, deep and all strata). Summary of coefficients of variation (CV), mean, maximum and minimum chlorophyll for 10m intervals.

Chlorophyll <i>a</i> level by stratum ($\mu\text{g l}^{-1}$)												
	Inshore				Coastal				Deep			
Depth	CV (%)	Mean	Max	Min	CV (%)	Mean	Max	Min	CV (%)	Mean	Max	Min
0	62.4	13.9	46.6	4.8	12.6	5.4	6.7	4.5	13.0	4.1	4.8	3.5
10	100.5	12.7	70.3	4.7	21.3	5.5	8.4	4.3	10.7	4.0	4.6	3.6
20	42.8	7.2	13.1	4.7	23.1	5.0	7.9	3.6	6.8	3.8	4.4	3.5
30	8.5	4.9	6.1	4.7	27.6	4.5	7.7	2.9	3.5	3.5	3.7	3.2
40					44.1	3.1	6.4		5.0	3.3	3.5	3.0
50					58.5	2.4	3.7		16.2	3.0	3.6	2.4
60									70.5	2.4	5.9	
Total	83.0	11.7	70.3	4.7	34.9	4.5	8.4	2.9	21.5	3.5	5.9	

Table 4 – Temperature by strata (inshore, coastal, deep and all strata). Summary of coefficients of variation (CV), mean, maximum and minimum temperature for 10m intervals.

Temperature by stratum ($^{\circ}\text{C}$)												
	Inshore				Coastal				Deep			
Depth	CV (%)	Mean	Max	Min	CV (%)	Mean	Max	Min	CV (%)	Mean	Max	Min
0	1.3	25.0	26.2	24.5	0.3	25.0	25.1	24.8	0.1	25.0	25.0	24.9
10	0.7	24.8	25.1	24.5	0.1	24.9	25.0	24.9	0.0	25.0	25.0	25.0
20	0.6	24.9	25.0	24.5	0.1	24.9	24.9	24.9	0.1	25.0	25.0	25.0
30	0.0	24.9	24.9	24.9	0.1	24.9	24.9	24.8	0.1	25.0	25.0	25.0
40					0.7	24.8	24.9	24.2	0.1	25.0	25.0	25.0
50					0.8	24.5	24.8	24.2	0.5	24.9	25.0	24.6
60									0.6	24.6	25.0	24.6
Total	1.0	24.9	26.2	24.5	0.6	24.9	25.1	24.2	0.5	25.0	25.0	24.6

Appendix VI – Relation between the limnological variables

6.1. Relation between limnological variables for each stratum

Graphs 1 to 3 done using PASGEAR.

6.1.1. Oxygen against chlorophyll

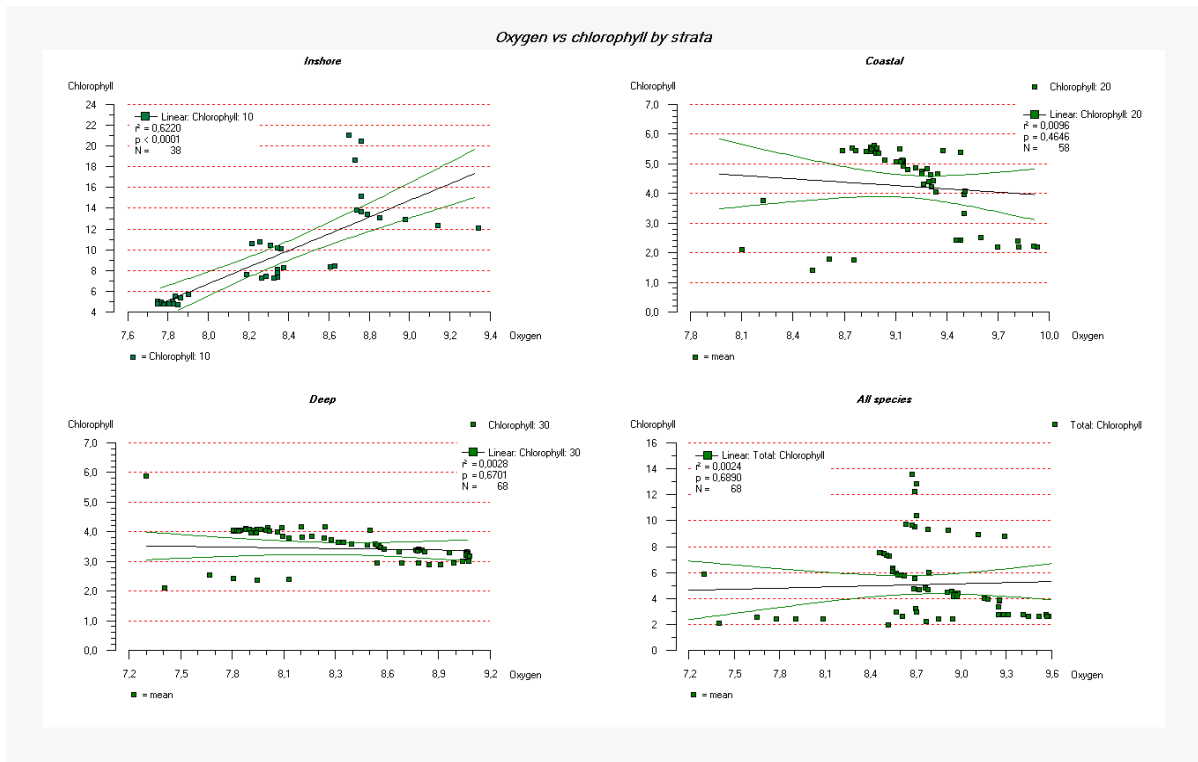


Figure 1 – Variation of chlorophyll *a* in function of oxygen for the three strata.

6.1.2. Oxygen against temperature

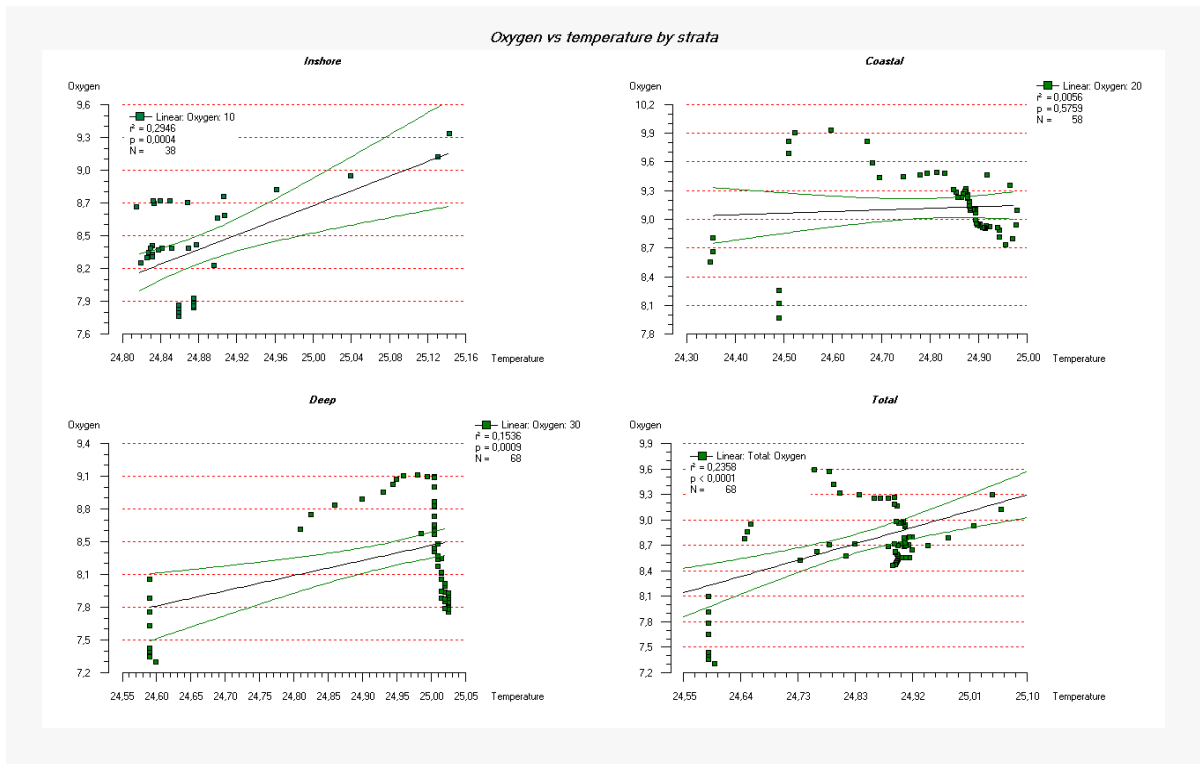


Figure 2 – Variation of oxygen in function of temperature for the three strata.

6.1.3. Chlorophyll against temperature

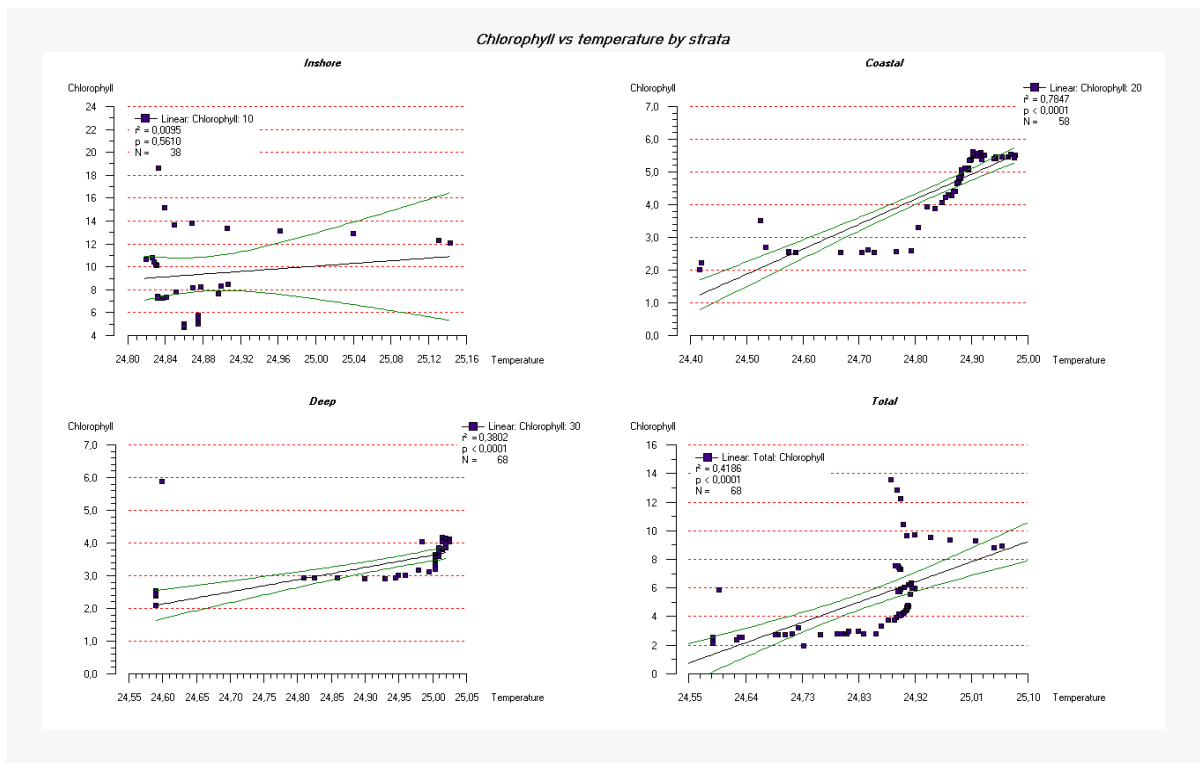


Figure 3 – Variation of chlorophyll *a* in function of temperature for the three strata.

6.2. Statistical analysis results

6.2.1. Results from the Spearman rank correlation non parametric test

Significant values are highlighted in red.

Table 1 – Correlation matrix between the limnological parameters

		<i>N</i>	<i>Spearman R</i>	<i>t(N-2)</i>	<i>p-level</i>
Inshore	Depth & Oxygen	134	-0,266	-3,171	0,002
	Depth & Chlorophyll	134	-0,657	-10,024	0,000
	Depth & Temperature	134	-0,135	-1,567	0,119
	Oxygen & Chlorophyll	134	0,456	5,892	0,000
	Oxygen & Temperature	134	0,716	11,787	0,000
	Chlorophyll & Temperature	134	0,130	1,510	0,133
	Depth & Oxygen	176	0,113	1,506	0,134
Coastal	Depth & Chlorophyll	197	-0,745	-15,613	0,000
	Depth & Temperature	197	-0,832	-20,903	0,000
	Oxygen & Chlorophyll	176	-0,260	-3,549	0,000
	Oxygen & Temperature	176	0,136	1,806	0,073
	Chlorophyll & Temperature	197	0,761	16,380	0,000
	Depth & Oxygen	101	0,429	4,726	0,000
	Depth & Chlorophyll	101	-0,793	-12,965	0,000
Deep	Depth & Temperature	101	-0,356	-3,795	0,000
	Oxygen & Chlorophyll	101	-0,491	-5,614	0,000
	Oxygen & Temperature	101	-0,124	-1,243	0,217
	Oxygen & Conductivity	101	0,162	1,629	0,107
	Chlorophyll & Temperature	101	0,504	5,806	0,000

6.2.2. Results from the Kruskal-wallis Anova non parametric test

Oxygen, chlorophyll a and temperature were selected as dependent variables; strata was selected as the independent (grouping) variable

Dependent variable: Mean Oxygen

Kruskal-Wallis test: H (2, N= 411) =57,45872 p =,0000

Median Test, Overall Median = 8.97453

Chi-Square = 80,10381 df = 2 p = ,0000

Multiple Comparisons p values;

Kruskal-Wallis test: H (N= 411) p =,0000

	Coastal	Deep	Inshore
Coastal		0.000000	0.000001
Deep	0.000000		0.050497
Inshore	0.000001	0.050497	

Dependent variable: Mean chlorophyll a

Kruskal-Wallis test: H (2, N= 432) =234,0787 p =0,000

Median Test, Overall Median = 4,36297

Chi-Square = 231,0772 df = 2 p = 0,000

Multiple Comparisons p values (2-tailed);

Kruskal-Wallis test: H (2, N= 432) =234,0787 p =0,000

	Coastal	Deep	Inshore
Coastal		0.000670	0.00
Deep	0.000670		0.00
Inshore	0.000000	0.000000	

Dependent variable: Mean temperature

Kruskal-Wallis test: H (2, N= 432) =109,7692 p =0,000

Median Test, Overall Median = 24,8890;

Chi-Square = 75,52193 df = 2 p = ,0000

Multiple Comparisons p values (2-tailed

Kruskal-Wallis test: H (2, N= 432) =109,7692 p =0,000

	Coastal	Deep	Inshore
Coastal		0.000670	0.00
Deep	0.000670		0.00
Inshore	0.000000	0.000000	

Appendix VII – Biological data analysis results

Table 1 – Weight (kg haul⁻¹) of each species in the bottom trawl catches.

<i>Location</i>	<i>Ln</i>	<i>On</i>	<i>H</i>	<i>Si</i>	<i>Ra</i>	<i>Bp</i>	<i>Cn</i>	<i>Bs</i>	<i>TC</i>
Kome Channel	15.9	0	31	1	0	0	0	0	47.9
Maisome Channel	33	0.5	0	0	0	0	0	0	33.5
Emin Pasha	2	0	78	0	0	0	0	0	80
Luega Point	65	0	121	0	0	0	0	0	186
Iroba Isl.	93	0	0.5	0	0	0.25	0.75	0	94.5
Kerebe Isl.	72	0	6.4	0	0	7.47	2.13	0	88
Kerebe Isl.North	71.05	0	5	0	0	14	0.05	0	90.1
Bumbure Channel	195.75	0	105.53	0	2.63	2.1	0	0	306.01
Makibwa Isl.	175	0	14	0	0	0	0	0	189
Nafuba Isl.	82	0	44	0	0	0	0	0.05	126.05
Bulamba (Speke Gulf)	24.75	7.5	62.7	0	8.25	0	0	2.97	106.17

Ln - Lates niloticus (Kg/haul)

Bp - Barbus profundus (Kg/haul)

On - Oreochromis niloticus (Kg/haul)

Cn- Caridina niloticus(Kg/haul)

H - Haplochromine (Kg/haul)

Bs - B. sadleri (Kg/haul)

Si - Schilbe intermedius (Kg/haul)

TC - Total Catch Weight (Kg)

Ra - Rastrineobola argentea (Kg/haul)

Table 2 – Proportion of each species in the bottom trawl catches (% of weight).

Percentage of species in the Total Catch								
Location	<i>Ln</i>	<i>On</i>	<i>H</i>	<i>Si</i>	<i>Ra</i>	<i>Bp</i>	<i>Cn</i>	<i>Bs</i>
Kome Channel	33.2		64.7	2.1				
Maisome Channel	98.5	1.5						
Senga (Emin Pasha Gulf)	2.5		97.5					
Ruega	34.9		65.1					
Iroba Isl.	98.4		0.5			0.3	0.8	
Kerebe Isl.	81.8		7.3			8.5	2.4	
Kerebe Isl.North	78.9		5.5			15.5	0.1	
Bumbure Channel	64.0		34.5		0.9	0.7		
Makibwa Isl.	92.6		7.4					
Nafuba Isl. (Speke Gulf)	65.1		34.9					0.1
Bulamba (Speke Gulf)	23.3	7.1	59.1		7.8			2.8

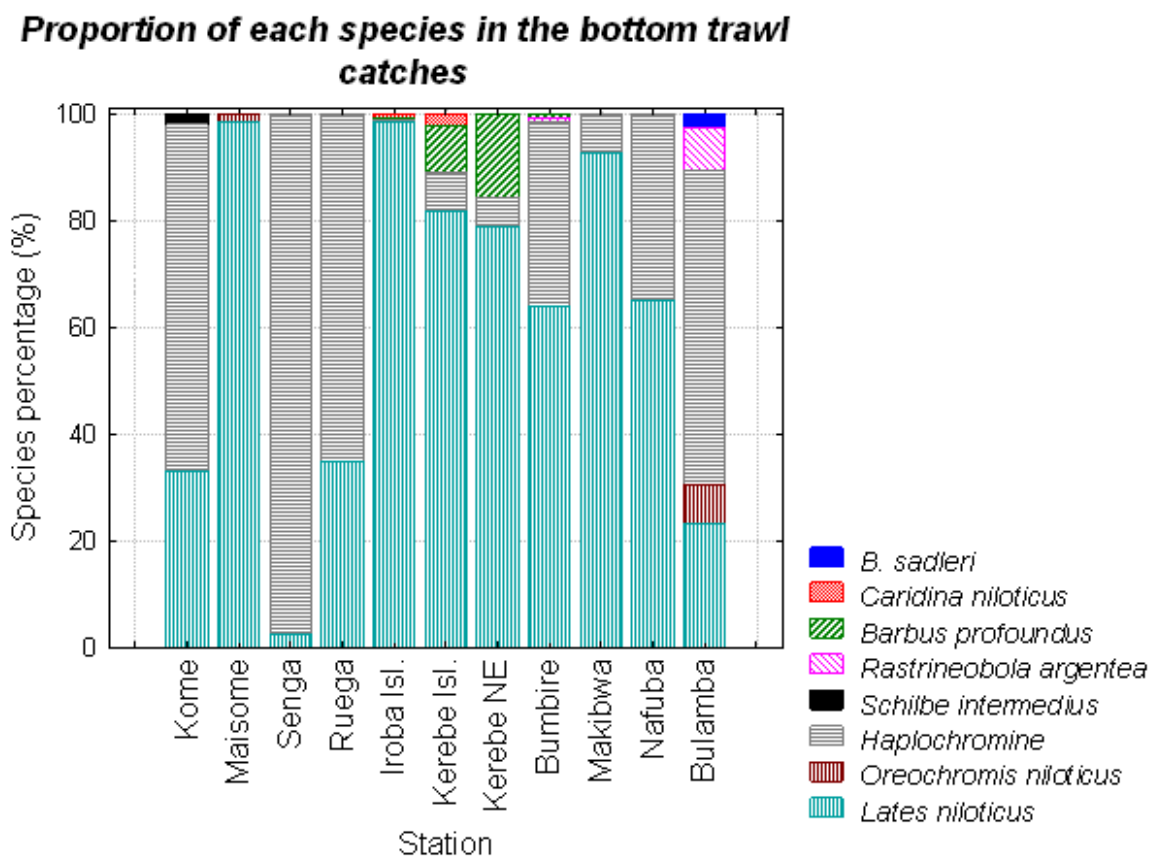


Figure 1 – Proportion of each species in the bottom trawl catches (% of weight).

Appendix VII – Biological Data Analysis Results

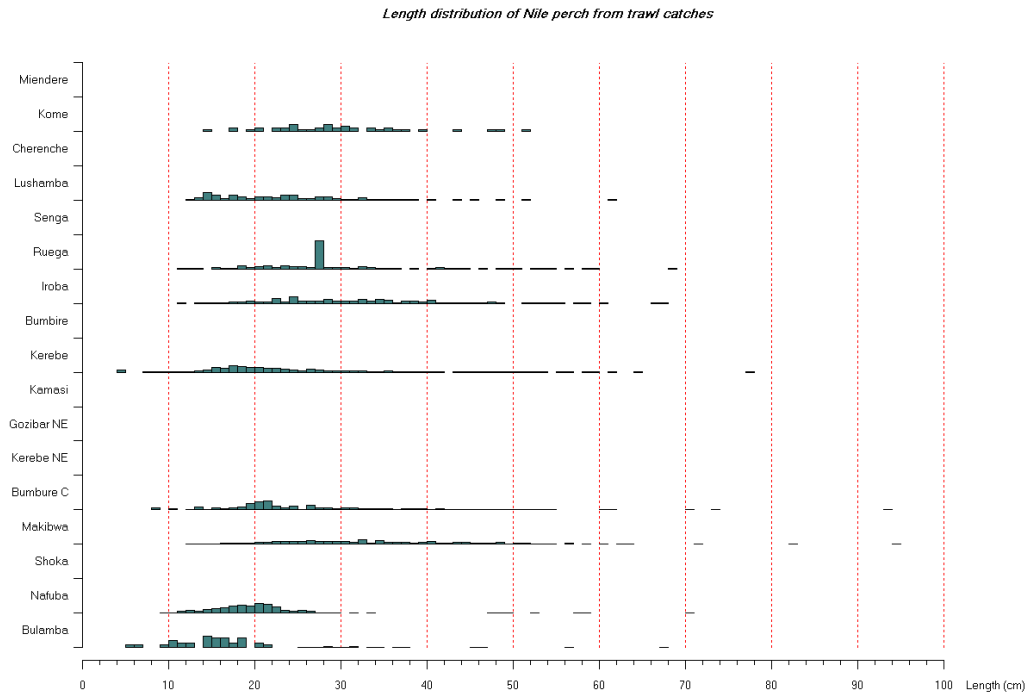


Figure 2 - Length distribution from Nile perch, for each trawl station (graphs shown in percentage).

8.2. Mean TS results

Table 2 – Mean TS calculated for each station. Values calculated from the acoustic data from the entire water column ($TS_{Station}$), back-calculated from the trawl catches ($TS_{Trawl\ catches}$), calculated from selected single targets ($TS_{Selected}$) and from 3 m above the bottom ($TS_{Trawl\ area}$). The number of values (N) used for the calculations is also displayed.

Station	$TS_{Station}$	N	$TS_{Trawl\ catches}$	N	$TS_{Selected}$	N	$TS_{Trawl\ area}$	N
Miendere	-48,56	21482	<i>a</i>	<i>a</i>	-52,60	616		
Kome	-49,60	3682	-36,40	41	<i>b</i>	<i>b</i>	-52,61	1497
Cherenche	-47,46	14437	<i>a</i>	<i>a</i>	-50,89	588		
Maisome	-49,25	9848	-37,81	123	-52,97	271	-49,19	1642
Senga	-48,77	6350	<i>c</i>	<i>c</i>	<i>b</i>	<i>b</i>	-48,79	5420
Ruega	-47,88	14998	-36,65	231	-52,83	154	-48,30	3603
Iroba	-47,98	12989	-35,67	193	-51,98	786	-47,84	2089
Bumbire	-49,05	11165	<i>a</i>	<i>a</i>	-50,12	487		
Kerebe	-49,81	16238	-38,16	310	-52,30	921	-49,55	537
Kamasi	-49,87	7818	<i>a</i>	<i>a</i>	-51,15	869		
Gozibar NE	-50,36	25946	<i>a</i>	<i>a</i>	-51,88	1054		
Kerebe NE	-48,67	15669	-38,36	327	-52,30	921	-48,76	880
Bumbure C	-51,02	8567	-37,67	665	-53,67	463	-51,20	4572
Makibwa	-51,05	9051	-35,15	287	-52,82	814	-50,78	2191
Shoka	-48,24	12091	<i>a</i>	<i>a</i>	-48,18	128		
Nafuba	-50,72	7927	-40,08	727	<i>b</i>	<i>b</i>	-51,30	4268
Bulamba	-49,12	654	-41,66	556	<i>b</i>	<i>b</i>	-47,70	395

a – there was no bottom trawl haul in this location.

b – it was not possible to select Nile perch isolated targets for TS calculations due to the high fish densities and/or to the shallow waters.

c – no data for this station.

Appendix VIII – Target Strength Analysis Results

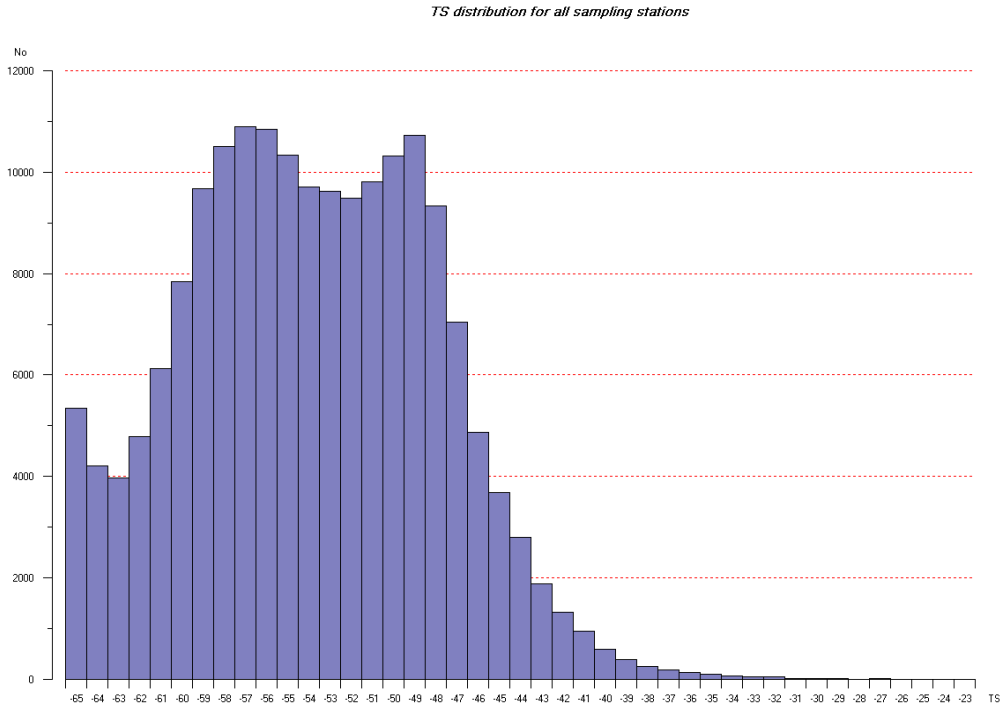


Figure 1 – TS frequency distribution from all stations sampled.

8.3. Mean TL calculated for each station from acoustic data and from trawl data

Table 3 – Results for the mean total length, by station, obtained from the acoustic data (TL station), from the trawl catches (RMSL) and from the acoustic from isolated Nile perch targets (TL selected).

Station	TL station (cm)	RMSL trawl catches (cm)	TL selected (cm)
Miendere	7,45	-	4,68
Kome	6,61	30,20	-
Cherenche	8,45	-	5,69
Maisome	6,88	25,67	4,48
Senga	7,27	-	-
Luega	8,06	29,33	4,56
Iroba	7,96	32,83	5,02
Bumbire	7,04	-	6,22
Kerebe	6,45	24,65	4,84
Kamasi	6,41	-	5,53
Gozibar NE	6,06	-	5,08
Kerebe NE	7,35	24,10	4,84
Bumbure	5,61	26,08	4,13
Makibwa	5,59	34,86	4,56
Shoka	7,72	-	7,78
Nafuba	5,80	19,78	-
Bulamba	6,98	16,47	-
All	6,97	25,79	5,27

8.4. Results from the Kruskal-wallis Anova non parametric test

Mean TS (dependent variable) against strata (grouping variable)

Kruskal-Wallis test: H (2, N= 391) =20,22814 p =,0000

Median Test, Overall Median = -50,619

Chi-Square = 16,57822 df = 2 p = ,0003

Multiple Comparisons p values (2-tailed);

Kruskal-Wallis test: H (2, N= 391) =20,22814 p =,0000

	Coastal	Deep	Inshore
Coastal		0.000307	1.000000
Deep	0.000307		0.000103
Inshore	1.000000	0.000103	

Appendix IX – Graphs of TS and fish density distribution

A more detailed analysis of the fish distribution and of the size of the returned echoes for each of the stations shows the differences among the several sampling locations. The patterns of oxygen, mean TS, number of TS detections, as volume area backscattering (s_v , [$m^2 m^{-3}$]), are shown. Stations are displayed by its sampling order.

Miendere

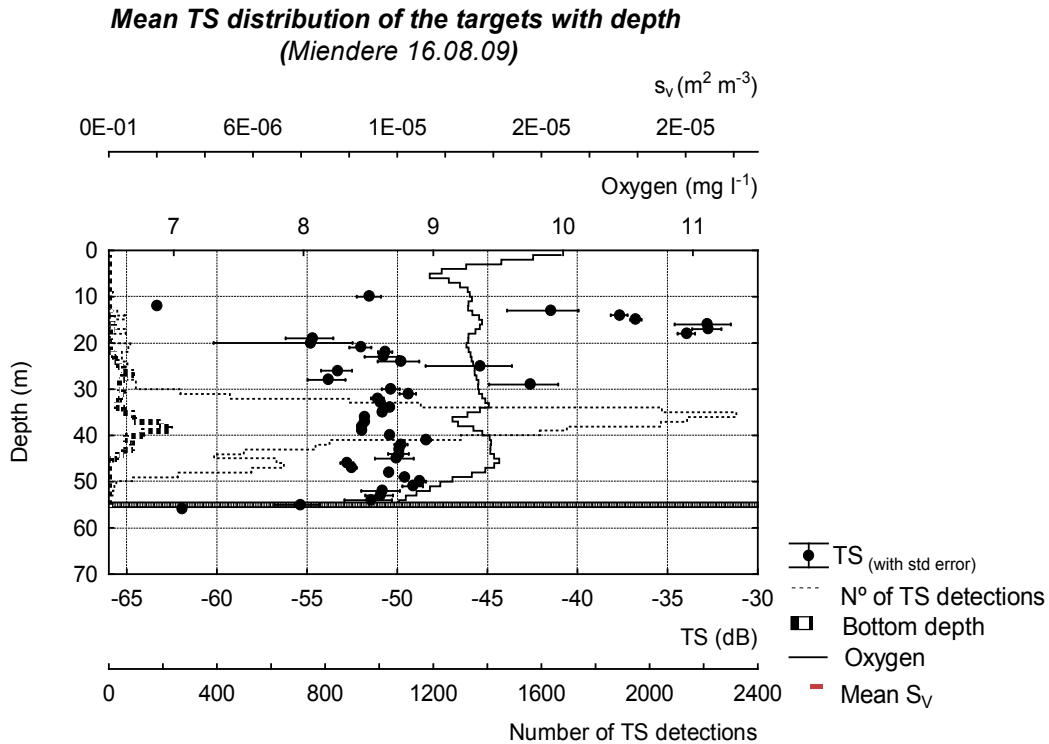


Figure 1 – Graph showing the mean TS distribution, over depth, of the fish targets for the Miendere sampling station. The correspondent values for the number of TS detections, oxygen level and volume backscattering coefficient (s_v), as well as the bottom depth are illustrated.

Kome

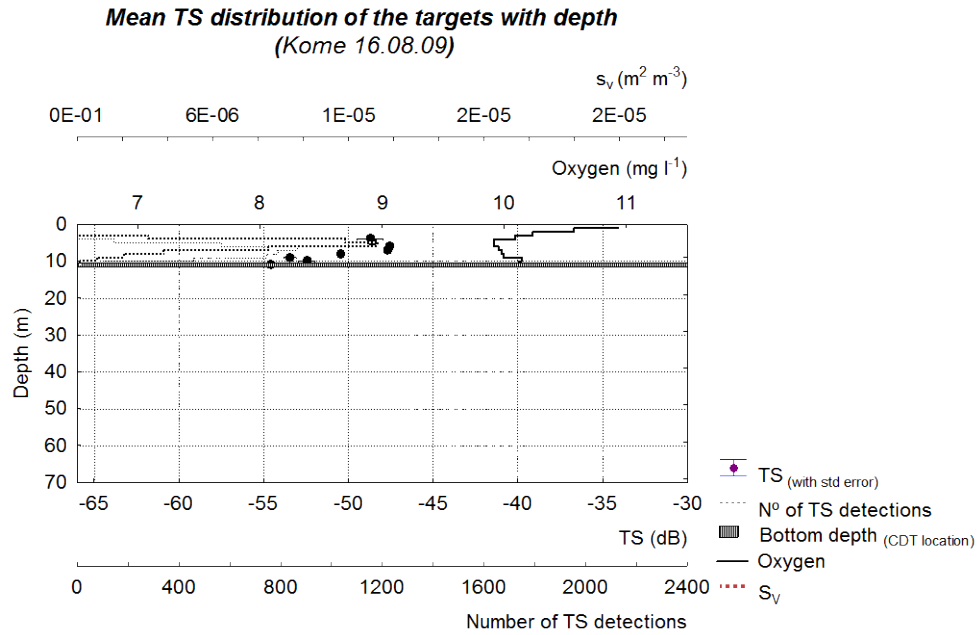


Figure 2 – Graph showing the mean TS distribution, over depth, of the fish targets for Kome sampling station. The correspondent values for the number of TS detections, oxygen level and volume backscattering coefficient (s_v), as well as the bottom depth are illustrated.

Cherenche

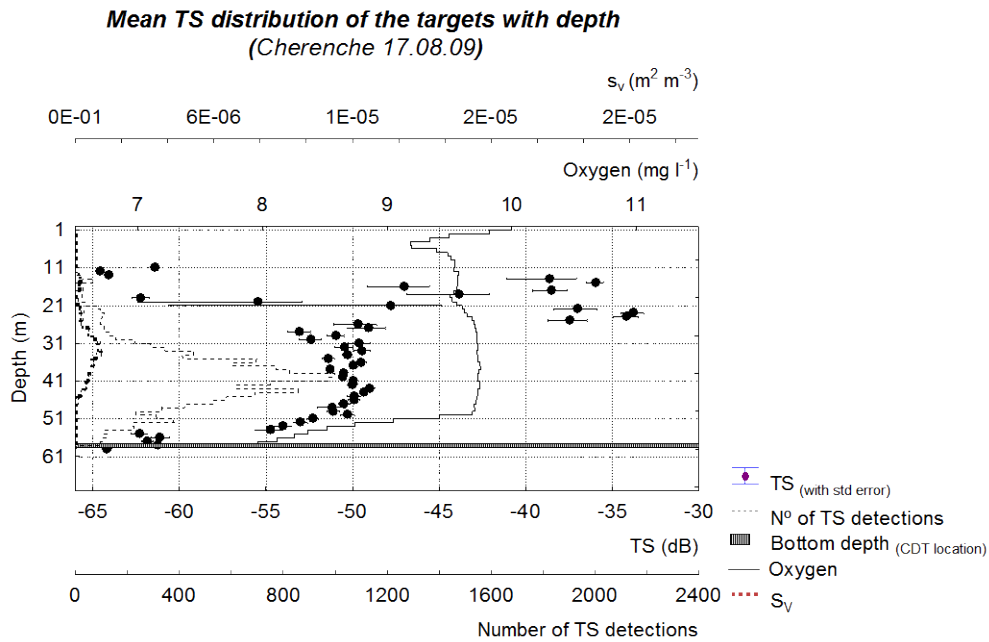


Figure 3 – Graph showing the mean TS distribution, over depth, of the fish targets for Cherenche sampling station. The correspondent values for the number of TS detections, oxygen level and volume backscattering coefficient (s_v), as well as the bottom depth are illustrated.

Maisome

The data used in Maisome, for exporting the fish scatters, was selected from 1nmi prior to the CTD sampling (correspondent to the 1st half of the echogram). This was done as way of correcting the large standard error values caused by the differences in the bottom depth along the 2nmi sampled.

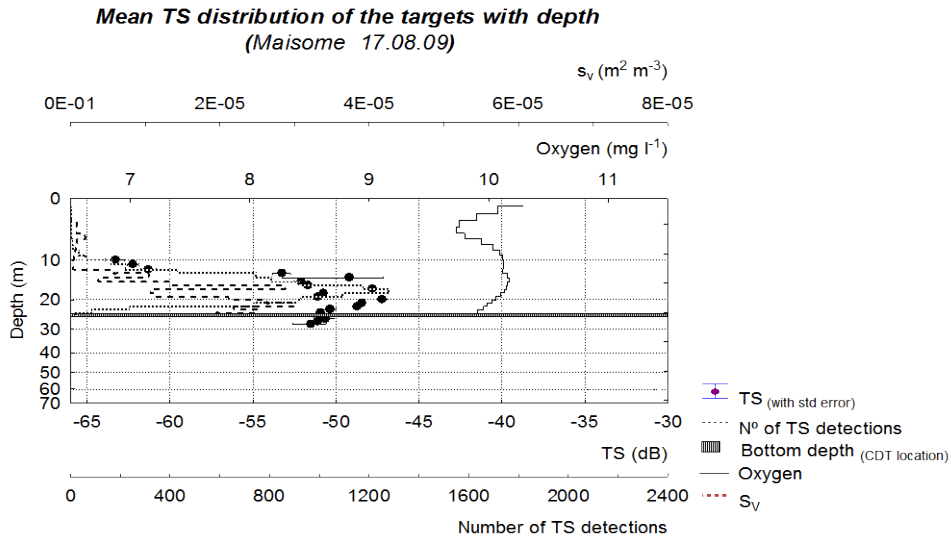


Figure 4 – Graph showing the mean TS distribution, over depth, of the fish targets for Maisome sampling station. The correspondent values for the number of TS detections, oxygen level and volume backscattering coefficient (s_v), as well as the bottom depth are illustrated.

Senga

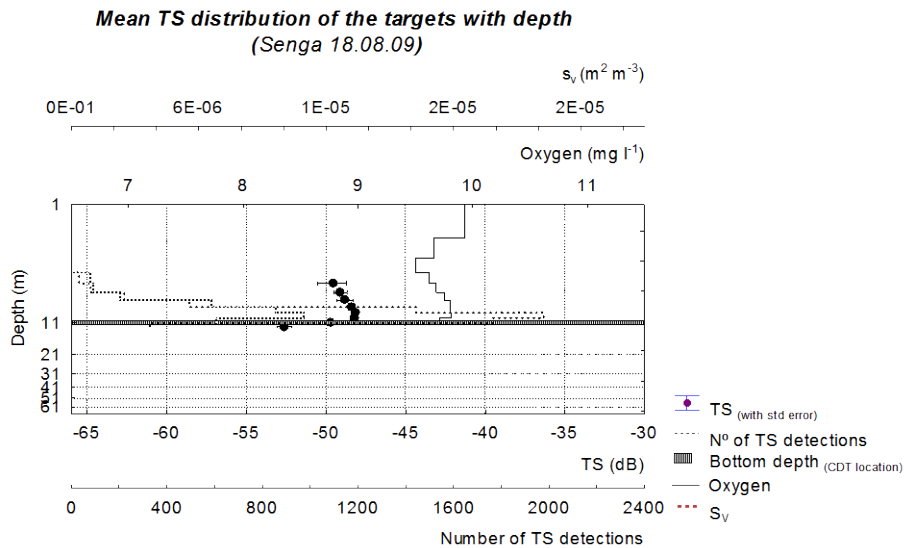


Figure 5 – Graph showing the mean TS distribution, over depth, of the fish targets for Senga sampling station. The correspondent values for the number of TS detections, oxygen level and volume backscattering coefficient (s_v), as well as the bottom depth are illustrated.

Ruega

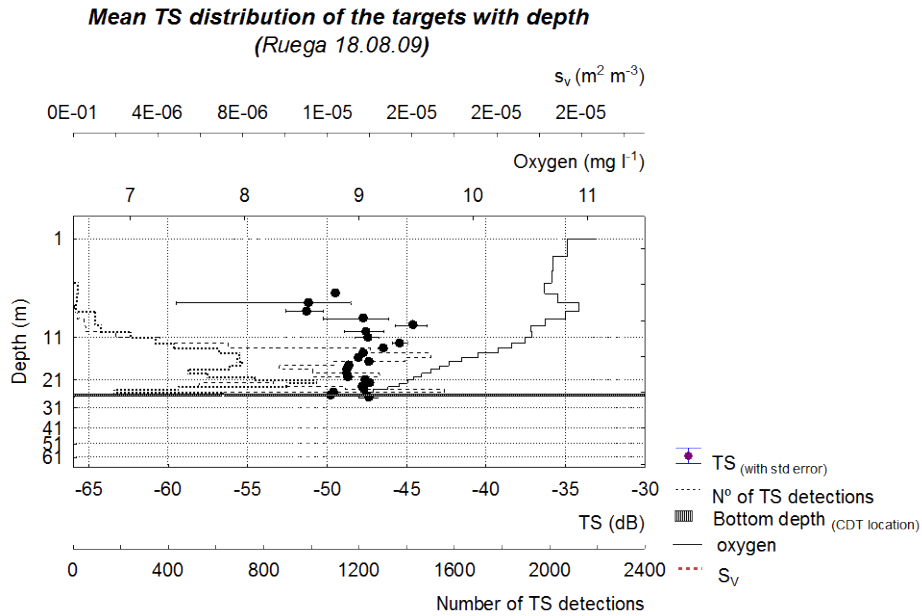


Figure 6 – Graph showing the mean TS distribution, over depth, of the fish targets for the Ruega sampling station. The correspondent values for the number of TS detections, oxygen level and volume backscattering coefficient (s_v), as well as the bottom depth are illustrated.

Iroba

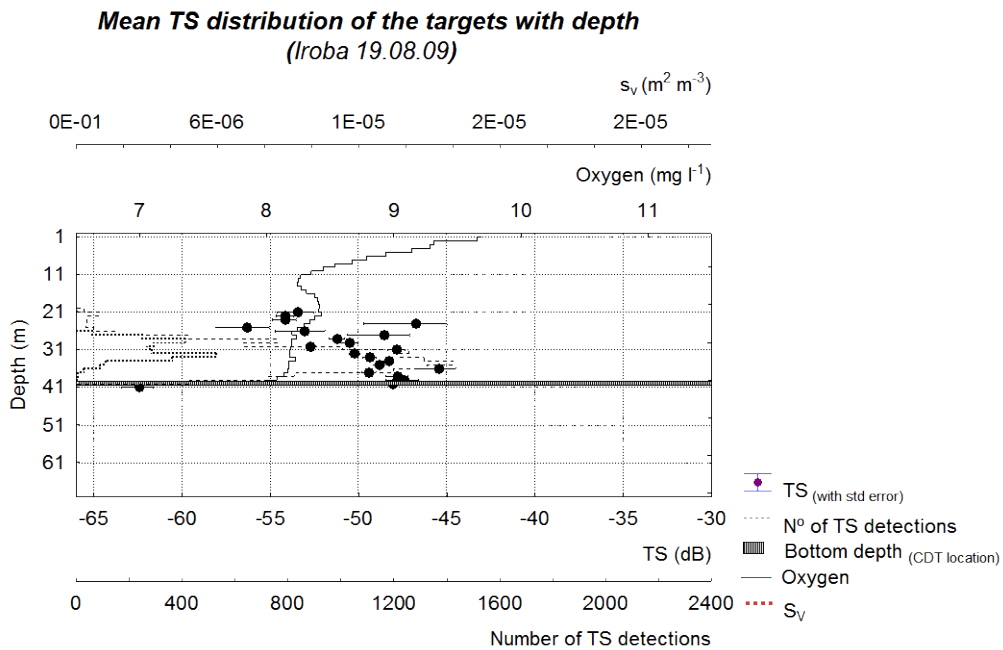


Figure 7 – Graph showing the mean TS distribution, over depth, of the fish targets for Iroba sampling station. The correspondent values for the number of TS detections, oxygen level and volume backscattering coefficient (s_v), as well as the bottom depth are illustrated.

Bumbire

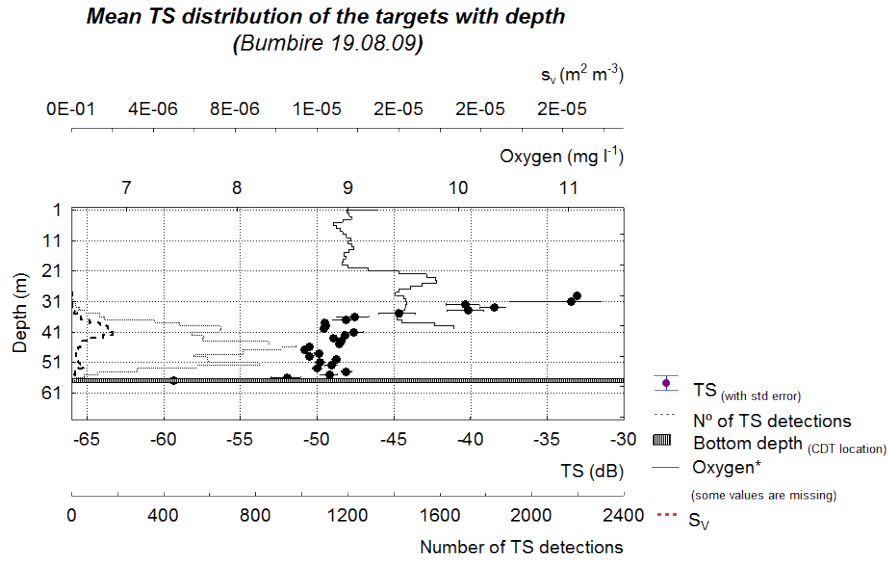


Figure 8 – Graph showing the mean TS distribution, over depth, of the fish targets for the Bumbire sampling station. The correspondent values for the number of TS detections, oxygen level and volume backscattering coefficient (s_v), as well as the bottom depth are illustrated.

Kerebe Island

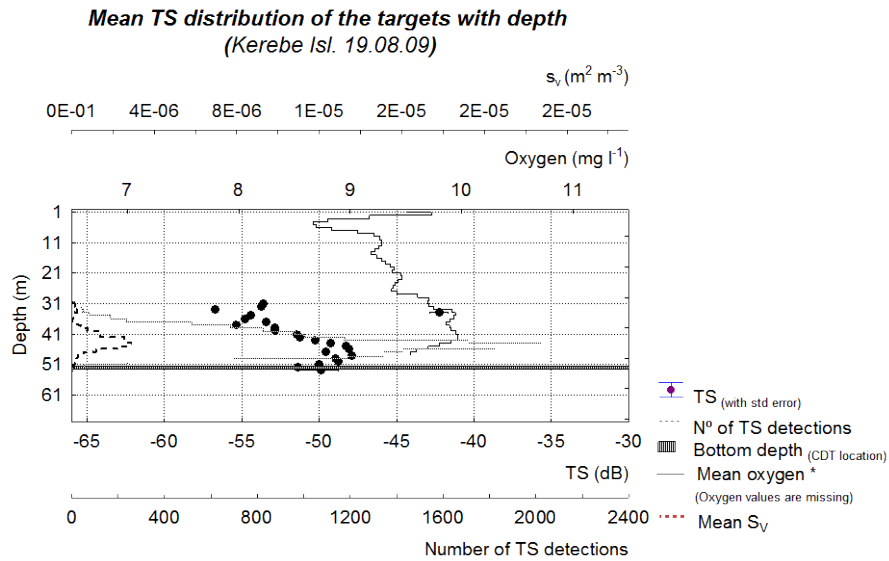


Figure 9 – Graph showing the mean TS distribution, over depth, of the fish targets for the Kerebe Island sampling station. The correspondent values for the number of TS detections, oxygen level and volume backscattering coefficient (s_v), as well as the bottom depth are illustrated.

Kamasi

For the density calculations for Kamasi, only 0,6nmi distance (before the CTD sampling) was considered. The other parameters included in the graph, mean TS and number of TS detections corresponds to values extracted from the whole echogram (2nmi total).

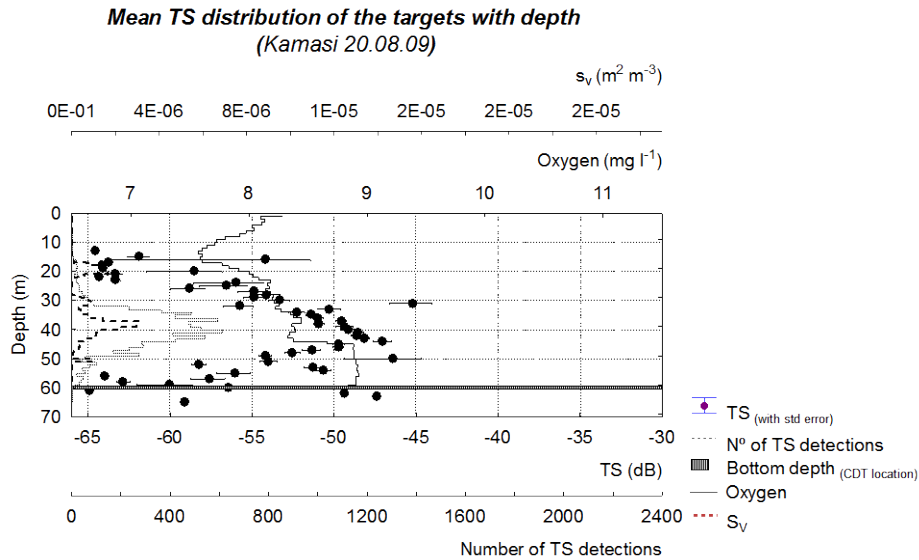


Figure 10 – Graph showing the mean TS distribution, over depth, of the fish targets for Kamasi sampling station. The correspondent values for the number of TS detections, oxygen level and volume backscattering coefficient (s_v), as well as the bottom depth are illustrated.

Gozibar

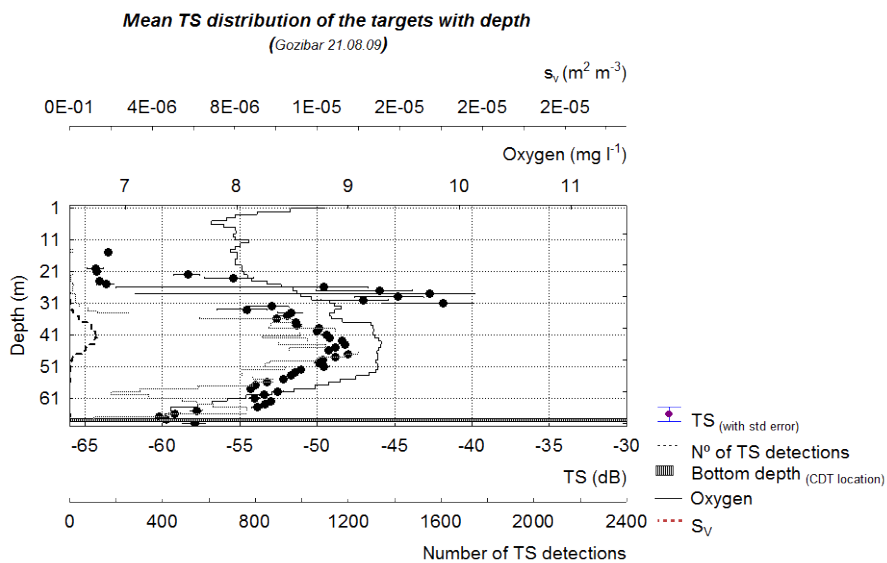


Figure 11 – Graph showing the mean TS distribution, over depth, of the fish targets for Gozibar sampling station. The correspondent values for the number of TS detections, oxygen level and volume backscattering coefficient (s_v), as well as the bottom depth are illustrated.

Kerebe Island North

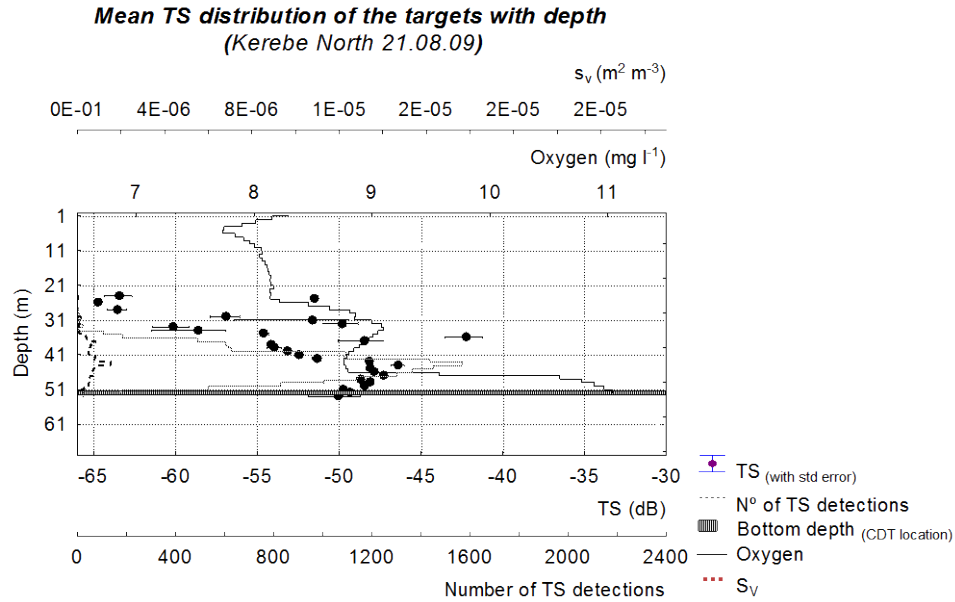


Figure 12 – Graph showing the mean TS distribution, over depth, of the fish targets for Kerebe North sampling station. The correspondent values for the number of TS detections, oxygen level and volume backscattering coefficient (s_v), as well as the bottom depth are illustrated.

Bumbure

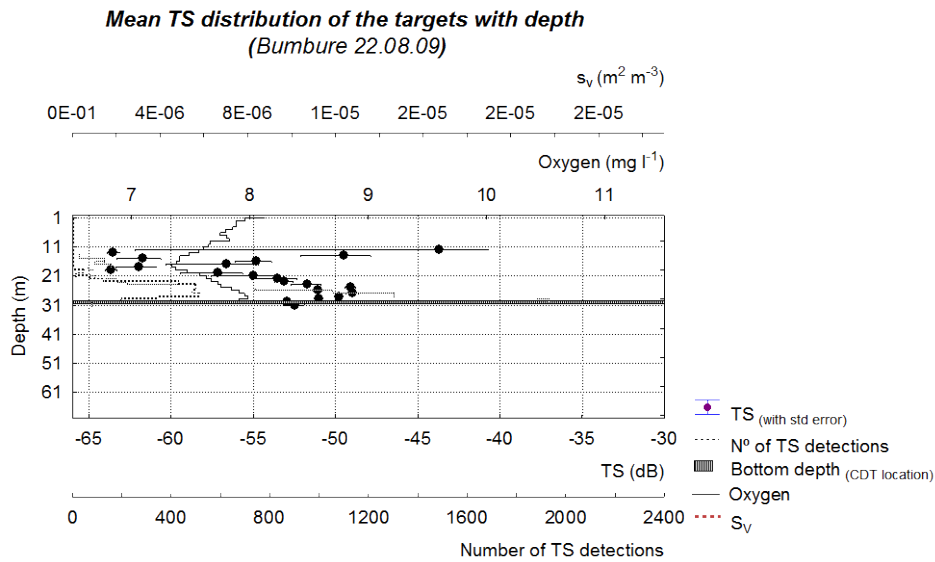


Figure 13 – Graph showing the mean TS distribution, over depth, of the fish targets for Bumbure sampling station. The correspondent values for the number of TS detections, oxygen level and volume backscattering coefficient (s_v), as well as the bottom depth are illustrated.

Makibwa

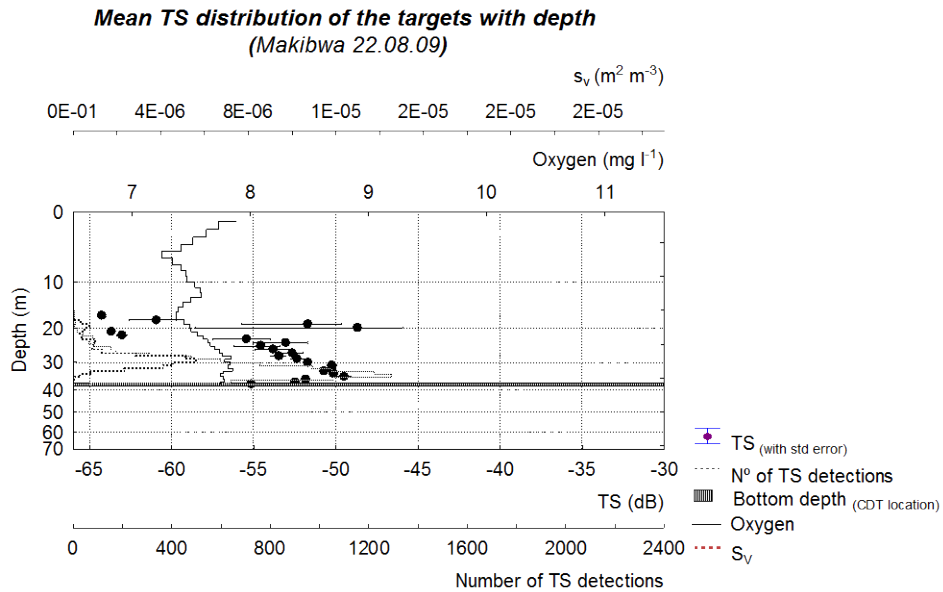


Figure 14 – Graph showing the mean TS distribution, over depth, of the fish targets for Makibwa sampling station. The correspondent values for the number of TS detections, oxygen level and volume backscattering coefficient (s_v), as well as the bottom depth are illustrated.

Shoka

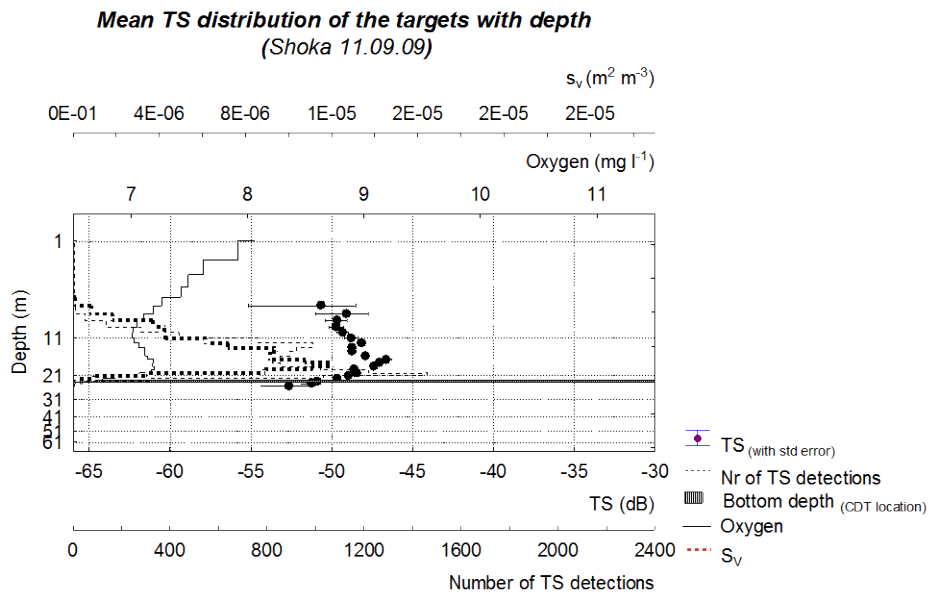


Figure 15 – Graph showing the mean TS distribution, over depth, of the fish targets for Shoka sampling station. The correspondent values for the number of TS detections, oxygen level and volume backscattering coefficient (s_v), as well as the bottom depth are illustrated.

Nafuba

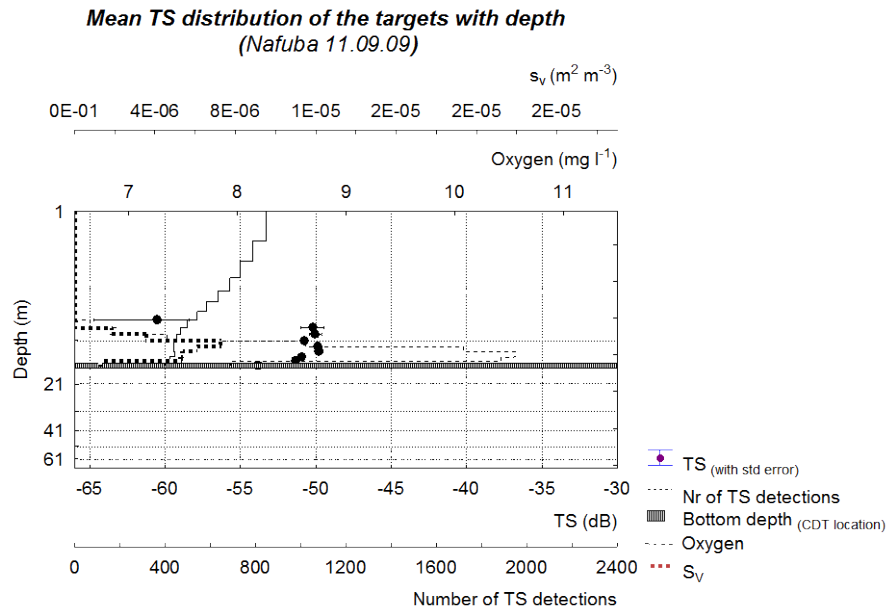


Figure 16 – Graph showing the mean TS distribution, over depth, of the fish targets for Nafuba sampling station. The correspondent values for the number of TS detections, oxygen level and volume backscattering coefficient (s_v), as well as the bottom depth are illustrated.

Bulamba

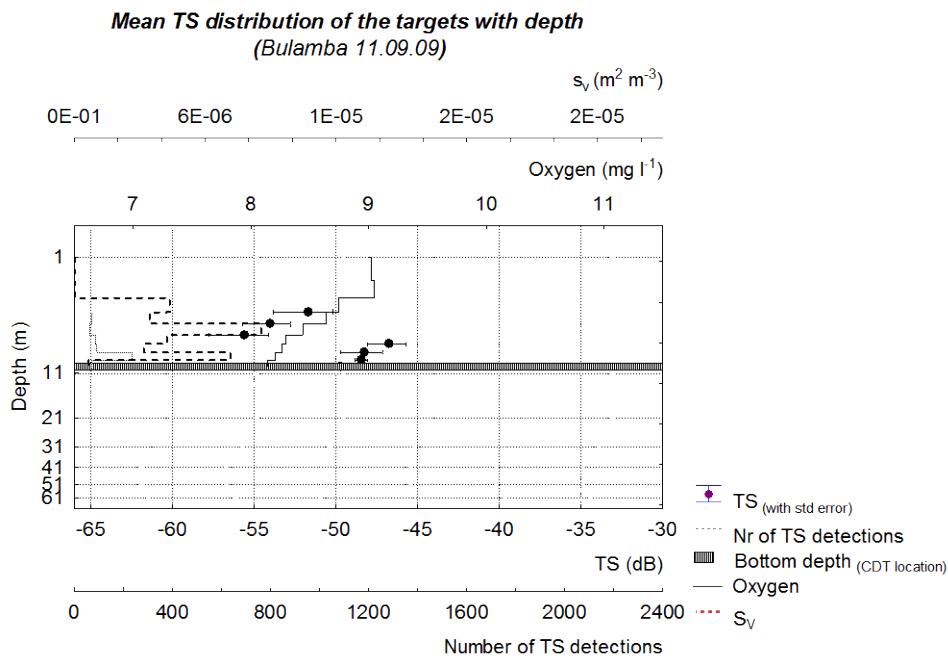


Figure 17 – Graph showing the mean TS distribution, over depth, of the fish targets for Bulamba sampling station. The correspondent values for the number of TS detections, oxygen level and volume backscattering coefficient (s_v), as well as the bottom depth are illustrated.

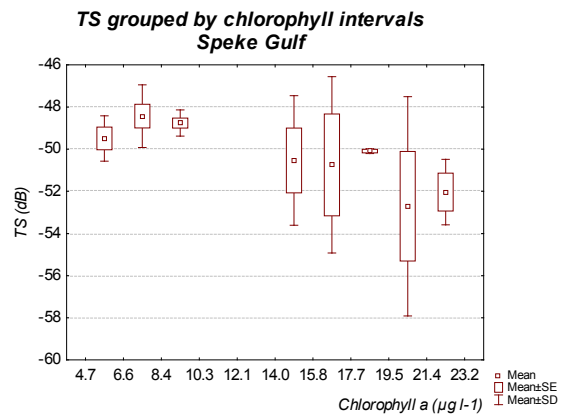
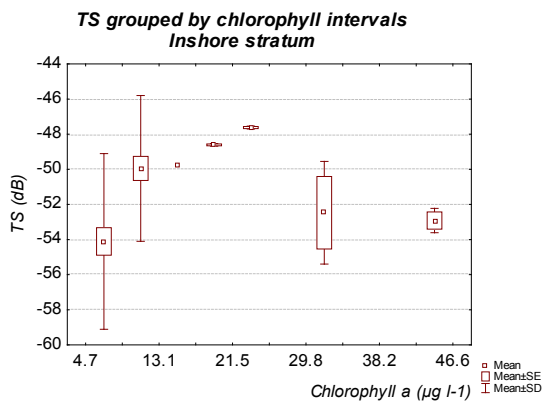
Appendix X – Relation between TS and the limnological data

10.1. Results from the statistical analysis

Table 1 – Results from the Spearman’s Rank correlation test

		Valid N	Spearman R	t(N-2)	p-level
Inshore	TS & Depth	128	-0,222	-2,551	0,012
	TS & Oxygen	128	0,203	2,321	0,022
	TS & Chloro	128	0,347	4,146	0,000
	TS & Temperature	128	0,090	1,010	0,314
	TS & Conductivity	128	0,419	5,177	0,000
Coastal	TS & Depth	166	0,015	0,193	0,847
	TS & Oxygen	145	0,168	2,039	0,043
	TS & Chloro	166	-0,005	-0,063	0,950
	TS & Temperature	166	0,067	0,856	0,393
	TS & Conductivity	166	-0,097	-1,244	0,215
Deep	TS & Depth	97	0,184	1,822	0,072
	TS & Oxygen	97	0,556	6,524	0,000
	TS & Chloro	97	-0,267	-2,706	0,008
	TS & Temperature	97	-0,032	-0,313	0,755
	TS & Conductivity	97	0,100	0,977	0,331

10.2. Range plot showing the TS distribution in function of chlorophyll a



Appendix X – Relation between TS and Limnological Data

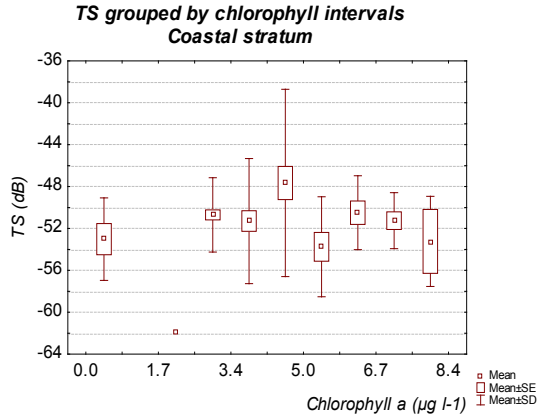


Figure 3

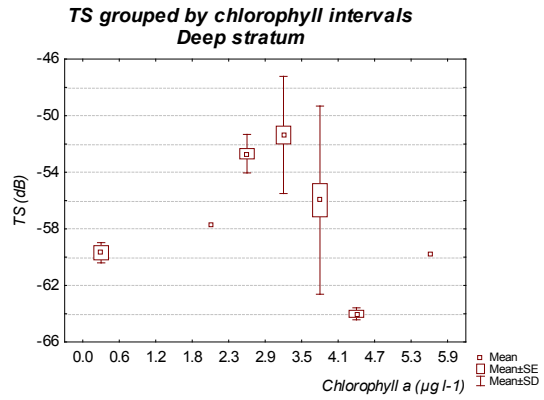


Figure 4

Figures 1 to 4 – Range plots of TS distribution (TS averaged for each meter depth) in function of chlorophyll *a* (with standard error and standard deviation).

Scatterplot of mean TS against chlorophyll a, categorized by stratum

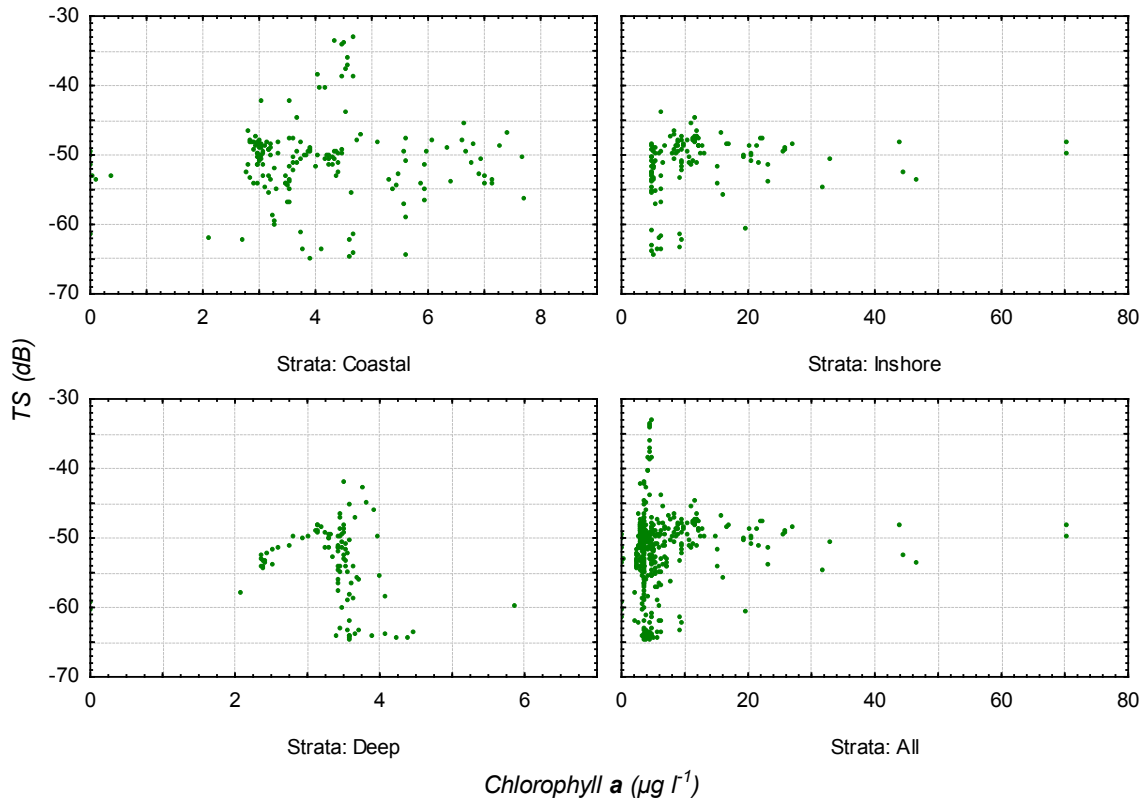


Figure 5 – Scatterplot showing TS (averaged for each meter depth) against chlorophyll a.

10.3. Range plot showing the TS distribution in function of temperature

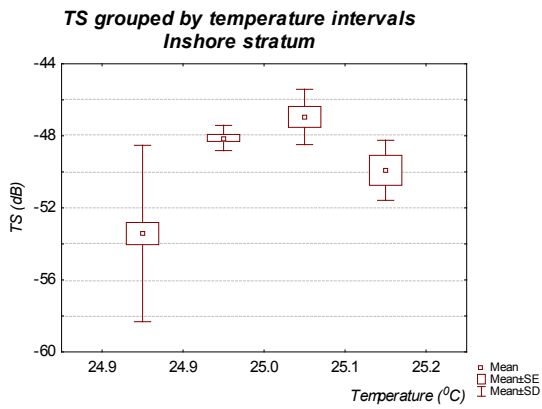


Figure 6

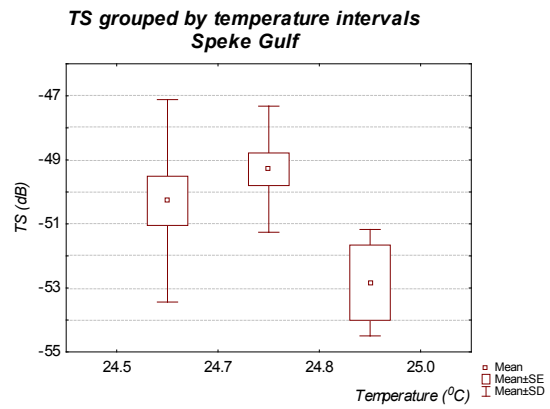


Figure 7

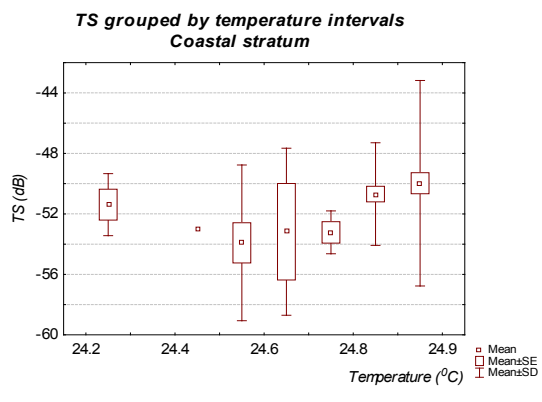


Figure 8

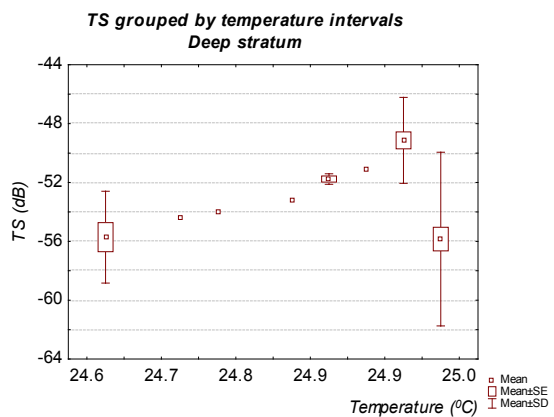


Figure 9

Figures 6 to 9 – Range plots of TS distribution (TS averaged for each meter depth) in function of temperature (with standard error and standard deviation).

Appendix XI – Validation of the TS measurements

The following graphs (figure1 to 26) show the TS distribution from the single targets extracted from the whole water column (left column) and from selected Nile perch targets (right column). Graphs are at the same scale (from -65 to -20dB).

11.1. Comparison of TS distributions from the water column and selected targets

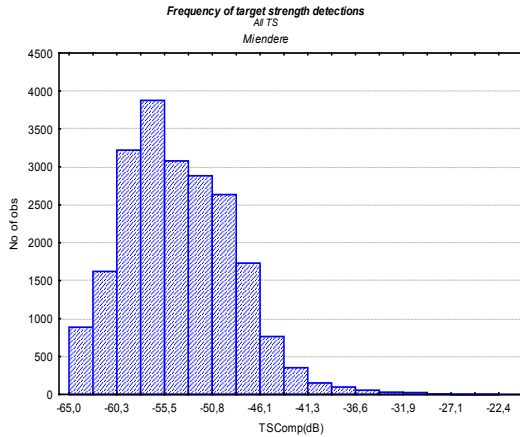


Figure 1

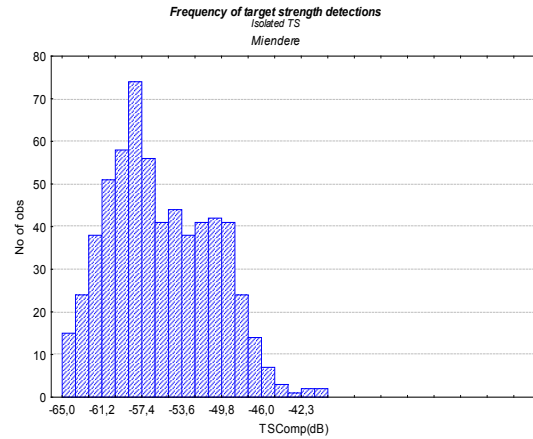


Figure 2

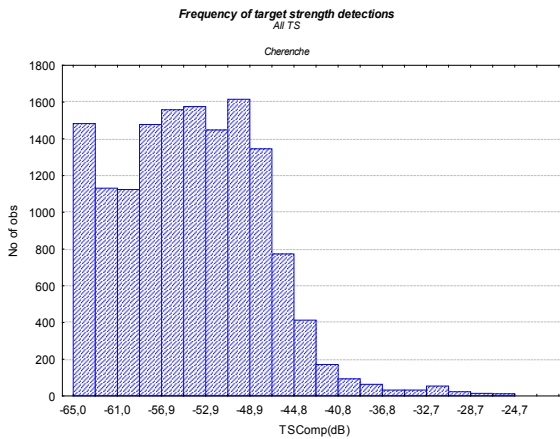


Figure 3

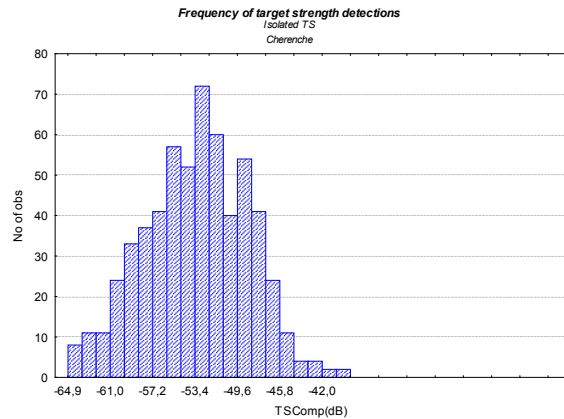


Figure 4

Appendix XI – Validation of the TS Measurements

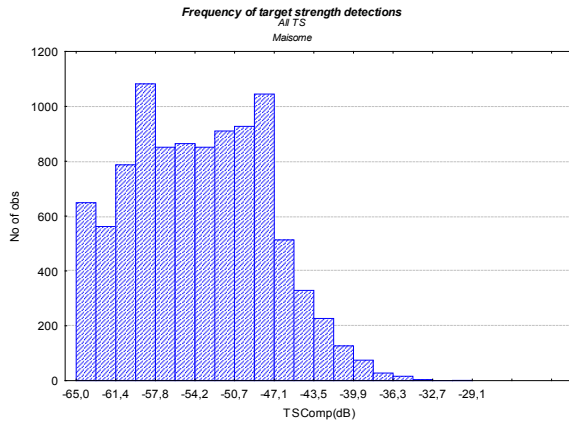


Figure 5

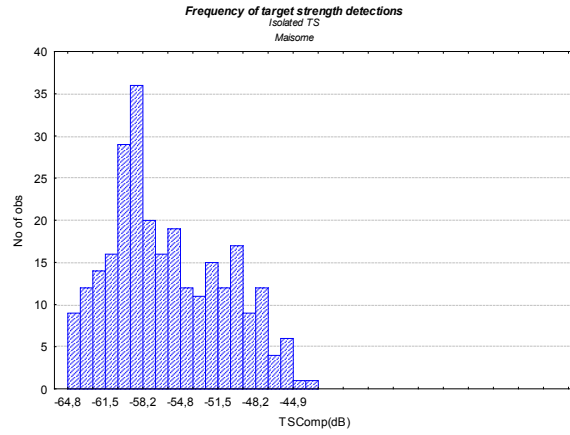


Figure 6

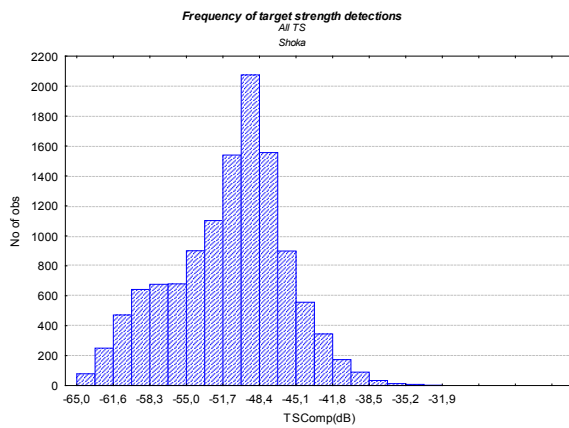


Figure 7

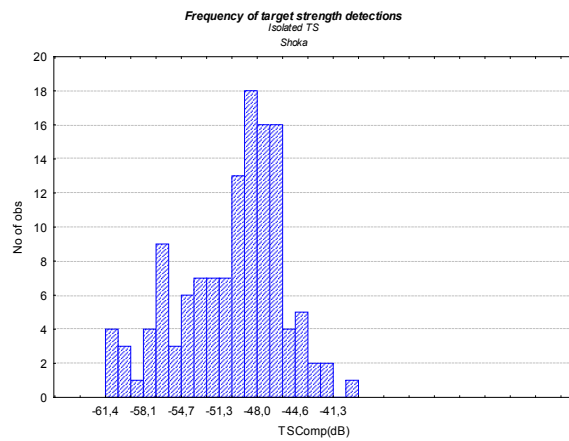


Figure 8

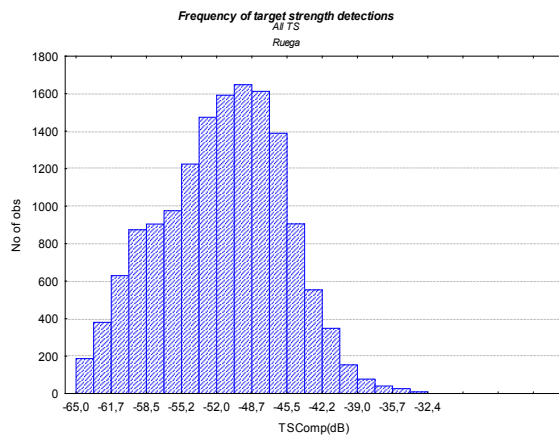


Figure 9

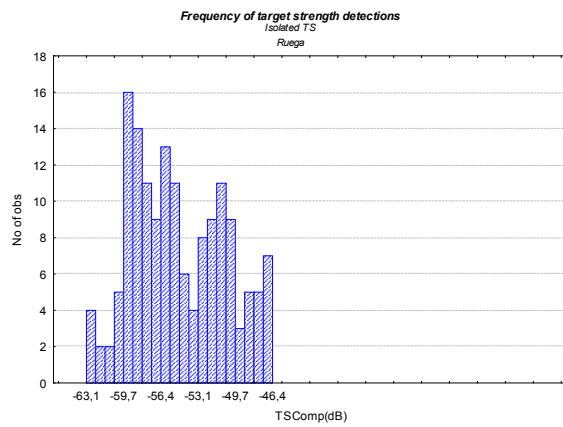


Figure 10

Appendix XI – Validation of the TS Measurements

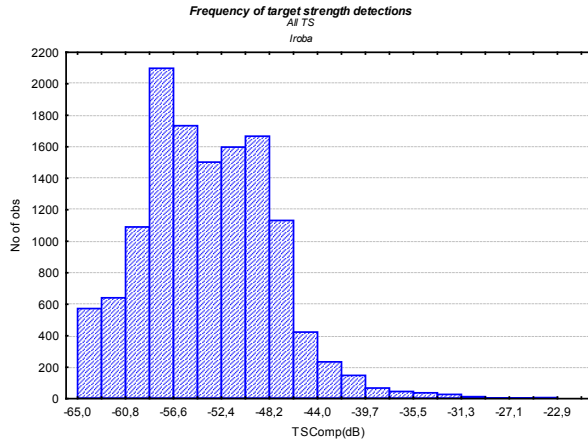


Figure 11

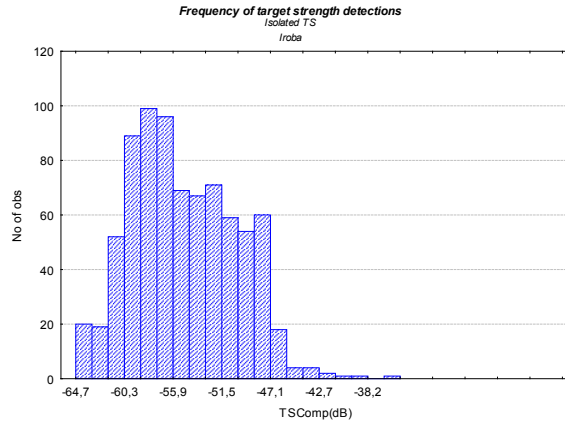


Figure 12

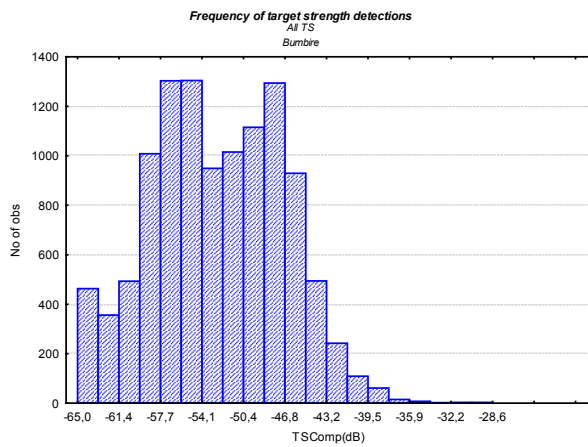


Figure 13

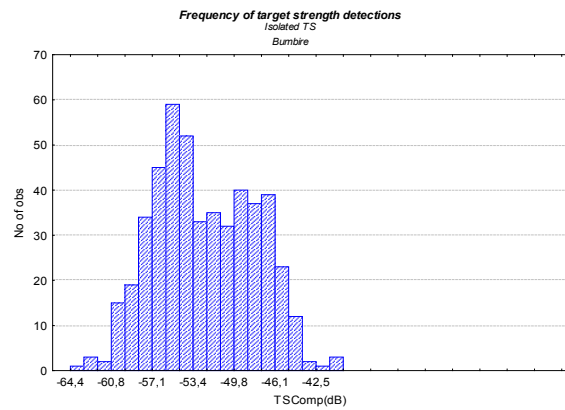


Figure 14

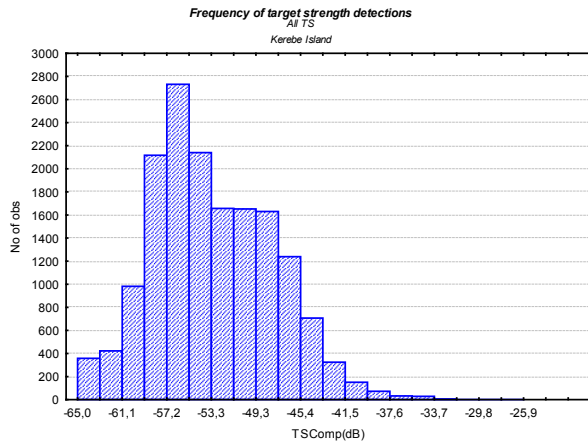


Figure 15

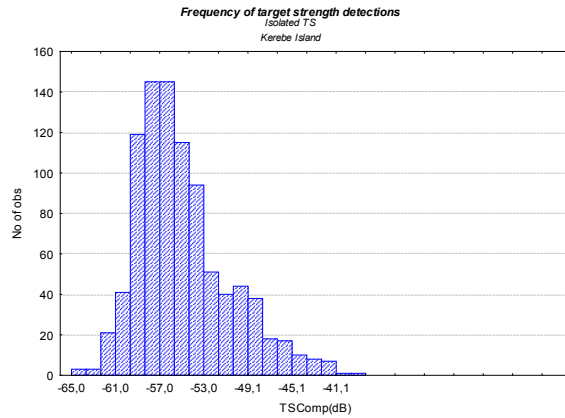


Figure 16

Appendix XI – Validation of the TS Measurements

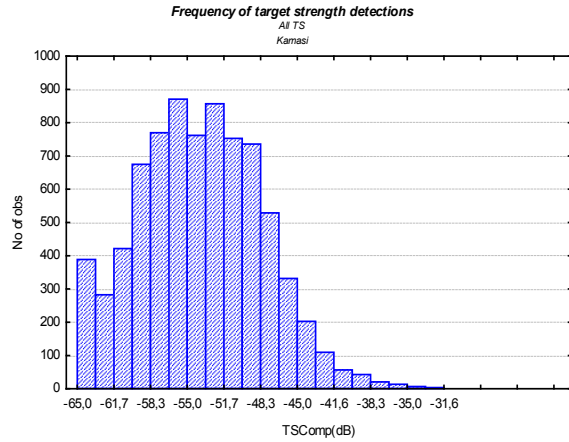


Figure 17

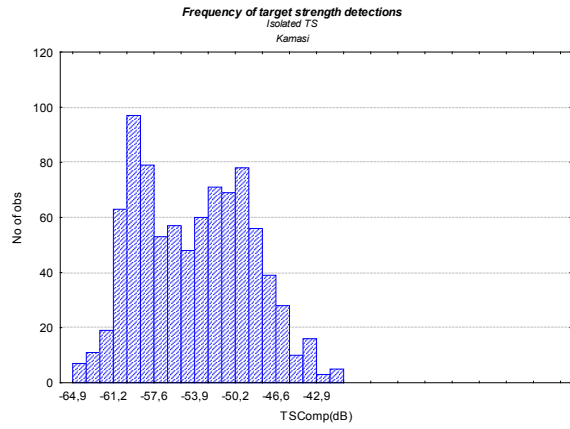


Figure 18

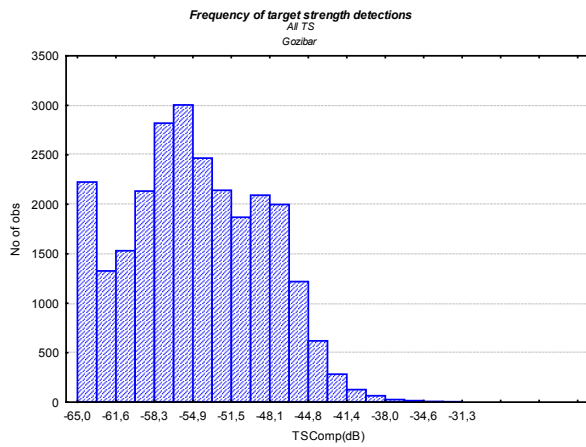


Figure 19

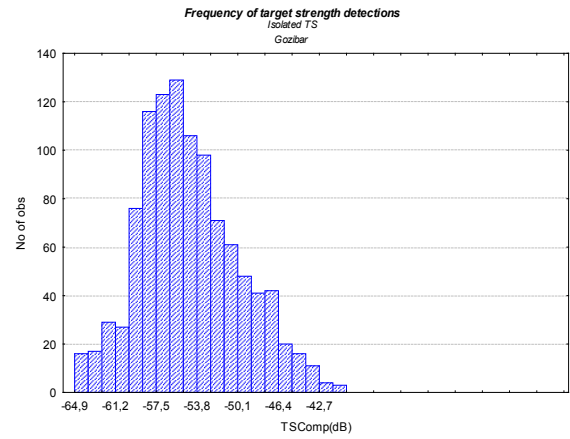


Figure 20

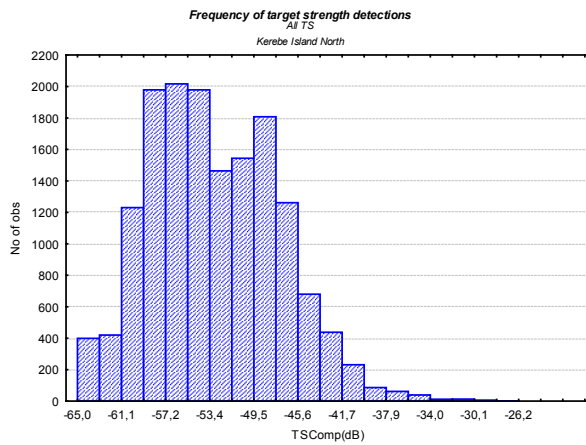


Figure 21

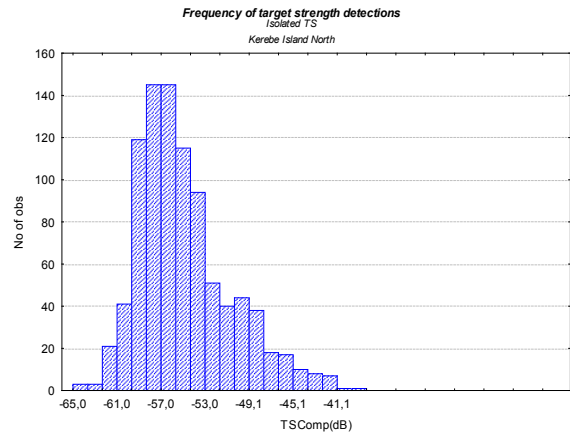


Figure 22

Appendix XI – Validation of the TS Measurements

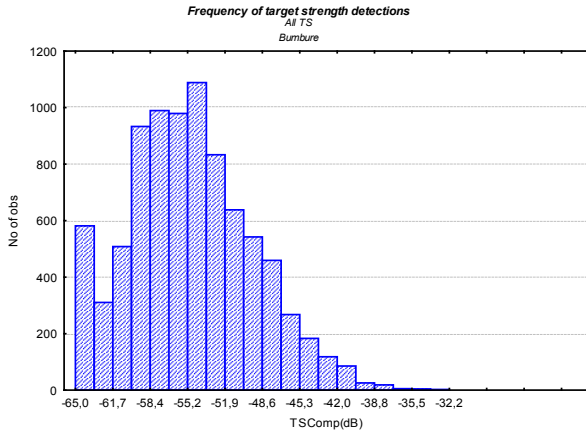


Figure 23

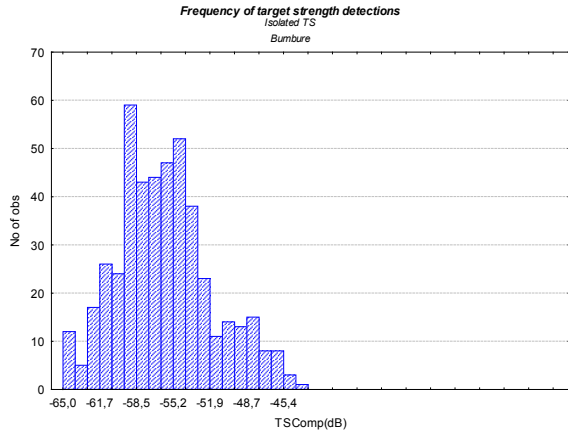


Figure 24

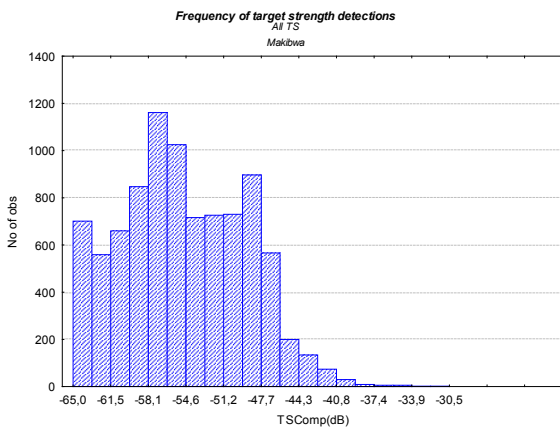


Figure 25

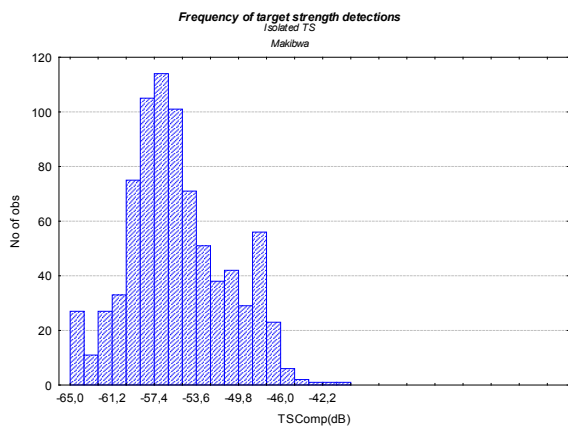


Figure 26

Figures 1 to 26 – Frequency distribution of TS values for each station sampled. The left column show the distribution for the entire water column and the right column show the distribution from TS from selected targets. Note: graphs from left and right column are not at the same scale.

11.2. Regression of TS in function of number of fish inside the acoustic beam

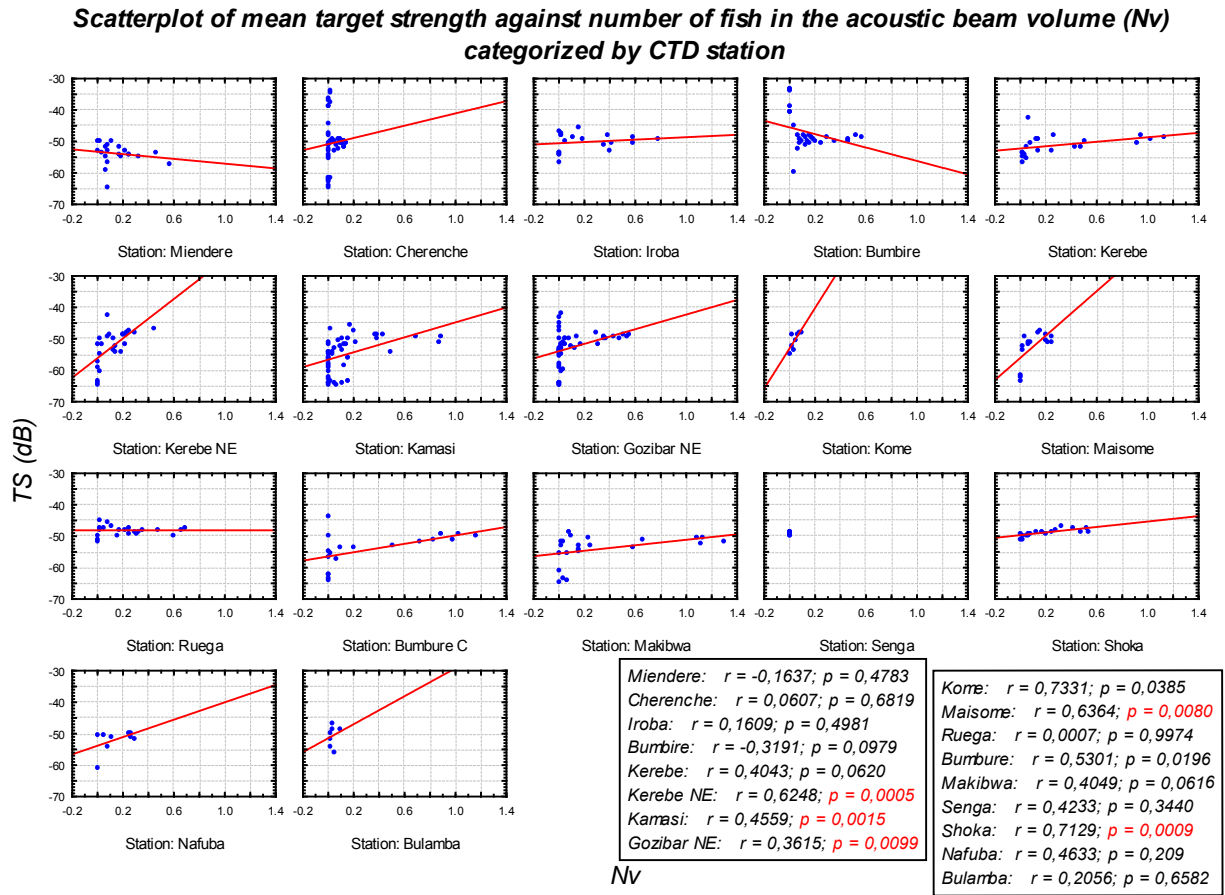


Figure 27 – Scatterplot of TS (average for each meter depth) against number of fish inside the acoustic beam (N_V) for each station. Results from TS regressed against N_V is shown on the bottom right corner (significant values are highlighted in red).

Appendix XII – Echograms

12.1. Echograms Inshore stratum stations

The figures 1 to 9 correspond to the echograms from the sampling stations for the inshore stratum (2nmi distance).

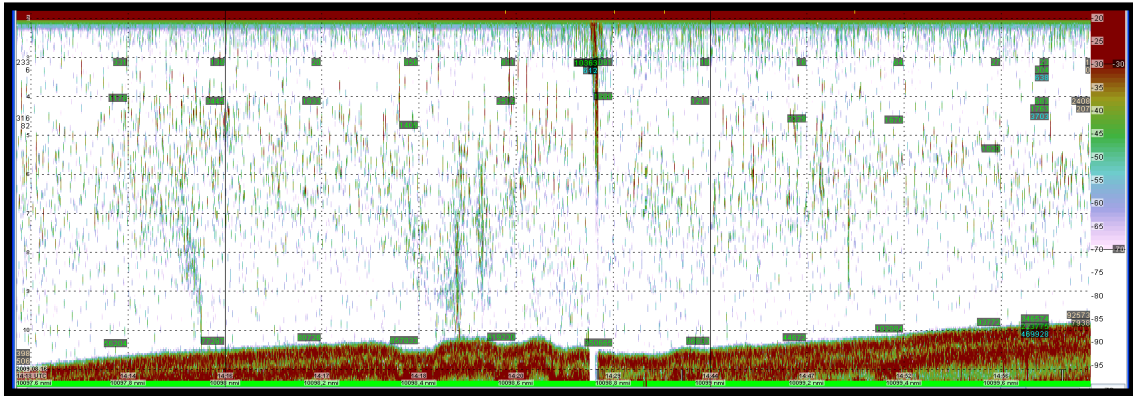


Figure 1 – Echogram from Kome. Bottom depth: 10,22 m; horizontal grids seen every at 1 m depth.

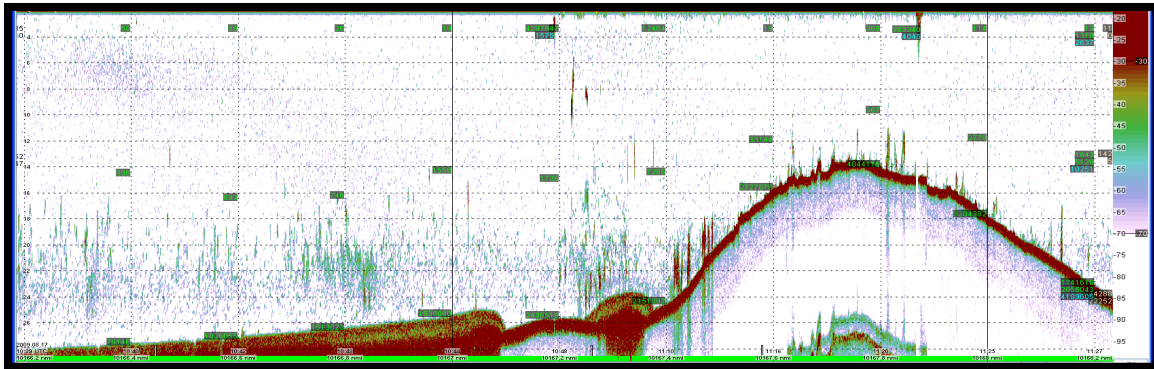


Figure 2 – Echogram from Maisome. Bottom depth: 24,76 m; horizontal grids seen at every 2 m depth.

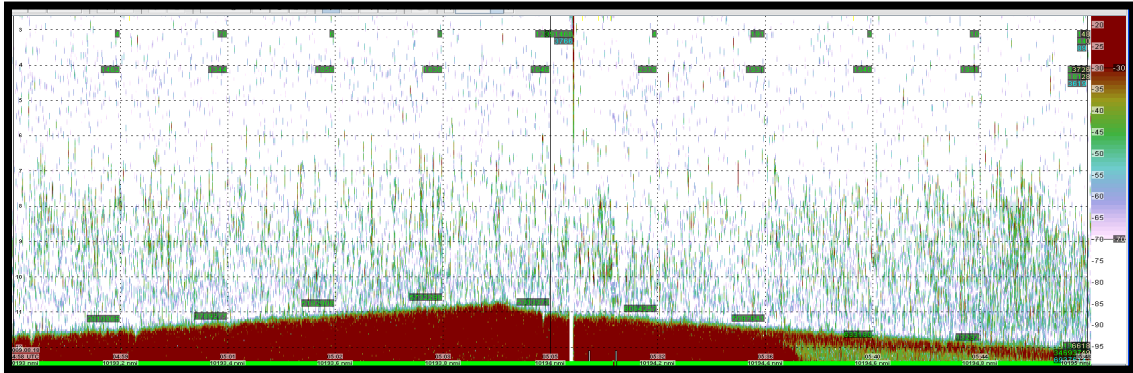


Figure 3 – Echogram from Senga. Bottom depth: 10,73 m; horizontal grids seen at every 1 m depth.

Appendix XII – Echograms

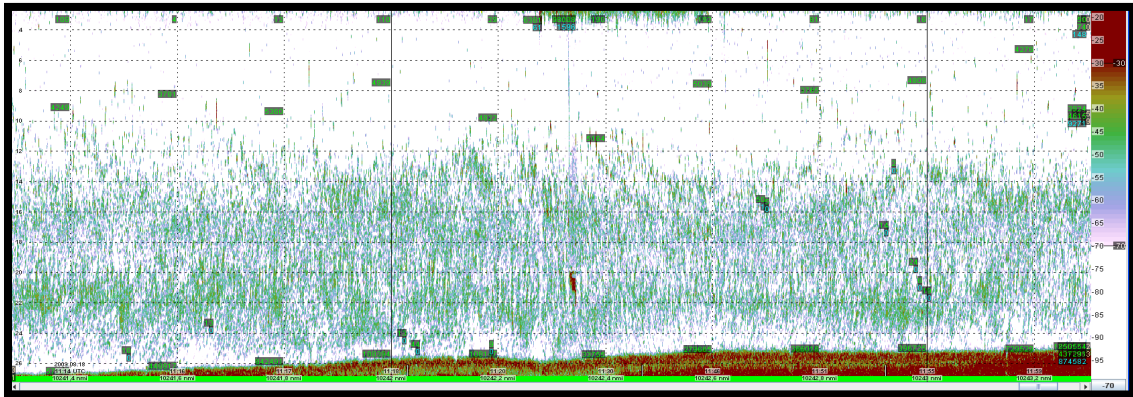


Figure 4 – Echogram from Ruega. Bottom depth: 25.03 m; horizontal grids seen at every 2 m depth.

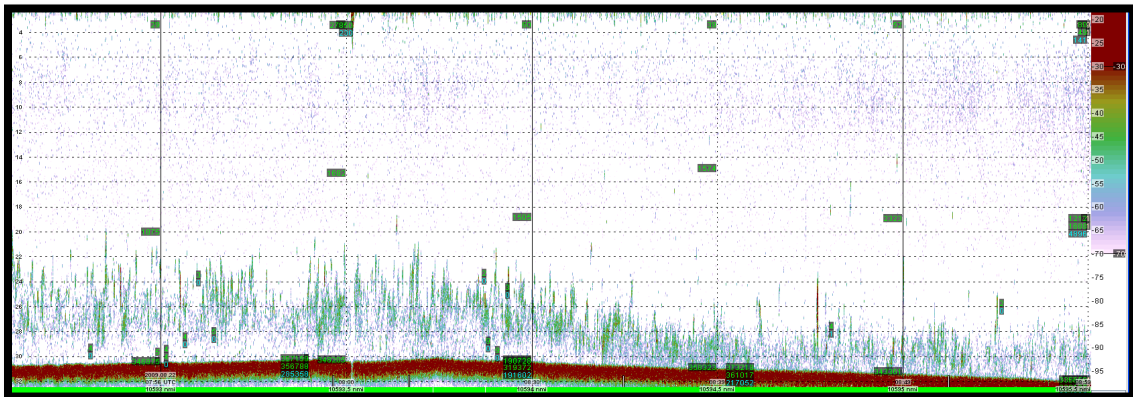


Figure 5 – Echogram from Bumbure. Bottom depth: 29.44 m; horizontal grids seen at every 2 m depth.

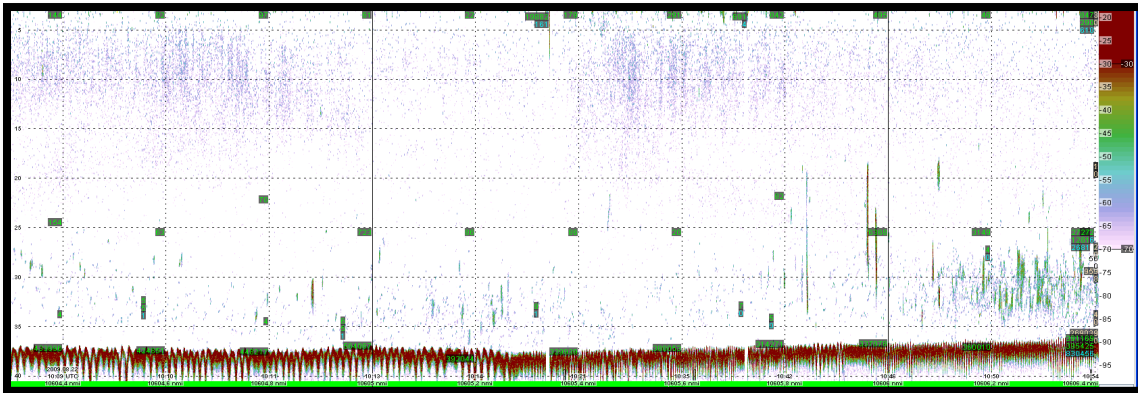
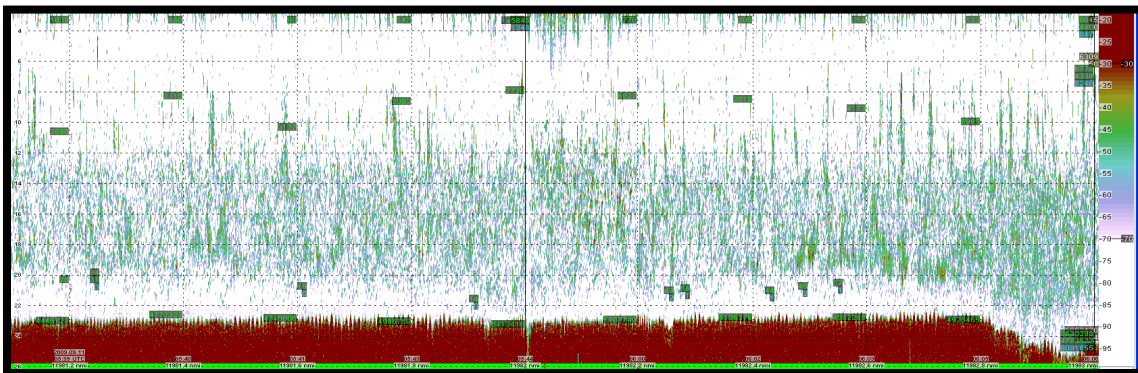


Figure 6 – Echogram from Makibwa. Bottom depth: 37.71 m; horizontal grids seen at every 5 m depth.



Appendix XII – Echograms

Figure 7 – Echogram from Shoka. Bottom depth: 22,32 m; horizontal grids seen at every 2 m depth.

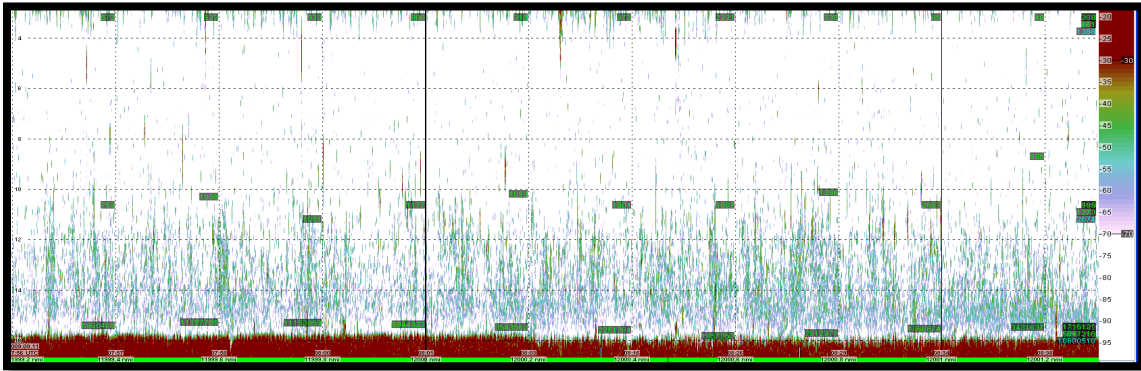


Figure 8 – Echogram from Nafuba. Bottom depth: 15,44 m; horizontal grids seen at every 2 m depth.

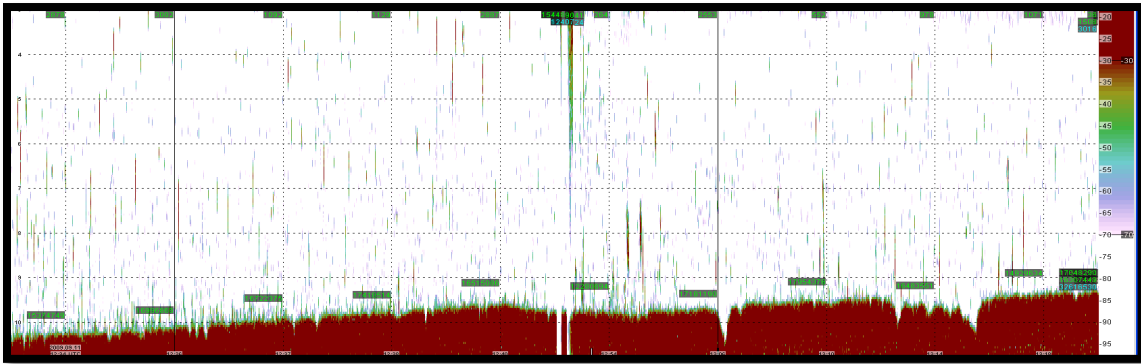


Figure 9 – Echogram from Bulamba. Bottom depth: 9.32 m; horizontal grids seen at every 1 m depth.

12.2. Echograms Coastal stratum stations

The figures 10 to 15 correspond to the echograms from the sampling stations for the coastal stratum (2nmi distance).

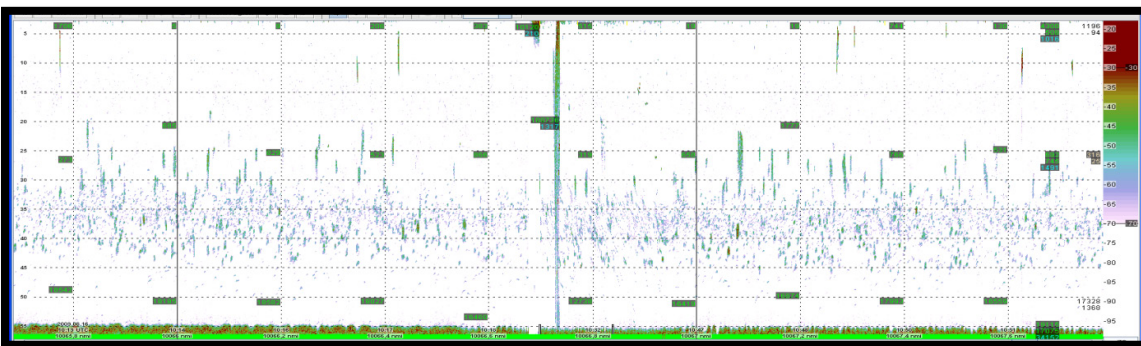


Figure 10 – Echogram from Miendere. Bottom depth: 54,55 m; horizontal grids seen at every 5 m depth.

Appendix XII – Echograms

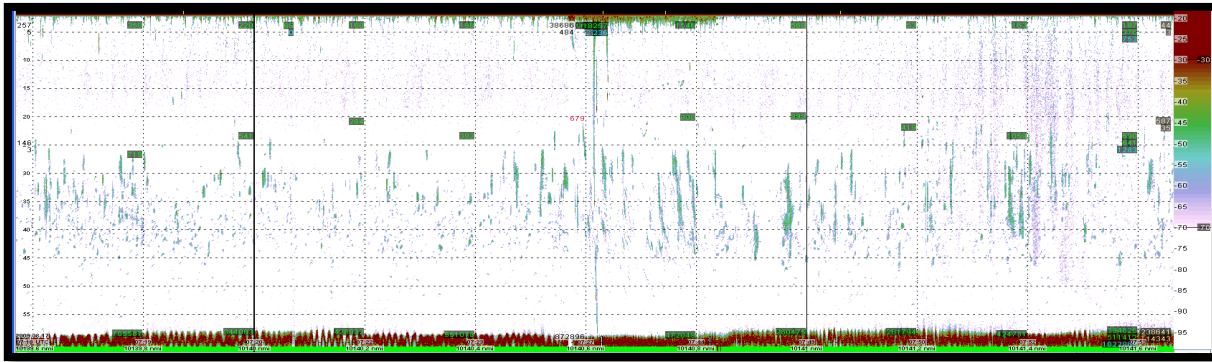


Figure 11 – Echogram from Cherenche. Bottom depth: 57,81 m; horizontal grids seen at every 5 m depth.

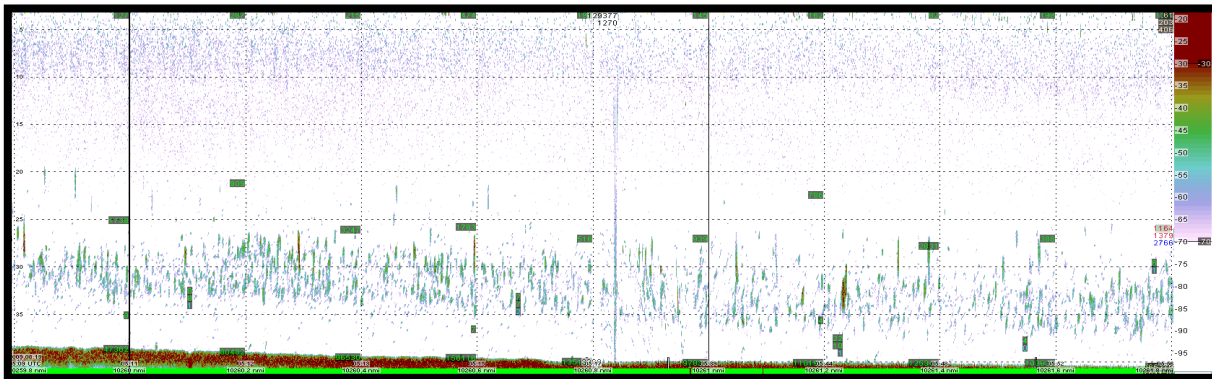


Figure 12 – Echogram from Iroba. Bottom depth: 39,34 m; horizontal grids seen at every 5 m depth.

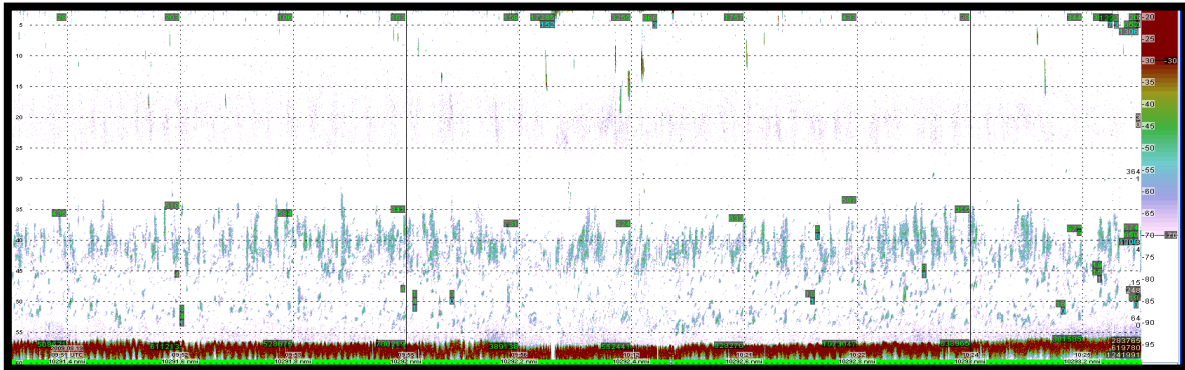


Figure 13 - Echogram from Bumbire. Bottom depth: 56.31 m; horizontal grids seen at every 5 m depth.

Appendix XII – Echograms

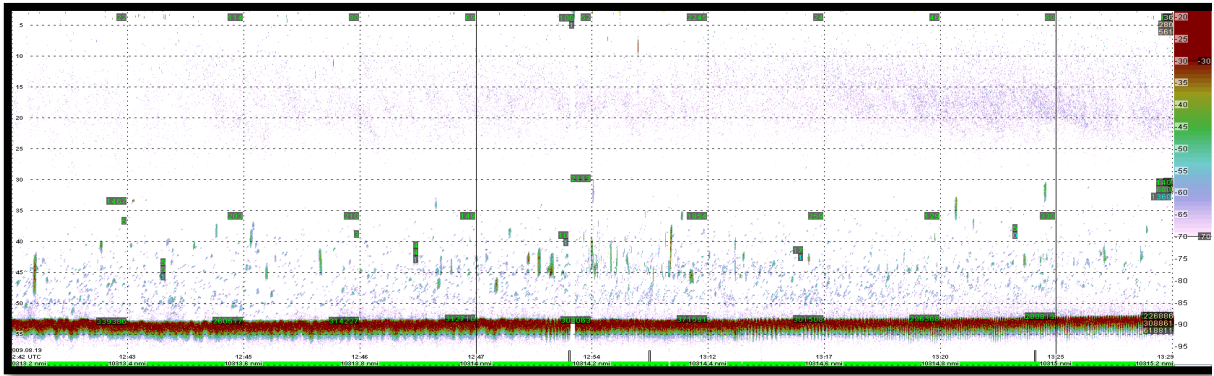


Figure 14 – Echogram from Kerebe Island. Bottom depth: 51.50 m; horizontal grids seen at every 5 m depth.



Figure 15 – Echogram from Kerebe Island North. Bottom depth: 51,79 m; horizontal grids seen at every 5 m depth.

12.3. Echograms deep stratum stations

The figures 16 to 17 correspond to the echograms from the sampling stations for the deep stratum (2nmi distance).

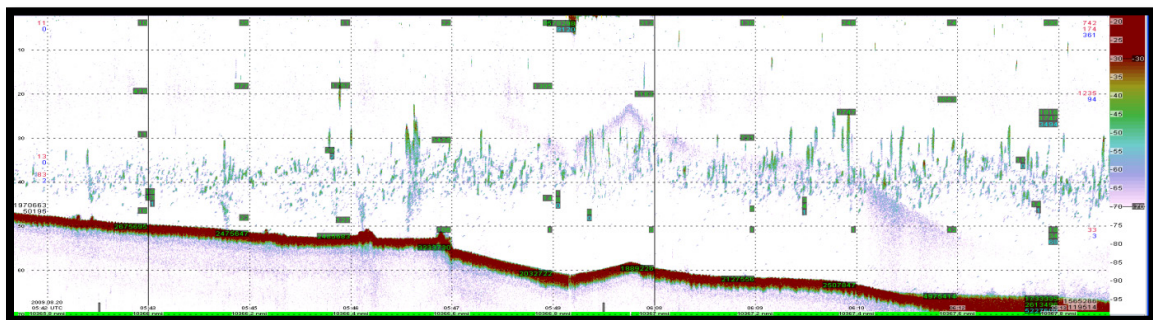


Figure 16 – Echogram from Kamasi. Bottom depth: 59,70 m; horizontal grids seen at every 10 m depth.

Appendix XII – Echograms

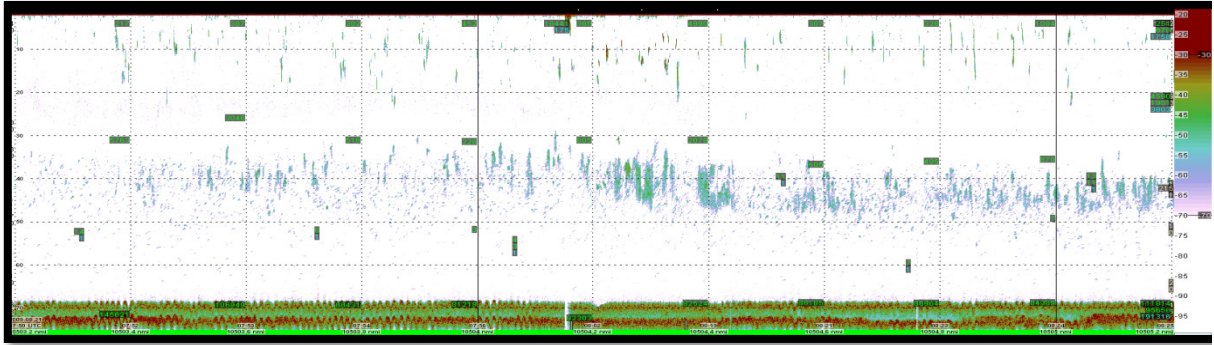


Figure 17 – Echogram from Gozibar. Bottom depth: 67,82 m; horizontal grids seen at every 10 m depth.

Appendix XIII – Fish density results

13.1. Fish densities for each station

Table 1 – Average fish density calculated for each station (values averaged from 0.1nmi from the entire water column).

Station	ρ_A (fish nmi⁻²)
Miendere	4579189
Kome	13651051
Cherenche	2753832
Maisome	13559521
Senga	9884192
Ruega	22931475
Iroba	6593500
Bumbire	4223633
Kerebe Isl.	5830918
Kamasi	8761766
Gozibar	4830534
Kerebe NE	2940708
Bumbure C	15794660
Makibwa	14033799
Shoka	23632958
Nafuba	12474211
Bulamba	8865092

13.2. Correlation between fish density and chlorophyll a

Scatterplot fish density against chlorophyll a, categorized by stratum

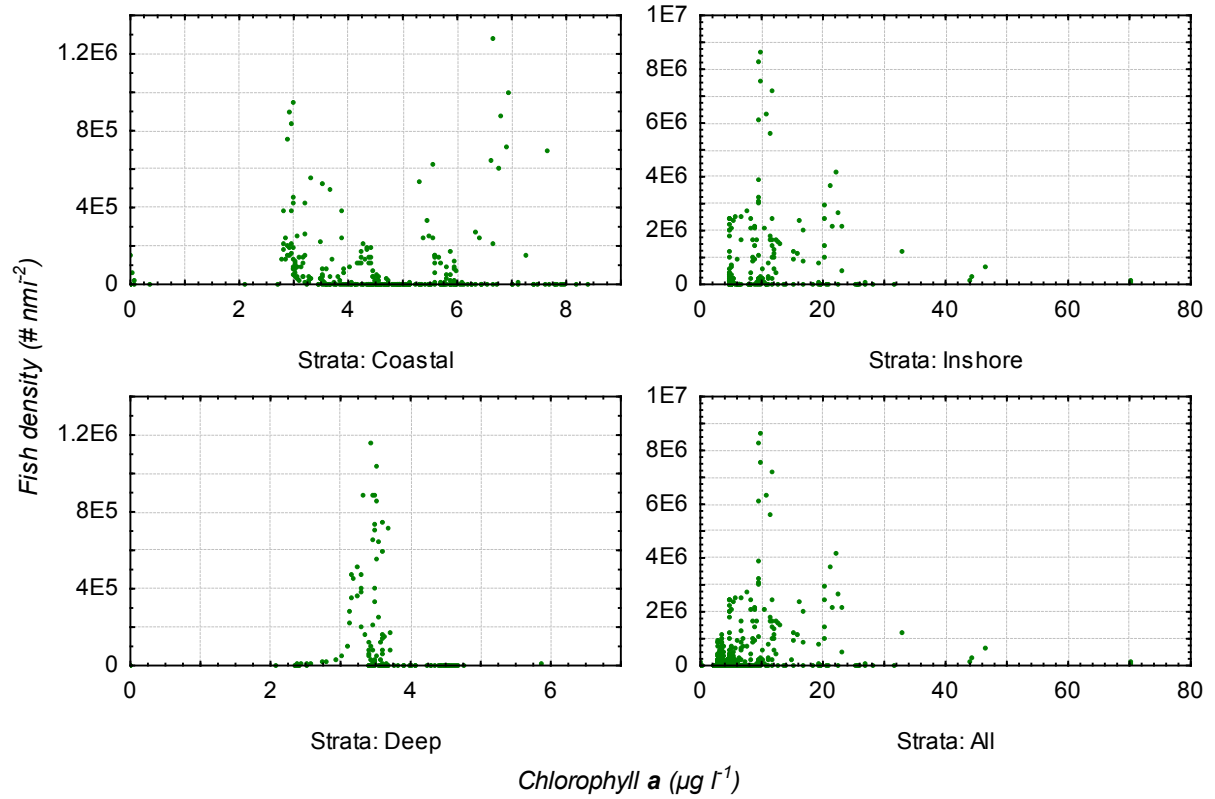


Figure 1 – Scatterplot of fish density distribution in function of Chlorophyll a, divided by stratum. Note: graphs are not at the same scale.

13.3. Statistical analysis results

Table 2 – Results from the Spearman Rank correlation test (fish density was tested against depth, Oxygen, chlorophyll a and temperature) by strata. Significant correlations are highlighted in red.

		<i>N</i>	<i>Spearman R</i>	<i>t(N-2)</i>	<i>p-level</i>
Inshore	ρ_A (#/nmi ²) & Depth	134	0,22	2,60	0,010
	ρ_A (#/nmi ²) & Oxygen	134	0,13	1,54	0,125
	ρ_A (#/nmi ²) & Chlorophyll	134	0,12	1,38	0,171
	ρ_A (#/nmi ²) & Temperature	134	-0,02	-0,28	0,778
Coastal	ρ_A (#/nmi ²) & Depth	197	0,20	2,79	0,006
	ρ_A (#/nmi ²) & Oxygen	176	0,20	2,75	0,007
	ρ_A (#/nmi ²) & Chlorophyll	197	-0,04	-0,51	0,612
	ρ_A (#/nmi ²) & Temperature	197	-0,04	-0,52	0,607
Deep	ρ_A (#/nmi ²) & Depth	101	0,03	0,29	0,775
	ρ_A (#/nmi ²) & Oxygen	101	0,31	3,23	0,002
	ρ_A (#/nmi ²) & Chlorophyll	101	-0,20	-1,99	0,050
	ρ_A (#/nmi ²) & Temperature	101	0,32	3,34	0,001

Appendix XIV – List of equations used

$$r(f) = \frac{s_v(f)}{s_v} \quad (1)$$

$$\sigma = 4\pi 10^{TSc/0,1} \quad (2)$$

$$TS = 10 \text{Log}_{10} \left(\frac{\bar{\sigma}}{4\pi} \right) \quad (3)$$

$$\bar{\sigma} = \frac{1}{n} \sum_{i=1}^n \sigma_i \quad (4)$$

$$N_V = \frac{c \tau \psi R^2 \rho_v}{2} \quad (5)$$

$$\bar{x} = \frac{1}{n} \sum_{i=1}^n x_i \quad (6)$$

$$\text{Std. Error} = \frac{s}{\sqrt{n}} \quad (7)$$

$$s_A = 4\pi (1852^2) s_a \quad (8)$$

$$s_v = \frac{s_a}{\Delta z} \quad (9)$$

$$\rho_A = \frac{s_A}{\bar{\sigma}} \quad (10)$$

$$\rho_v = \frac{s_a}{\bar{\sigma}} \quad (11)$$

$$RMSL = \sqrt{\frac{\sum n_j L_j^2}{\sum_{i=1}^n n_j}} \quad (12)$$

$$TS = m \text{Log}_{10} (TL) + b_{20} \quad (13)$$

Appendix XIV – List of Equations Used

$$TS = 20 \text{ Log}_{10} (RMSL) - 66 \quad (14)$$

$$TS = 29,9 \text{ Log}_{10} (TL) - 79,3 \quad (15)$$

$$TS = 30,2 \text{ Log}_{10} (TL) - 84,6 \quad (16)$$

$$A_{i,j}^{sw} = V_{i,j} t_{i,j} h_{i,j} \chi \quad (17)$$

$$D_{i,j} = \frac{W_{i,j}}{A_{i,j}^{sw}} \quad (18)$$

$$C = \rho_{Trawl} A_{i,j}^{sw} \quad (19)$$